University of Alberta

Regulation of clavam metabolite production in *Streptomyces clavuligerus*

by

Thomas Kwong

A thesis submitted to the Faculty of Graduate Studies and Research
in partial fulfillment of the requirements for the degree of

Doctor of Philosophy
in
Microbiology and Biotechnbology

Department of Biological Sciences

Spring, 2011
Edmonton, Alberta

Abstract

Streptomyces clavuligerus is capable of producing various secondary metabolites including clavulanic acid. The biosynthetic pathway of clavulanic acid is partially shared with other structurally related 5*S* clavams. The first reaction involved in clavam biosynthesis is catalyzed by carboxyethylarginine synthase (CeaS), which is encoded by two paralogous genes, *ceaS1* and *ceaS2*. However, *ceaS2* mutant was severely compromised in clavam biosynthesis when grown in liquid medium. This mutation was shown to affect *ceaS1* transcription, as reverse transcriptase-polymerase chain reaction (RT-PCR) and Western blot protein analyses showed that transcription of *ceaS1*, and CeaS1 production, were abolished in *ceaS2* mutants. Interestingly, clavam biosynthesis was restored when *ceaS2* mutants were grown on solid medium.

Production of 5*S* clavams in *S. clavuligerus* is controlled by a pathway specific transcriptional regulator, C7P, and an unusual two-component system that is composed of a sensor kinase, Snk, and two response regulators, Res1 and Res2. Null mutations in *snk* or *res2* completely abolished production of 5*S* clavams. In contrast, *res1* mutants overproduce 2-hydroxymethylclavam and alanylclavam. Phosphorylation sites of each protein involved in this two-component system were identified by changing the conserved histidine residues of Snk (H-365) and the asparatate residues of Res1 (D-65) and Res2 (D-52) to alanine residues. These mutations prevented auto-phosphorylation of Snk and transfer of phosphate molecules from phosphorylated Snk to response regulators as shown by *in vitro* phosphorylation assays. The phosphorylation dynamics between Res1 and Res2

were also analyzed. Phospho-transfer assays suggested that Res1 is capable of transferring its phosphate molecule to Res2, and dephosphorylation assays showed that Res1 may possess phosphatase activity.

The transcriptional regulator C7P is encoded by the *c7p* gene. RT-PCR analyses showed that transcription of *cvm1* and *cvm5*, which encode essential biosynthetic enzymes involved in 5*S* clavam production, ceased in *c7p* mutants. In addition, *c7p* transcription was severely reduced in a *snk* or *res2* mutant. Electrophoretic mobility shift assays showed that Res2 binds to the putative promoter region of *c7p*, and C7P binds to the intergenic region between *cvm1* and *cas1*. This suggests that the two-component system controls transcription of *c7p*, and C7P promotes transcription of clavam genes through direct binding.

Acknowledgements

First of all, I would like to express my sincere gratitude to my Ph.D supervisor, Dr. Susan Jensen, for giving me the opportunity to work in her lab as a graduate student. Without her support, encouragement and guidance over the last five years, this thesis would not have been possible.

I am grateful to my many student colleagues, Jingru Li, Nathan Zelyas, Mohamad Shaheen and Sarah Goomeshi Nobary, for providing a fun and supportive environment in which to grow and learn. I appreciate their help and sound advices throughout my study and introducing many valuable laboratory techniques to me. I would like to thank Annie Wong for her work and technical support, which contributed greatly to my thesis. I would also like to thank Troy Locke from MBSU for his help with the FPLC.

Lastly and most importantly, I wish to thank my family, especially my parents, and friends for their love and support through the good and difficult times. Without their caring and encouragement, this study would not have been completed. To them, I dedicate this thesis.

Table of Contents

1. Introduction **1**

1.1 *Streptomyces* 2

1.2 β-lactam metabolites 4

1.3 Biosynthesis of clavulanic acid and 5*S* clavams 9

1.3.1 "Early" steps in clavam production 10

1.3.2 Gene clusters involved in clavam production 13

1.3.3 "Late" genes in clavulanic acid production 24

1.3.4 "Late" genes in 5*S* clavam production 29

1.4 Regulation of antibiotic production 35

1.4.1 SARPS 35

1.4.2 Other pathway specific transcriptional regulators 38

1.4.3 Bald (*bld*) genes 39

1.4.4 γ-butyrolactone regulators 40

1.4.5 The stringent response 41

1.4.6 Two-component regulatory systems 42

1.5 Thesis objective 45

2. Materials and Methods **47**

2.1 Materials 48

2.2 Bacterial strains and plasmids 49

2.3 Centrifugation and culture harvesting 49

2.4 *E. coli* procedures 49

2.4.1 Culture media and growth conditions for *E. coli* 49

2.4.2 Storage of *E. coli* strains 58

2.4.3 Isolation of *E. coli* plasmid DNA 58

2.4.4 Electroporation of DNA into electrocompetent *E. coli* 58

2.5 *Streptomyces* procedures 59

2.5.1 Culture media and growth conditions for *S. clavuligerus* 59

2.5.2 Storage of *S. clavuligerus* strains 59
2.5.3 Introduction of DNA into *S. clavuligerus* 60
2.5.4 Fermentation of *S. clavuligerus* 61
2.5.5 RNA isolation 61
2.5.6 Cell-free extract preparation 64
2.6 Determination of antibiotic production 64
2.6.1 Clavulanic acid bioassay 64
2.6.2 High performance liquid chromatography 65
2.7 DNA methods 66
2.7.1 DNA quantification 66
2.7.2 Digestion and ligation reactions 66
2.7.3 Polymerase chain reaction 67
2.7.4 Agarose gel electrophoresis 68
2.7.5 DNA purification from agarose gels 75
2.7.6 Polyacrylamide gel electrophoresis 75
2.7.7 DNA purification from polyacrylamide gels 75
2.7.8 DNA labelling 76
2.7.9 DNA sequencing 76
2.8 RNA methods 77
2.8.1 RNA quantification 77
2.8.2 Reverse transcriptase-polymerase chain reaction 77
2.9 Protein methods 78
2.9.1 Protein quantification 78
2.9.2 SDS-Polyacrylamide gel electrophoresis 78
2.9.3 Overproduction of CeaS1 and CeaS2 79
2.9.4 Overproduction of Snk-His_7 and Res2-His_7 80
2.9.5 Overproduction of His_{10}-Res1, His_{10}-Res1-SD and His_{10}-C7P 80
2.9.6 Overproduction of MBP-Res1 and MBP-Res2 81
2.9.7 Purification of His-tagged proteins 81
2.9.8 Purification of MBP fusion protein 82

2.9.9 *In vitro* phosphorylation assays 84
2.9.10 Phospho-transfer assays 84
2.9.11 *In vitro* dephosphorylation assays 86
2.9.12 Western analysis 86
2.10 DNA-Protein interactions 87
2.10.1 Electrophoretic mobility shift assays 87
2.11 Confocal Microscopy 88
2.12 Software and web sources used for analysis 89
3. Results 90
3.1 Analysis of the regulation of *ceaS* involved in clavam biosynthesis 91
3.1.1 Overproduction of CeaS1 and CeaS2 92
3.1.2 Cross reaction of anti-CeaS2 antibody with CeaS1 protein 94
3.1.3 Western analyses to detect CeaS1 and CeaS2 production 99
3.1.4 Western analyses to detect Bls1 and Bls2 production 110
3.1.5 Reverse transcriptase-PCR analysis 116
1. Effect of Δ*ceaS2*-IF mutation on *ceaS1* and *bls2* transcription 116
2. Investigation of transcription of other clavam biosynthetic genes in the Δ*ceaS2*-IF mutant by RT-PCR 120
3.1.6 Promoter activity analysis by use of *egfp* 121
3.1.7 Clavulanic acid production revisited 128
3.2 Analysis of the regulation of the late steps of 5*S* clavam biosynthesis 133
3.2.1 Phenotype of Δ*snk*-IF, Δ*res1*::apra Δ*res2*::apra Δ*c7p*::apra mutants 133
3.2.2 Transcript analysis by RT-PCR 134
3.2.3 Protein overproduction and purification 137
1. Res2-His_7 overproduction and purification 145
2. Construction of a C7P overexpression vector 148
3. His_{10}-C7P overproduction and purification 155
3.2.4 Protein-DNA interactions 160
1. Analysis of Res2-DNA interactions by EMSA 160
2. Analysis of C7P-DNA interaction by EMSA 163

3.3 Analysis of proteins involved in the two-component system 173
3.3.1 Overproduction and purification of wild type proteins of the two-component regulatory system 173
3.3.2 Sequence comparison 179
3.3.3 Site-directed mutagenesis of phosphorylation site of Snk, Res1 and Res2 179
3.3.4 Overproduction and purification of two-component regulatory proteins with altered phosphorylation sites 184
3.3.5 *In vitro* phosphorylation assays 189
3.3.6 Phosphorylation dynamics between Res1 and Res2 196
1. Construction of MBP fusion protein overproduction vector 196
2. Purification of phosphorylated MBP-Res1 and MBP-Res2 200
3. *In vitro* dephosphorylation assays 207
4. Phospho-transfer assays 210
4. Discussion 213
4.1 Polar effect exerted on transcription of downstream genes 214
4.2 *ceaS1* and *ceaS2* regulation 217
4.3 Atypical two-component system and C7P on 5*S* clavam metabolite biosynthesis 221
4.4 Conclusions 229
5. References **231**

List of Tables

Chapter 1

1.1 Production of clavulanic acid and 5*S* clavams by mutants with defects in genes encoding enzymes involved in the early steps of clavam metabolite biosynthesis in *S. clavuligerus*.....19

Chapter 2

2.1 *Escherichia coli* strains used in this study..... 50

2.2 *Streptomyces* strains used in this study..... 51

2.3 *Escherichia coli* and *Streptomyces* plasmids used in this study..... 53

2.4 Oligionucleotides primers used in this study..... 69

Chapter 3

3.1 Bioassay detection of clavulanic acid production by various *S. clavuligerus* mutants after 48 hours of growth in Soy and SA media..... 93

3.2 Transcription profile of various *S. clavuligerus* strains as determined by RT-PCR..... 144

List of Figures

Chapter 1

1.1. Chemical structure of various secondary metabolites produced by *S. clavuligerus* 5

1.2. "Early" steps involved in biosynthesis of clavaminic acid, the branch point intermediate leading to production of clavulanic acid and 5*S* clavams..... 11

1.3. The β-lactam supercluster of *S. clavuligerus* 14

1.4. The clavam gene cluster of *S. clavuligerus*..... 17

1.5. The paralogue gene cluster of *S. clavuligerus*. 21

1.6. Proposed "late" steps involved in biosynthesis of clavulanic acid and 5*S* clavams..... 26

1.7. Proposed steps involved in alanylclavam biosynthesis 32

Chapter 3

3.1.1. Overproduction of CeaS1 and CeaS2 from *E. coli* BL21(DE3) carrying pET9c-*ceaS1* and pET24a-*ceaS2* 95

3.1.2. Western analysis of CeaS1 and CeaS2..... 97

3.1.3. Western analysis of CeaS using cell-free extracts isolated from wild type *S. clavuligerus* grown either in liquid complex soy (Soy) or defined starch asparagine (SA) medium..... 101

3.1.4. Western analysis of CeaS in *ceaS2* mutant strains and *ceaS1*/*ceaS2* double mutant.....103

3.1.5. Western analysis of CeaS in *ceaS1* mutant strains.....105

3.1.6. Western analysis of CeaS in complemented *ceaS2* mutants 108

3.1.7. Western analysis of Bls in wild type *S. clavuligerus* and *bls* mutants. 111

3.1.8. Western analysis of Bls in *ceaS2* mutants 114

3.1.9. Assessment of *ceas1*, *ceas2*, *bls1*, *bls2* and *hrdB* transcript levels in wild type *S. clavuligerus*, Δ*ceaS2*-IF and Δ*ceaS1*::apra mutants by RT-PCR 118

3.1.10. Assessment of *cvm5*, *c7p*, *c6p* and *hrdB* transcript levels in wild type *S. clavuligerus*, Δ*ceaS2*-IF, Δ*res2*::apra and Δ*res1*::apra mutants by RT-PCR 122

3.1.11. Assessment of *cas1*, *cvm1*, *res1* and *res2* transcript levels in wild type *S. clavuligerus*, Δ*ceaS2*-IF, Δ*res2*::apra and Δ*res1*::apra mutants by RT-PCR 124

3.1.12. Assessment of *orfA*, *ceaS1*, *ceaS2* and *snk* transcript levels in wild type *S. clavuligerus*, Δ*ceaS2*-IF, Δ*res2*::apra and Δ*res1*::apra mutants by RT-PCR 126

3.1.13. Detection of *ceaS1* promoter activity in wild type and Δ*ceaS2* mutant strains of *S. clavuligerus* by using EGFP as a reporter.....129

3.1.14. Clavam metabolites produced by wild type *S. clavuligerus* and Δ*ceaS2*-IF mutants grown on solid Soy medium.....131

3.2.1. Clavam metabolites produced by Δ*snk*-IF, Δ*res2*::apra, Δ*c7p*::apra and Δ*res1*::apra mutants grown on solid Soy medium 135

3.2.2. Assessment of *cas1*, *cvm5*, *cvm1* and *hrdB* transcript levels in Δ*ceaS1*::apra, Δ*c7p*::apra and Δ*snk*-IF mutants by RT-PCR.....138

3.2.3. Assessment of *res1, res2*, *snk* and *orfA* transcript levels in Δ*ceaS1*::apra, Δ*c7p*::apra and Δ*snk*-IF mutants by RT-PCR.....140

3.2.4. Assessment of *ceaS1*, *ceaS2*, *c6p* and *c7p* transcript levels in Δ*ceaS1*::apra, Δ*c7p*::apra and Δ*snk*-IF mutants by RT-PCR. 142

3.2.5. Purification of Res2-His_7 from *E. coli* BL21(DE3) carrying pT7-7His-*res2* 146

3.2.6. Schematic of the process leading to the construction of pET-19b-*c7p*.....149

3.2.7. DNA fragments used to construct the *c7p* expression vector 153

3.2.8. Restriction analysis of pET-19b-*c7p* protein expression vector 156

3.2.9. Purification of His_{10}-C7P from *E. coli* BL21(DE3) carrying pET-19b-*c7p* 158

3.2.10. DNA probes for electrophoretic mobility shift assays of various targets identified by RT-PCR 161

3.2.11. Analysis of binding of Res2-His_7 to promoter regions of genes in the clavam and paralogue gene clusters. 164

3.2.12. Analysis of binding of His_{10}-C7P to promoter regions of genes in the clavam and paralogue gene clusters. 166

3.2.13. Electrophoretic mobility shift of a 454 bp DNA fragment spanning the intergenic region between *cvm1* and *cas1* when bound by His_{10}-C7P.....169

3.2.14. Specificity of His_{10}-C7P binding to a 454 bp DNA fragment spanning the intergenic region between *cvm1* and *cas1* 171

3.3.1. Purification of Snk-His_7 from *E. coli* BL21(DE3) carrying pT7-7His-*snk*.....175

3.3.2. Purification of His_{10}-Res1 from *E. coli* BL21(DE3) carrying pET-19b-*res1* 177

3.3.3. *In vitro* phosphorylation of Snk-His_7, His_{10}-Res1 and Res2-His_7.....180

3.3.4. Sequence comparison through BLAST analyses of the proteins of the two-component regulatory system 182

3.3.5. Schematic representation of the two-step site-directed mutagenesis used to change the phosphorylation site of Snk, Res1 and Res2 to an alanine residue....185

3.3.6. Purification of Snk-SD-His_7 from *E. coli* BL21(DE3) carrying pT7-7His-*snk*-SD. 190

3.3.7. Purification of His_{10}-Res1-SD and Res2-SD- His_7 from *E. coli* BL21(DE3) carrying pET-19b-*res1*-SD and pT7-7His-*res2*-SD 192

3.3.8. *In vitro* phosphorylation of Snk-His_7, His_{10}-Res1 and Res2-His_7 and Snk-SD-His_7, His_{10}-Res1-SD and Res2-SD-His_7 194

3.3.9. Purification of MBP-Res1 and MBP-Res2 from *E. coli* BL21(DE3) carrying pMal-*res1* and pMal-*res2* 198

3.3.10. Phosphorylation of MBP-tagged response regulators.....201

3.3.11. Anion exchange chromatography of MBP fusion protein.....203

3.3.12. Schematic diagram of the process leading to the purification of phosphorylated MBP-Res1 and MBP-Res2. 205

3.3.13. *In vitro* dephosphorylation assays 208

3.3.14. Phospho-transfer activity between phosphorylated Res1 and Res2-His_7.....211

Chapter 4

4.1. The proposed mechanism for regulation of *ceaS1* transcription by *ceaS2* of *S. clavuligerus*.....222

4.2. The proposed mechanism between the Snk/Res1/Res2 atypical two-component system and transcriptional regulator C7P of *S. clavuligerus*.....227

List of Abbreviations

α	Alpha
β	Beta
Δ	Delta or deletion
γ	Gamma
g	Gravity
λ	Lambda bacteriophage
μ	Micro
Ω	Omega
σ	Sigma factor
ARE	Autoregulatory element
ATP	Adenosine triphosphate
BLAST	Basic Local Alignment Search Tool
bp	Base pair
BSA	Bovine serum albumin
C-	Carboxy
CDA	Calcium-dependent-antibiotic
cDNA	Complementary DNA
CFE	Cell free extract
Ci	Curie
D	Aspartate
Da	Dalton
DMSO	Dimethyl sulfoxide
DNA	Deoxyribonucleic acid
DNase	Deoxyribonuclease
dNTP	Deoxynucleoside triphosphate
DTT	Dithiothreitol

EBP	Enhancer binding protein
ECL	Enhanced chemiluminescence
EDTA	Ethylenediaminetetraacetic acid
EGFP	Enhanced Green Fluorescent Protein
EMSA	Electrophoretic mobility shift assay
F	Farad
FPLC	Fast protein liquid chromatography
GAF	cGMP-specific and -stimulated phosphodiesterases, adenylate cyclases and FhlA
H	Histidine
HPLC	High performance liquid chromatography
IAA	Isoamyl alcohol
IPTG	Isopropyl-β-D-thiogalactopyranoside
ISP-4	International Streptomyces project medium
kb	Kilobase
kDa	KiloDalton
LB	Lennox broth
LBA	LB agar
M	Molar
m	milli
Mb	Megabase
MBP	Maltose binding protein
mol	mole
MOPS	3-[N-morpholino]propanesulfonic acid
MYM	Maltose yeast extract malt extract medium
N-	Amino
ng	nanogram
NiNTA	Nickel-Nitrilotriacetate

OD	Optical density
PAG	Polyacrylamide gel
PAGE	Polyacrylamide gel electrophoresis
PCR	Polymerase chain reaction
pmol	Picomole
RNA	Ribonucleic acid
RNase	Ribonuclease
rpm	Revolutions per minute
RT-PCR	Reverse-transcriptase-PCR
SARP	*Streptomyces* Antibiotic Regulatory Protein
SD	Site-directed mutagenesis
SDS	Sodium dodecyl sulfate
TAE	Tris-acetate-EDTA buffer
TBE	Tris-borate-EDTA buffer
TCS	Two-component regulatory system
TE	Tris-EDTA buffer
U	Unit
UV	Ultraviolet
V	Volt
v/v	volume/volume
w/v	weight/volume
X-gal	5-bromo-4-chloro-3-β-D-galactopyranoside

Chapter 1

Introduction

1. Introduction

1.1 *Streptomyces*

Streptomycetes are Gram-positive, aerobic, filamentous, spore-forming bacteria that commonly inhabit soil and give it its characteristic smell. The genus *Streptomyces* was first proposed in 1943 by Waksman and Henrici (1943). Streptomycetes have a complex life cycle that is similar to fungi and the life cycle begins as the spore germinates. On solid substrates, growth then occurs at hyphal tips, and with frequent branching, develops into a network called the vegetative or substrate mycelium. During this vegetative growth phase, DNA replicates without cellular division. This results in the characteristic multinucleoid and filamentous structure of the bacterial cells (Chater, 1993). As nutrients begin to be depleted in its surrounding environment, morphological differentiation takes place, which leads to the formation of reproductive aerial hyphae that grow vertically and away from the surface. At the same time, secondary metabolite production begins. Many of these compounds have important medical value including various antibiotics, antitumor agents and immunosuppressants (Chater, 1993; Demain, 2000). The aerial hyphae obtain necessary nutrients for growth and further differentiation by lysing the substrate mycelium underneath (Mendez *et al*., 1985). Septation begins to occur between individual nucleoids along the aerial hyphae leading to development of uninucleoid spores (Hardisson and Manzanal, 1976; Wildermuth, 1970). Once sporulation is complete, the mature spores can then disperse and start the cycle again.

Streptomycetes chromosomes are typically 8-9 Mb in size and are among the largest found in prokaryotes; they are linear and have a high G+C content (69-78%). Due to their saprotrophic nature, *Streptomyces* species are capable of utilizing different carbon sources by producing a range of extracellular enzymes (McCarthy and Williams, 1992). This metabolic diversity is reflected in their extremely large genome. Determination of its complete genome sequence showed that the chromosome of *Streptomyces coelicolor* is about 8.7 Mb in length and contains 7,825 genes, where as in *Streptomyces avermitilis* and *Streptomyces griseus*, the chromosomes contain 7,574 and 7,138 genes and are 9.0 Mb and 8.5 Mb in length, respectively (Bentley *et al*., 2002; Ikeda *et al*., 2003; Ohnishi *et al*., 2008). A comparative analysis between these strains also revealed that the genes on the chromosomes are organized in a way such that a highly conserved core region, which carries most of the essential genes, can be found in the middle of the chromosome in all three organisms. However, the outer arms of the chromosomes are less conserved and contain genes with non-essential functions, such as secondary metabolite production (Bentley *et al*., 2002; Ikeda *et al*., 2003; Ohnishi *et al*., 2008). In *Streptomyces* spp., including *S. clavuligerus*, genes involved in secondary metabolite production tend to be grouped together as gene clusters, which are shown to be highly abundant. More than twenty gene clusters related to known or predicted secondary metabolite production were identified in *S. avermitilis*, *S. coelicolor* and *S. griseus* (Bentley *et al*., 2002; Chater and Bibb, 1997; Ikeda *et al*., 2003; Ohnishi *et al*., 2008). This clustering characteristic has

proven useful as a genetic tool for researchers to identify novel genes that may be involved in antibiotic biosynthetic pathways.

1.2 β-lactam metabolites

Since the discovery of penicillin by Alexander Fleming in 1928, intensive research has been undertaken to discover new antibiotics for treating infections. The β-lactam metabolites have different ring structures fused to the four-membered azetidinione ring (also known as the β-lactam ring) (Figure1.1), which contributes to their biological activity (Skatrud *et al*., 1997). The β-lactam ring acts as an analog of acyl-D-alanyl-D-alanine and binds to the transpeptidase enzyme that catalyzes the cross-linking reaction of the peptidoglycan network (Tipper and Strominger, 1965; Wise and Park, 1965). This weakens the peptidoglycan, which normally provides the structural support and rigidity to bacterial cells, and eventually leads to cell death as the cells are no longer protected from osmotic pressure. To date, β-lactam antibiotics are still one of the most important groups of chemotherapeutic agents, accounting for over 65% of antibiotics used worldwide (Elander, 2003; Paradkar *et al*., 1997). However, it was not until 1962 that researchers started to realize that, besides fungi, bacteria such as Streptomycetes were also capable of producing β-lactam antibiotics (Miller *et al*., 1962). *Streptomyces clavuligerus* NRRL 3585 was isolated from a South American soil sample in 1971 by Higgens and Kastner (1971). Subsequent analysis showed that this strain could produce penicillin N and cephamycin C (Nagarajan *et al*., 1971; Figure 1.1). In addition to the antibiotics mentioned above, five other clavam-type-β-lactam metabolites, including clavulanic acid, as

Figure 1.1. Chemical structure of various secondary metabolites produced by *S. clavuligerus*. A. β-lactam metabolites. B. other types of metabolites.

A.

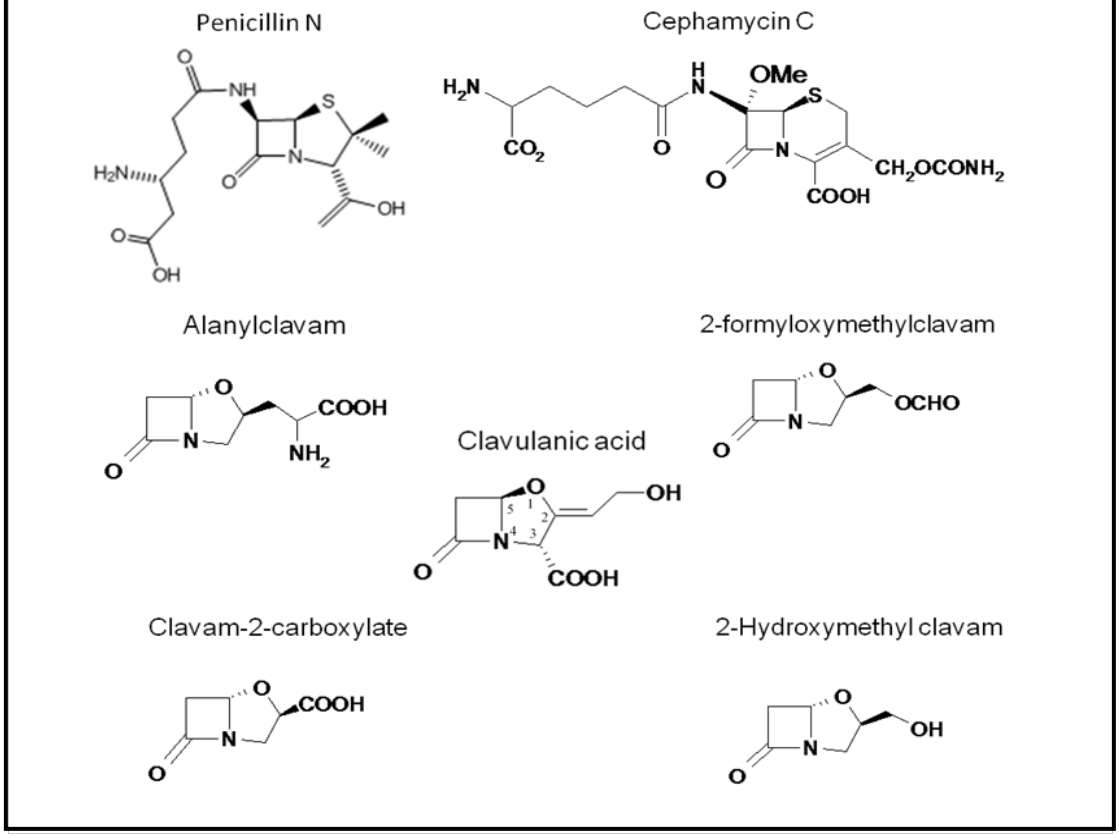
Penicillin N
Cephamycin C
Alanylclavam
2-formyloxymethylclavam
Clavulanic acid
Clavam-2-carboxylate
2-Hydroxymethyl clavam

B.

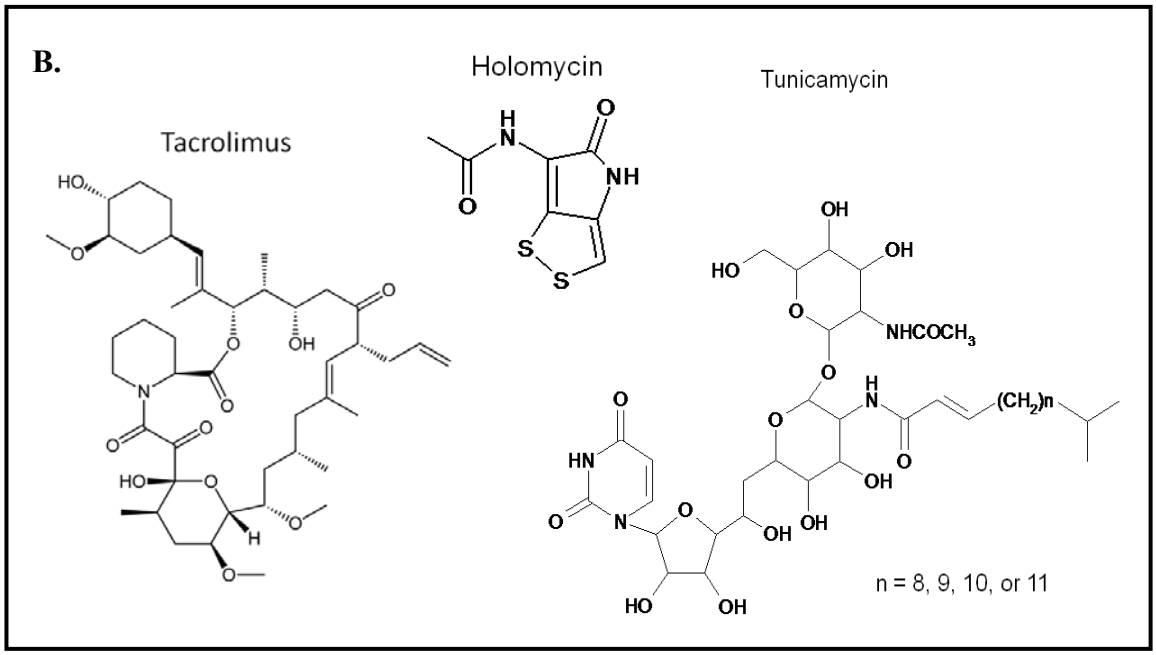
Tacrolimus
Holomycin
Tunicamycin
n = 8, 9, 10, or 11

well as non-β-lactam compounds including holomycin and tunicamycin were found to be produced by this strain (Kenig and Reading, 1979; Nagarajan *et al*., 1971; Figure1.1). The five clavam compounds have an oxygen-containing oxazolidine ring instead of the sulfur-containing thiazolidine ring found in penicillin or the six-membered dihydrothiazine ring found in cephamycin C (Demain and Elander, 1999; Figure 1.1). Another *S. clavuligerus* strain, CKD119, newly isolated from a south Korea soil sample, was shown to produce tacrolimus (FK-506), which has high clinical value because of its immunosuppressant activity (Kim and Park, 2008; Figure 1.1). Recently, sequencing of the *S. clavuligerus* genome has been completed. Although its chromosome is only 6.8 Mb in length, 48 secondary metabolite gene clusters have been identified that are distributed between the chromosome and a newly identified 1.8 Mb linear plasmid (pSCL4) (Medema *et al*., 2010). This suggests that *S. clavuligerus* is capable of producing a large number of yet unidentified secondary metabolites.

Unfortunately, improper and over usage of antibiotics has led to the development of β-lactam antibiotic resistance in many organisms. One of the resistance mechanisms employed by these organisms is the production of β-lactamase, which hydrolyzes the β-lactam ring structure and therefore inactivates its function. The four recognized classes of β-lactamases produced by various bacteria can be arranged into two groups, in which class A, C, and D enzymes are serine hydrolases while class B β-lactamases are metalloenzymes with zinc being the common co-factor (Ambler, 1980).

The spread of β-lactamase encoding genes to pathogenic organisms led to large scale screening for β-lactam antibiotics that are resistant to β-lactamase hydrolysis, and alternatively, for compounds that are capable of inhibiting the reaction catalyzed by β-lactamases. This latter approach led to the identification of clavulanic acid. Although clavulanic acid itself is a weak antibiotic, it is a potent β-lactamase inhibitor (Brown *et al*., 1976), which binds by acting as a structural analogue of penicillin and therefore inhibits a wide range of β-lactamases that belong to classes A and D (Walsh, 2003). Beside the carboxyl group that is present at the C3 position, clavulanic acid also has a 5*R* stereochemistry compared to the 5*S* stereochemistry of the other four clavams (Figure 1.1), which are therefore referred to as the 5*S* clavams. Although clavulanic acid and the 5*S* clavams are very similar in structure, only clavulanic acid is capable of inhibiting β-lactamase. Thus, it is believed that this unique stereochemistry confers the β-lactamase inhibitory activity (Baggaley *et al*., 1997). Despite the fact that the 5*S* clavams are not β-lactamase inhibitors, they still possess biological activity. Clavam-2-carboxylate, 2-hydroxymethylclavam and 2-formyloxymethylclavam were shown to be antifungal (Brown *et al*., 1979), and alanylclavam was found to be bacteriostatic for certain organisms by inhibiting methionine biosynthesis (Pruess and Kellett, 1983).

Since the discovery of this β-lactamase inhibitory activity, clavulanic acid has been used in combination with β-lactam antibiotics to treat infections caused by β-lactamase-producing pathogenic bacteria (Jensen and Paradkar, 1999). Augmentin™, a commercial product that contains clavulanic acid and

amoxicillin, was the second largest selling antibacterial with a world sales value of ~$1.3 billion (US) in 1995 (Elander, 2003). As the emergence of antibiotic resistant strains increased rapidly and in view of the great difficulty in identifying new functional antibiotics, the need for clavulanic acid has increased dramatically. Since *S. clavuligerus* is the only organism used to produce clavulanic acid through industrial fermentation (Jensen, personal communication), the biosynthetic pathway and its regulation has become a point of great interest. It is now known that clavulanic acid and the 5*S* clavams share a common biosynthetic pathway up to the intermediate called clavaminic acid and then the pathway branches off leading to the production of clavulanic acid on the one hand, or the various 5*S* clavams on the other hand (Egan *et al*., 1997). However, the biosynthetic pathway has not been completely elucidated and it is still unclear how clavaminic acid proceeds to clavulanic acid or the 5*S* clavams.

1.3 Biosynthesis of clavulanic acid and 5*S* clavams

Similar to the biosynthetic pathway for cephamycin C, which has been well studied in *S. clavuligerus*, the biosynthetic pathway for clavulanic acid and the 5*S* clavams can be divided into two parts that are commonly referred to as the "early" and "late" steps. The "early" steps are shared between clavulanic acid and 5*S* clavam biosynthesis up to the branch point intermediate called clavaminic acid (Egan *et al*., 1997; Figure 1.2). The "late" steps are specific and either lead to the formation of clavulanic acid or 5*S* clavams from clavaminic acid. Even though the pathway leading to clavaminic acid production has been well characterized (Jensen and Paradkar, 1999), steps beyond clavaminic acid are uncertain.

1.3.1 "Early" steps in clavam production

The first reaction in the "early" steps involves the condensation of L-arginine and D-glyceraldehyde-3-phosphate to produce N^2-(2-carboxyethyl) arginine (Khaleeli *et al*., 1999; Figure 1.2). This reaction is catalyzed by carboxyethylarginine synthase (CeaS), which is encoded by the gene *ceaS* and requires thiamine pyrophosphate and Mg^{2+} for activity (Khaleeli *et al*., 1999). The crystal structure of this enzyme showed that it is a tetramer consisting of two closely associated dimers (Caines *et al*., 2004). β-lactam synthetase (BLS), which is encoded by *bls*, then catalyzes the formation of a β-lactam ring structure in N^2-(2-carboxyethyl) arginine leading to formation of deoxyguanidinoproclavaminate (Bachmann *et al*., 1998; Figure 1.2). The crystal structure of this enzyme showed that the holoenzyme consists of a dimer and requires ATP and Mg^{2+} to function (Miller *at al*., 2001). Clavaminate synthase (CAS), which is encoded by *cas*, then catalyzes the hydroxylation of deoxyguanidinoproclavaminate to form guanidinoproclavaminate (Baldwin *et al*., 1993; Marsh *et al*., 1992; Figure 1.2). This enzyme is a dioxygenase, which requires α-ketoglutarate, molecular oxygen, and Fe^{2+} in order to function (Salowe *et al*., 1990). Proclavaminate amidino-hydrolase (PAH), which is encoded by *pah*, then catalyzes the removal of the guanidino group from guanidinoproclavaminate leading to the formation of proclavaminate (Elson *et al*., 1993a). PAH requires Mn^{2+} to function and the holoenzyme was shown to be to a hexamer (Elkins *et al*., 2002). Finally, CAS catalyzes another two reactions, which involve the oxidative cyclization of proclavaminate to produce dihydroclavaminate followed by desaturation of

Figure 1.2. “Early” steps involved in biosynthesis of clavaminic acid, the branch point intermediate leading to production of clavulanic acid and 5*S* clavams. Gene designations are shown in italics.

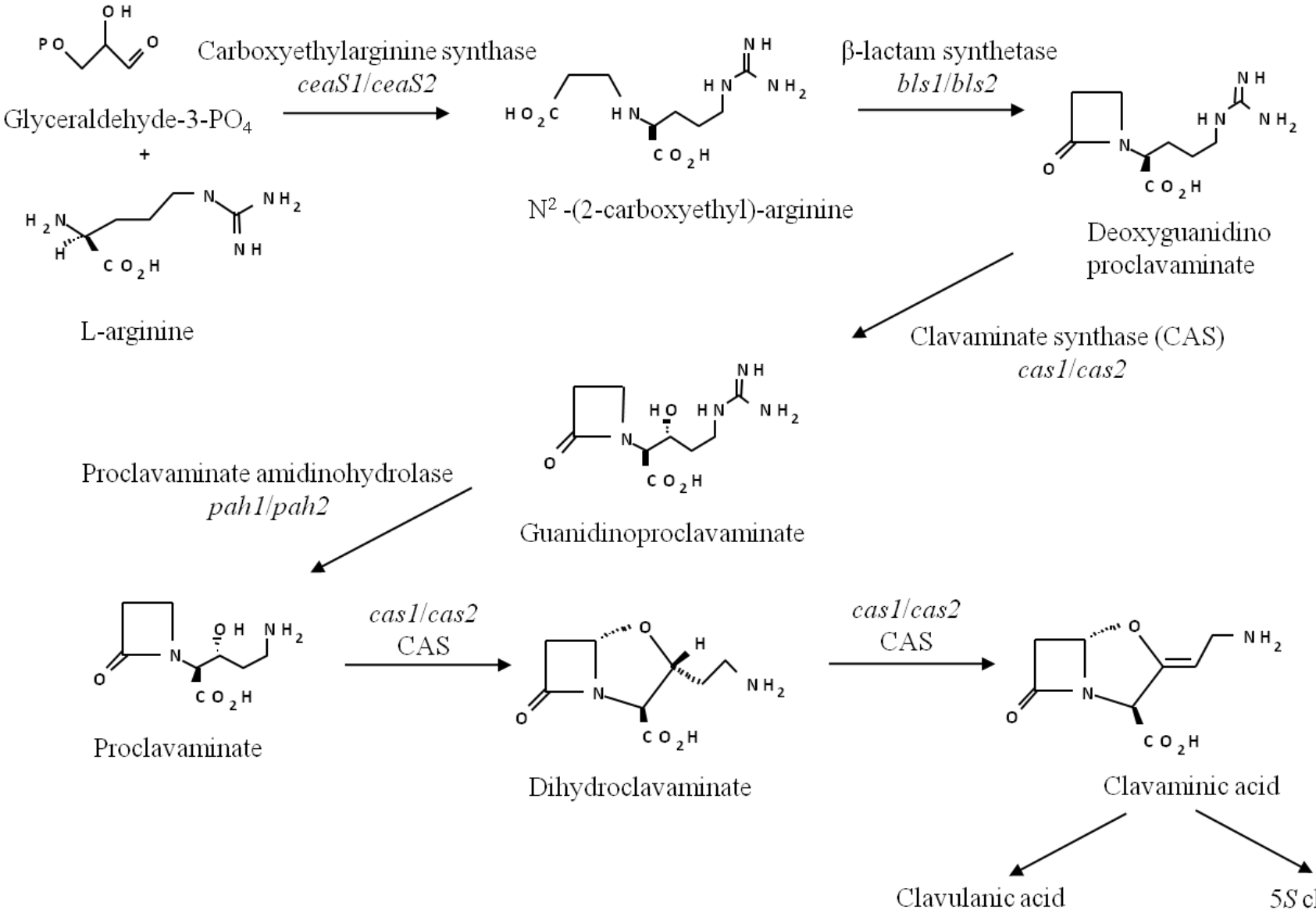
Glyceraldehyde-3-PO4
+
L-arginine
Carboxyethylarginine synthase
ceaS1/ceaS2
N2 -(2-carboxyethyl)-arginine
β-lactam synthetase
bls1/bls2
Deoxyguanidino proclavaminate
Clavaminate synthase (CAS)
cas1/cas2
Guanidinoproclavaminate
Proclavaminate amidinohydrolase
pah1/pah2
Proclavaminate
cas1/cas2 CAS
Dihydroclavaminate
cas1/cas2 CAS
Clavaminic acid
Clavulanic acid
5S clavams

dihydroclavaminate leading to the formation of clavaminic acid (Salowe *et al*., 1991; Figure 1.2).

1.3.2 Gene clusters involved in clavam production

When CAS was purified from *S. clavuligerus*, two active forms of the enzyme, which have slightly different kinetic constants and molecular weights, were observed (Salowe *et al*., 1990). Subsequent analysis revealed that the two CAS isozymes were encoded by two different genes, that shared 82% identity and 87% similarity at the amino acid level, and therefore the two genes were named *cas1* and *cas2* (Marsh *et al*., 1992). *cas2*, along with *ceaS*, *bls*, *pah* and *oat* (later called *ceaS2*, *bls2*, *pah2* and *oat2*), are located downstream of the cephamycin C gene cluster (Jensen *et al*., 2000; Figure 1.3). It is now known that genes specific for clavulanic acid production are also located in this region of the chromosome. As a result, this region is now referred to as the clavulanic acid gene cluster (Figure 1.3). For organisms, such as *Streptomyces jumonjinensis* and *S. clavuligerus*, that can produce clavulanic acid and cephamycin C, it is common for both gene clusters to reside adjacent to each other (Ward and Hodgson, 1993). Therefore, these two clusters together are also referred to as the β-lactam supercluster.

In contrast, *cas1* is located on another part of the *S. clavuligerus* chromosome. Investigation of the region surrounding *cas1* showed that it also formed a separate cluster with genes that are only involved in the 5*S* clavam biosynthesis and therefore, this cluster was named the clavam gene cluster

Figure 1.3. The β-lactam supercluster of *S. clavuligerus.* The yellow arrows represent genes in the cephamycin C gene cluster; the rest belong to the clavulanic acid gene cluster. The black arrows represent genes that are important or essential for clavulanic acid biosynthesis. The white arrows represent genes that are not essential for clavam production. The grey arrow represents an apparently essential gene. Gene designations for the cephamycin C gene cluster are described by Tahlan (2005). Gene designations for the clavulanic acid gene cluster are described in the text.

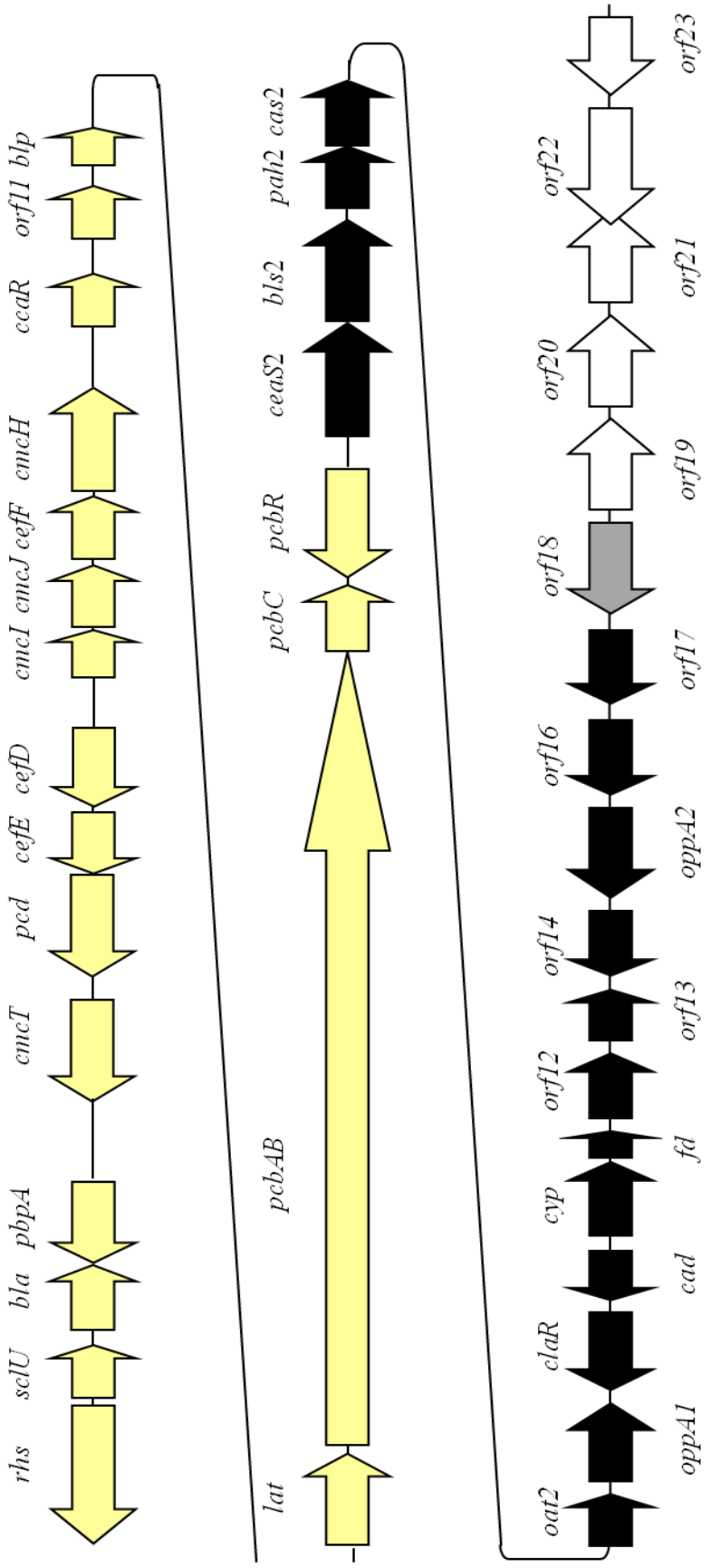
rhs
sclU
bla
pbpA
cmcT
pcd
cefE
cefD
cmcI
cmcJ
cefF
cmcH
ccaR
orf11
blp
lat
pcbAB
pcbC
pcbR
ceaS2
bls2
pah2
cas2
oat2
claR
oppA1
cyp
cad
fd
orf12
orf13
orf14
oppA2
orf16
orf17
orf18
orf19
orf20
orf21
orf22
orf23

(Mosher *et al*., 1999; Figure 1.4). Mutational analysis showed that a *cas2* null mutant was capable of producing clavulanic acid and 5*S* clavams but at a reduced level compared to wild type *S. clavuligerus* in complex soy (Soy) medium (Table 1.1). However, production of all clavam compounds was abolished in defined starch asparagine (SA) medium (Paradkar and Jensen, 1995). Mutational analysis showed that a *cas1* null mutant exhibited a phenotype similar to the *cas2* mutant when grown in Soy medium, but it could still produce clavulanic acid when grown in SA medium (Mosher *et al*., 1999). Transcriptional analysis showed that *cas1* and *cas2* are subjected to different nutritional regulation, where *cas1* is only expressed in Soy medium, while *cas2* can be expressed in both media (Paradkar and Jensen, 1995). A *cas1*/*cas2* double mutant cannot produce any clavam metabolites when growing either in Soy or SA media (Table 1.1). This result excluded the possibility that a third copy of *cas* is present in *S. clavuligerus*. All of these data together indicated that CAS1 and CAS2 are functionally equivalent enzymes and both are involved in clavulanic acid production when the organism is grown in Soy medium while CAS2 is solely responsible for the production of clavulanic acid when grown in SA medium.

When separate mutations were made in the *ceaS*, *bls* and *pah* genes that lie upstream of *cas2* in *S. clavuligerus*, phenotypes similar to that seen in the *cas2* mutant were observed (Table 1.1). Only partial loss of production of clavams was seen, although the severity of the defect in production was far more prominent in *ceaS* and *bls* mutants. These mutants were still capable of producing at least some clavulanic acid and 5*S* clavams in Soy medium but clavam production was

Figure 1.4. The clavam gene cluster of *S. clavuligerus*. The grey arrows represent genes that are essential or important for clavam biosynthesis. The white arrows represent genes that are not essential for clavam production. The black arrows represent genes whose importance in clavam biosynthesis has not been examined. Gene designations for the clavam gene cluster are described in the text.

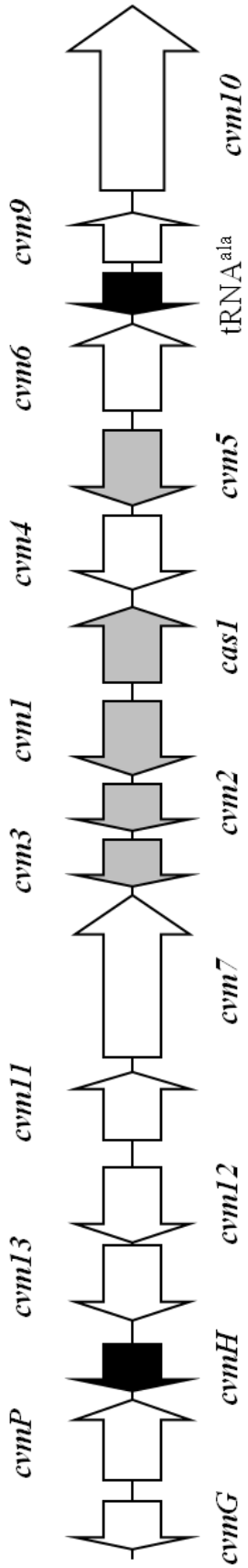
cvmG
cvmH
cvmP
cvm13
cvm12
cvm11
cvm7
cvm3
cvm2
cvm1
cas1
cvm4
cvm5
cvm6
tRNA^{ala}
cvm9
cvm10

Table 1.1. Production of clavulanic acid and 5*S* clavams by mutants with defects in genes encoding enzymes involved in the early steps of clavam metabolite biosynthesis in *S. clavuligerus* [a].

Mutant Strain	**Amount of metabolites produced (in %) as compared to the wild type strain grown in Soy medium** [b]				**Reference**
	Clavulanic acid		**5S clavams**		
	SA	**S oy**	**SA**	**Soy**	
Wild type	20	100	5-10	100	Jensen *et al*. (2000)
ceaS2	0	2-5	0	2-5	Jensen *et al*. (2000)
ceaS1	17-63	2-63	ND [c]		Tahlan *et al*. (2004c)
ceaS1/*ceaS2*	0	0	0	0	Tahlan *et al*. (2004c)
bls2	0	10	0	15	Jensen *et al*. (2000)
bls1	103-162	107-173	ND [c]		Tahlan *et al*. (2004c)
bls1/*bls2*	0	0	0	0	Tahlan *et al*. (2004c)
pah2	0	60	ND [c]	100	Jensen *et al*. (2000)
pah1	4-6	33-41	0	ND [c]	Jensen *et al*. (2004b)
pah1/ *pah2*	0	0	0	0	Jensen *et al*. (2004b)
cas2	0	60	0	60	Jensen *et al*. (2000)
cas1	20	27-71	0	28-87	Mosher *et al*. (1999)
cas1/ *cas2*	0	0	0	0	Mosher *et al*. (1999)
oat2	0	40	0	2-5 [d]	Jensen *et al*. (2000)
oat1	30-154	57-145	ND [c]		Tahlan *et al*. (2004c)
oat1/ *oat2*	12-62	31-67	ND [c]		Tahlan *et al*. (2004c)

[a] This table is adapted from Jensen *et al*. (2000)
[b] The amount of respective metabolite produced by wild type *S. clavuligerus* grown in Soy medium was taken as 100%
[c] Not determined, or too much variation was observed in the production levels to make any deductions
[d] Clavams were not detected in culture supernatants by HPLC analysis but some alanylclavam bioactivity was detected

abolished in SA medium. This suggested that, just as was seen for the *cas* genes, another copy of each of these other early genes may also exist in *S. clavuligerus* (Jensen *et al*., 2000). Indeed, a paralogue of *pah*, which is called *pah1* in order to differentiate it from the *pah* gene located in the clavulanic acid cluster (now called *pah2*), was found by Southern analysis and the two PAH isozymes they encode shared 71% identity at the amino acid level (Jensen *et al*., 2004b). Although clavam production was not greatly affected in a *pah1* mutant, a *pah1*/*pah2* double mutant was incapable of producing clavam metabolites. The region surrounding *pah1* was then sequenced and subsequent analysis revealed three more genes that showed significant similarity to the "early" genes in the clavulanic acid gene cluster (Tahlan *et al.,* 2004a). This region is therefore called the paralogue gene cluster (Figure 1.5). All of the "early" genes located in the clavulanic acid cluster are therefore renamed to become *ceaS2*, *bls2*, *pah2* and *oat2* in order to differentiate them from their respective paralogous copies. *ceaS1* encodes a protein that has 66% identity to CeaS2 at the amino acid level. It was proposed that these two genes may also be under different regulation, as was seen in *cas1* and *cas2*. Indeed, transcriptional analysis indicated that *ceaS1* and *ceaS2* are nutritionally regulated in different ways, where *ceaS2* was expressed in Soy and SA media while *ceaS1* was only expressed in Soy medium (Tahlan *et al*., 2004a). The same study also revealed that *ceaS2* but not *ceaS1* was under the regulation of the transcriptional regulator CcaR, where in a *ccaR* deletion mutant, *ceaS2* expression was completely abolished but *ceaS1* expression was retained (Tahlan *et al*., 2004a).

Figure 1.5. The paralogue gene cluster of *S. clavuligerus*. The grey arrows represent genes that are essential or important for clavam biosynthesis. The black arrows represent genes that are specifically involved in alanylclavam biosynthesis. The white arrows represent genes that are not essential for 5*S* clavam biosynthesis. Gene designations for the paralogue gene cluster are described in the text.

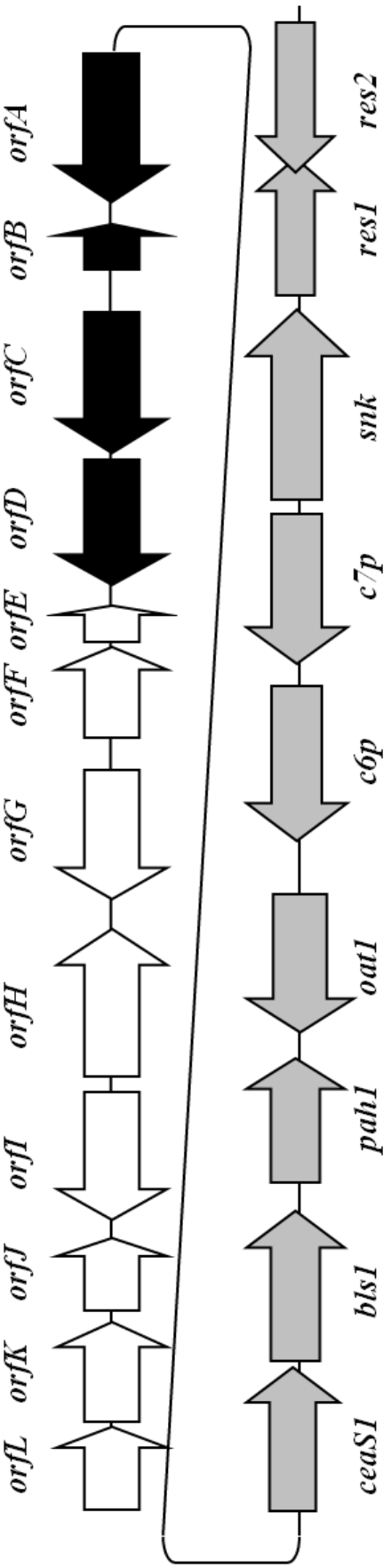
orfA
orfB
orfC
orfD
orfE
orfF
orfG
orfH
orfI
orfJ
orfK
orfL
res2
res1
snk
c7p
c6p
oat1
pah1
bls1
ceaS1

Despite the presence of the *ceaS1* gene encoding a CeaS enzyme functionally equivalent to CeaS2, *ceaS2* mutants were severely impaired in clavulanic acid production even in Soy medium (Table 1.1). This suggested that, in addition to being under different nutritional regulation, some kind of cross regulation is taking place between *ceaS1* and *ceaS2*, which prevents the expression of *ceaS1* in the *ceaS2* mutants.

bls1, which encodes a protein that shares 49% identity to BLS2 at the amino acid level, is located downstream of *ceaS1*. The next gene found in the cluster is *pah1*. Further downstream of *pah1* is *oat1*, encoding an ornithine acetyltransferase enzyme (OAT1), which shares 47% identity with OAT2 at the amino acid level. While clavulanic acid production was shown to be reduced in a *ceaS1* mutant, mutating either *bls1* or *oat1* had no apparent effect on clavam production when grown in Soy medium. Not surprisingly, *ceaS1/ceaS2* and *bls1/bls2* double mutants were incapable of producing clavams, indicating that third copies of these genes do not exist (Tahlan *et al*., 2004a; Table 1.1). OAT, encoded by *oat1* and *oat2*, is believed to play a non-essential role in clavam production by increasing arginine production and channelling it towards the biosynthesis of clavam metabolites (Kershaw *et al*., 2002). This suggestion is supported by data showing that *oat1*/*oat2* double mutants are still capable of producing clavams although at a reduced level (Jensen *et al*., 2000; Table 1.1).

To date, there are three gene clusters that comprise genes involved in the biosynthesis of identified clavam metabolites in *S. clavuligerus*. They are the clavulanic acid (Jensen and Paradkar, 1999), paralogue (Tahlan, 2005) and the

clavam (Mosher *et al*., 1999) gene clusters. These gene clusters are not physically linked as was originally shown by chromosome walking (Tahlan, 2004b) and the paralogue gene cluster has recently been found through genome sequencing to be located on the pSCL4 giant linear plasmid whereas the other two are located on the chromosome (Medema *et al*., 2010). As antibiotic biosynthetic genes are always grouped together, the discovery of these clusters provided a useful handle in order to identify genes that may play a role in clavam production. Long before the genome sequence of *S. clavuligerus* become available, sequence analyses of the regions surrounding the known "early" genes within the gene clusters revealed the presence of a large number of open reading frames (ORFs) that have been shown to be involved specifically in the "late" steps of the biosynthetic pathway. Some of these ORFs are also involved in regulating clavam production.

1.3.3 "Late" genes in clavulanic acid production

Extensive investigation through sequencing and mutational analyses has expanded the clavulanic acid gene cluster further. It is composed of all the "early" genes as well as genes involved specifically in clavulanic acid biosynthesis. Downstream of *oat2* resides *oppA1*, which has significant similarity to *oppA2* (encoded proteins show 48% identity at the amino acid level), located further downstream in the clavulanic acid gene cluster (Hodgson *et al*., 1995; Jensen *et al*., 2000; Lorenzana *et al*., 2004; Mellado *et al*., 2002; Figure 1.3). Both genes were predicted to encode oligopeptide binding proteins and contain a conserved domain found in bacterial extracellular solute-binding proteins (Mellado *et al*., 2002). Analysis of *oppA1* and *oppA2* mutants indicated that these genes are

involved in peptide transport, and disrupting either of these two genes separately impaired or eliminated clavulanic acid production (Jensen *et al*., 2000; Jensen *et al*., 2004a; Lorenzana *et al*., 2004). It is believed that OppA1 and OppA2 function to bind and transport arginine and arginine-containing peptides into *S. clavuligerus* for clavam biosynthesis (Mackenzie *et al*., 2010).

claR and *cad*, which are located downstream of *oppA1*, are another two genes in the clavulanic acid cluster that have well defined roles. *claR* encodes the pathway-specific transcriptional regulator for clavulanic acid biosynthesis (Paradkar *et al*., 1998) and *cad* encodes clavaldehyde dehydrogenase (CAD). CAD catalyzes the final step in clavulanic acid biosynthesis by reducing clavaldehyde, which is a known intermediate between clavaminic acid and clavulanic acid, to clavulanic acid (Nicholson *et al*., 1994; Figure 1.6). The crystal structure of CAD has been solved recently and was shown to be a tetramer that requires NADPH as a cofactor to function (MacKenzie *et al*., 2007). Clavulanic acid production was blocked when *cad* was mutated, while over-expressing *cad* increased clavulanic acid production (Jensen *et al*., 2000; Perez-Redondo *et al*., 1998). c*yp*, *fd*, *orf12*, *orf13* and *orf14* are located beside *cad* and were shown to be important for clavulanic acid production since disrupting any of these genes severely compromised the ability of *S. clavuligerus* to produce clavulanic acid (Jensen *et al*., 2000; Jensen *et al*., 2004a). Proteins encoded by *cyp* and *fd* showed homologies to P-450 cytochromes and ferredoxin proteins, respectively, and as a pair, they were proposed to participate in the oxidative deamination of clavaminic acid to clavaldehyde (Jensen *et al*., 2000; Li *et al*., 2000). However, this remains

Figure 1.6. Proposed “late” steps involved in biosynthesis of clavulanic acid and 5*S* clavams. Known processes are shown as solid black arrows. Hypothetical enzymes and chemical structures are shown in grey. (adapted from Tahlan *et al*. 2007).

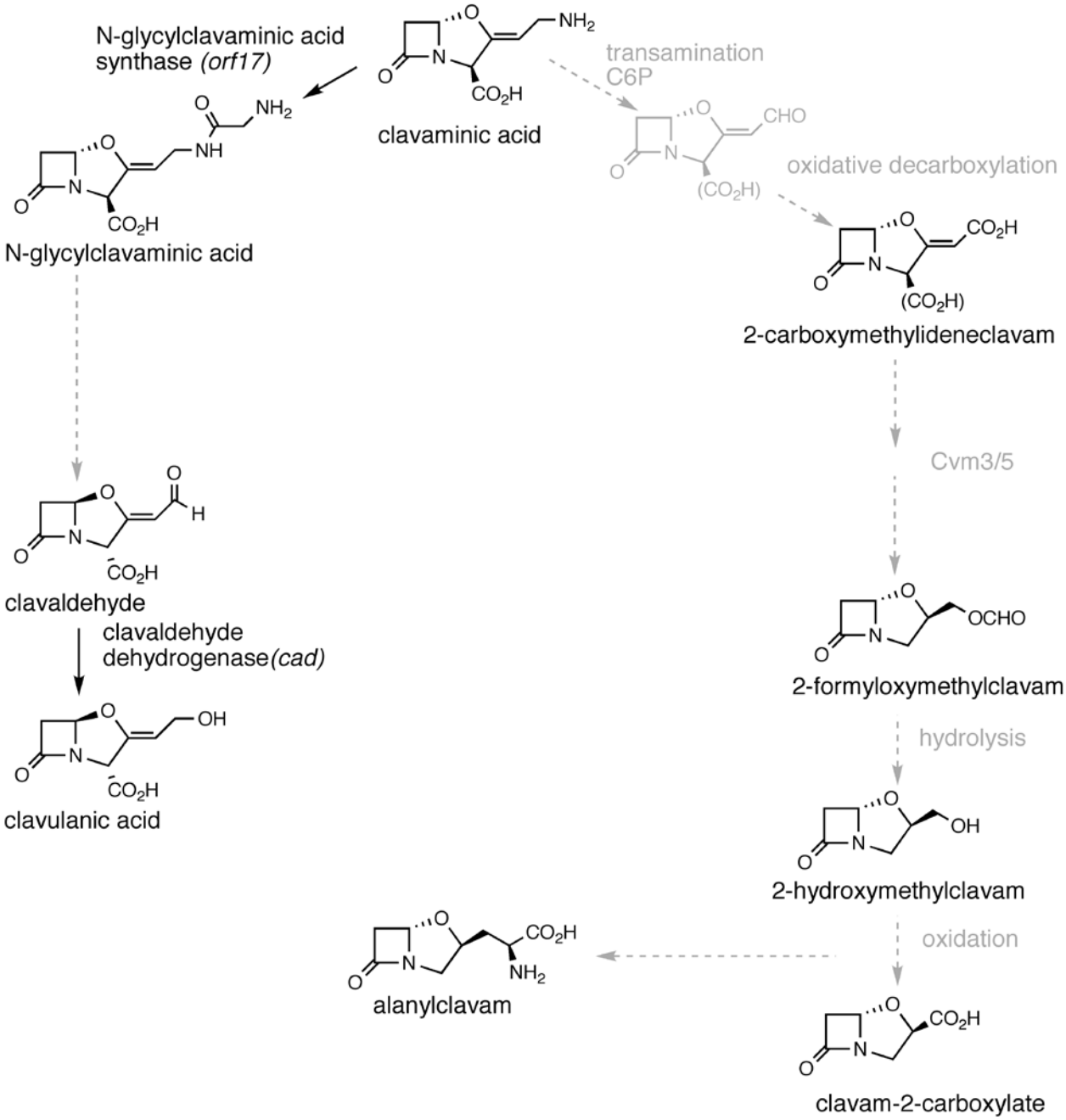
N-glycylclavaminic acid synthase (orf17)
clavaminic acid
transamination C6P
oxidative decarboxylation
N-glycylclavaminic acid
2-carboxymethylideneclavam
Cvm3/5
clavaldehyde
2-formyloxymethylclavam
clavaldehyde dehydrogenase(cad)
hydrolysis
clavulanic acid
2-hydroxymethylclavam
oxidation
alanylclavam
clavam-2-carboxylate

elusive as the reaction has not been demonstrated experimentally. Based on sequence analysis, *orf12*, *orf13* and *orf14* encode proteins showing some similarity to β-lactamases, efflux pump proteins and acetyltransferases, respectively (Jensen *et al*., 2004a; Li *et al*., 2000). Despite their obvious influence on clavulanic acid biosynthesis, the exact roles of these gene products remain unclear.

Similar to *oppA2*, disrupting *orf16* abolished clavulanic acid production and led to the accumulation of two novel intermediates that are proposed to lie between clavaminic acid and clavaldehyde, N-glycyl-clavaminic acid and N-acetyl-glycyl-clavaminic acid (Jensen *et al*., 2004a). Disrupting *orf17* also blocked clavulanic acid production, again indicating its essential role in the biosynthetic pathway (Jensen *et al*., 2004a). Recently, a new step in the process to produce clavulanic acid from clavaminic acid was proposed. Arulanantham *et al*. (2006) showed that ORF17 is an N-glycyl-clavaminic acid synthetase (GCAS), which belongs to the ATP-grasp fold superfamily and catalyzes a carboxylate-amine ligation reaction using ATP and glycine in the presence of Mg^{2+} and K^{+}. *In vitro* analysis confirmed that clavaminic acid was converted by ORF17 to *N*-glycylclavaminic acid, which is another novel intermediate that lies between clavaminic acid and clavaldehyde (Arulanantham *et al*., 2006; Figure 1.6). Based on these results, an acetyltransferase encoded by *orf14* mentioned above, was proposed to catalyze acetylation of *N*-glycylclavaminic acid, leading to N-acetyl-glycyl-clavaminic acid, which is another proposed intermediate in the "late" part of the pathway.

orf 18 and *orf19* encode proteins with high similarity to penicillin-binding proteins (PBPs) in *S. coelicolor* and *S. avermitilis*, respectively. While mutations in *orf19*, and in *orf20*, which encodes a putative cytochrome P-450, showed no effect on clavulanic acid production, the effect of disrupting *orf18* could not be assessed as no *orf18* mutants could be isolated, suggesting *orf18* may be an essential gene. Recently three more ORFs named *orf21*, *orf22* and *orf23*, which encode a putative sigma factor, a sensor kinase and a response regulator, respectively, were identified downstream of *orf 20* (Song *et al*., 2009). Although the effects were subtle, cephamycin C production was reduced in *orf21* mutants while both cephamycin C and clavulanic acid production were reduced in *orf22* mutants. A more prominent effect was observed in an *orf23* mutant, where both morphological differentiation and antibiotic production were retarded (Song *et al*., 2009).

Interestingly, the gene that encodes an enzyme to carry out the stereochemical inversion of the 3*S*, 5*S* stereochemistry in clavaminic acid to the 3*R*, 5*R* stereochemistry, believed to confer its β-lactamase inhibitory activity, in clavulanic acid, has not been identified as yet.

1.3.4 "Late" genes in 5*S* clavam production

Initial sequencing around the *cas1* gene in the clavam gene cluster revealed seven open reading frames termed *cvm1* to *cvm7* (Figure 1.4), of which some are involved in the "late" steps for 5*S* clavam biosynthesis, as determined by mutational studies (Mosher *et al*., 1999). Predicted amino acid sequence of *cvm1*

showed similarity to aldo-keto reductases. Mutation of *cvm1* blocked 5*S* clavam production but clavulanic acid production was unaffected in *S. clavuligerus* (Mosher *et al*., 1999). A similar phenotype was observed in a *cvm4*/*cvm5* double mutant (Mosher *et al*., 1999). Since mutations in *cvm4* have no apparent effect on clavam biosynthesis, this indicated the essential role of *cvm*5 in 5*S* clavam production. *cvm*5 was predicted to encode a mono-oxygenase and mutants with defects in *cvm5* accumulated a novel intermediate called 2-carboxymethylideneclavam (Tahlan *et al*., 2007). Based on limited data, a series of "late" steps were proposed for 5*S* clavam biosynthesis in which Cvm5 is believed to carry out a Baeyer-Villiger oxidation to convert 2-carboxymethylideneclavam to 2-formyloxymethylclavam (Tahlan *et al*., 2007; Zelyas, 2007; Figure 1.6). *cvm3* encodes a putative flavin reductase, which is believed to supply the reduced flavin that is required for the Cvm5 mono-oxygenase to function (Tahlan *et al*., 2007; Mosher *et al*., 1999). However, mutants in *cvm*3 produced normal level of 5*S* clavams, thus suggesting Cvm3 can be functionally substituted by other flavin reductases encoded by *S. clavuligerus* (Tahlan *et al*., 2007).

The predicted amino acid sequence of the protein encoded by *cvm2* showed similarity to isomerases (Mosher *et al*., 1999). Although its function is uncertain, 5*S* clavam production was severely depressed in *cvm2* mutants (Tahlan *et al*., 2007). Conversely, mutations in *cvm6* and *cvm7* showed no effect on clavam biosynthesis, despite the fact that *cvm7* encodes a putative protein that belongs to the *Streptomyces* antibiotic regulatory proteins (SARPs) (Tahlan *et al*.,

2007). A number of genes, named *cvm9, cvm10, cvm11, cvm12, cvm13, cvmH*, *cvmP*, and *cvmG*, were also identified in the clavam gene cluster (Tahlan *et al*., 2007; Figure 1.4). Disruption of these genes, except *cvmH*, showed that they are not involved in clavam production (Tahlan *et al*., 2007). Since mutants in *cvmH* could not be isolated, its role in clavam biosynthesis is not known.

Since the initial discovery of the paralogue gene cluster, it has been expanded considerably with the identification of additional open reading frames that flank the paralogous copies of the early genes (Figure 1.5). *orfA-L* are located upstream of *ceaS1* (Cai, 2003). Mutants of *orfA*, *orfB*, *orfC* or *orfD* are incapable of producing alanylclavam while production of other clavams is unaffected. This indicated that they are specifically involved in alanylclavam production. Disruption of the remaining ORFs (E through L) had no apparent effect on clavam biosynthesis (Zelyas *et al*., 2008). *orfA* is predicted to encode a protein similar to glycine/serine hydroxymethyltransferase while *orfB* encodes a YjgF/YER057c/UK114 family protein (Cai, 2003). *orfC* and *orfD* are predicted to encode aminotransferase and threonine dehydratase type enzymes, respectively, and mutations in these two genes abolished alanylclavam production and led to accumulation of a novel clavam metabolite, 8-hydroxyalanylclavam (Zelyas *et al*., 2008). Based on the predicted function of these proteins, a mechanism for alanylclavam biosynthesis was proposed, although this has not been proved experimentally (Zelyas *et al*., 2008; Figure 1.7). On the other side of the paralogue gene cluster, *c6p*, *c7p*, *snk*, *res1* and *res2* reside upstream of *oat1* (Figure 1.5). Mutants of *c6p* and *c7p*, which are paralogues of *cvm6* and *cvm7*

Figure 1.7. Proposed steps involved in alanylclavam biosynthesis. Hypothetical steps are showed in grey. (adapted from Zelyas *et al*. 2008).

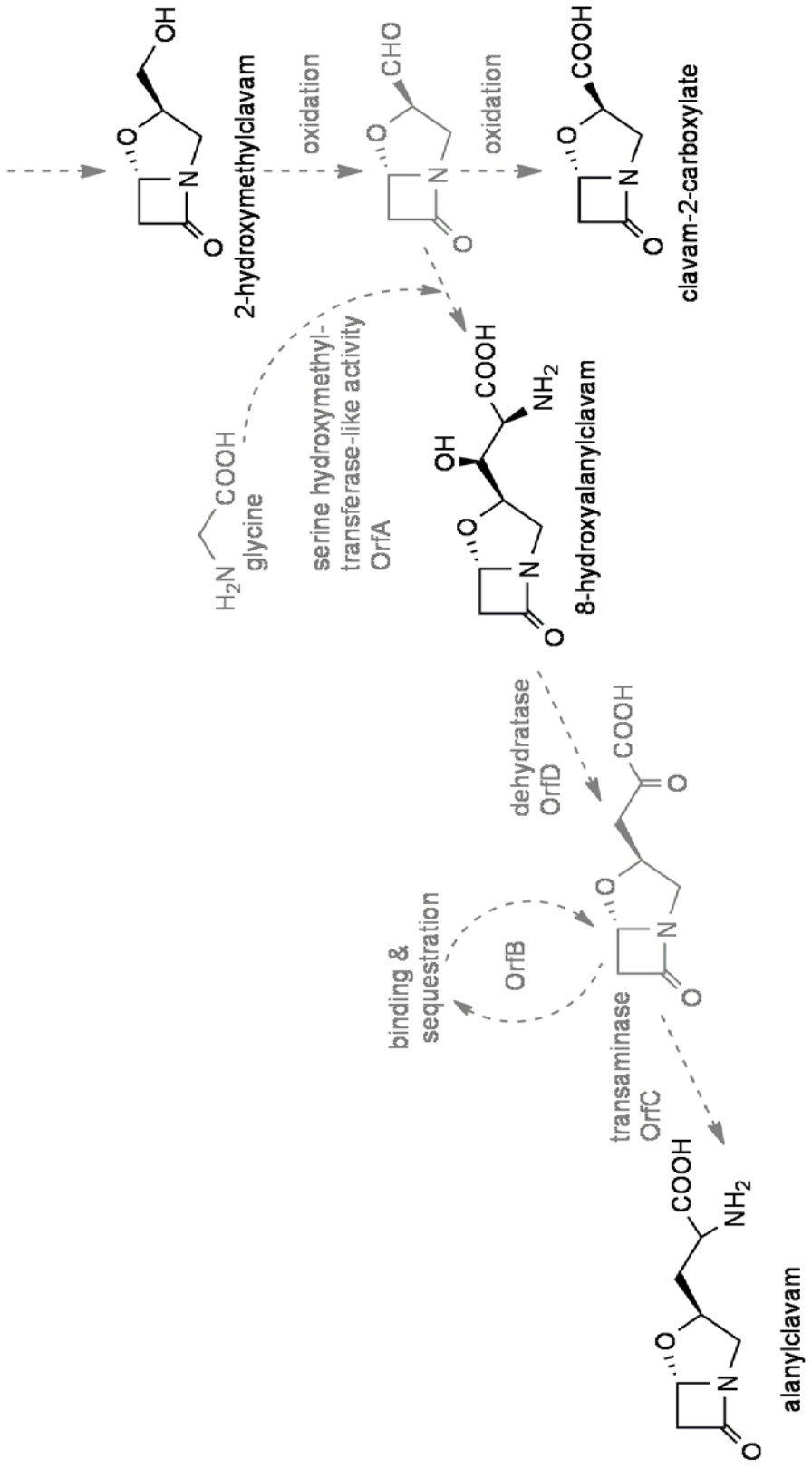
2-hydroxymethylclavam
oxidation
oxidation
clavam-2-carboxylate
glycine
serine hydroxymethyl-transferase-like activity
OrfA
8-hydroxyalanylclavam
dehydratase
OrfD
binding & sequestration
OrfB
transaminase
OrfC
alanylclavam

from the clavam gene cluster, were blocked in 5*S* clavam production while clavulanic acid production was unaffected (Tahlan, 2007). Since *c7p*, like *cvm7*, belongs to a class of antibiotic regulatory proteins that has an N-terminal SARP-like domain and a C-terminal ATPase domain, it was proposed to act as a pathway-specific transcriptional activator for 5*S* clavam production in *S. clavuligerus* (Tahlan, 2007). s*nk* encodes a product with similarity to sensor kinases from two-component systems in *S. avermitilis* and *S. coelicolor* (Tahlan, 2005). A mutant disrupted in *snk* was incapable of producing 5*S* clavams but clavulanic acid production was unaffected (Tahlan, 2005). Sequence analysis suggested that Snk is a soluble sensor kinase with two tandem GAF (cGMP-specific and -stimulated phosphodiesterases, adenylate cyclases and FhlA) domains, which may be involved in substrate binding, located at its N-terminus (Tahlan, 2005). *res1* and *res2* both encode response regulators and mutation in *res1* caused overproduction of 2-hydroxymethylclavam and alanylclavam. On the other hand, mutants in *res2* were unable to produce 5*S* clavams (Zelyas, 2007). Sequence analysis of Res2 suggested the presence of an N-terminal phosphorylation pocket and a C-terminal DNA-binding domain, which are characteristics of response regulators from different bacteria. In contrast, Res1 retained the phosphorylation pocket but lacked the DNA-binding domain (Zelyas, 2007). The reason for employing two response regulators is not clear at this point. Nonetheless, both C7P and the atypical two-component system were shown to be involved specifically in 5*S* clavam production. With the identification of various

enzymatic and regulatory genes, attention also turned to how the clavam biosynthetic pathway is being regulated.

1.4 Regulation of antibiotic production

In streptomycetes, secondary metabolite production is linked to growth phase and usually starts when entering stationary phase. Furthermore, it is often coordinated with morphological differentiation (Demain, 2000) and is subject to different levels of regulation, which are organized in a hierarchical manner (Chater and Bibb, 1997). Pathway-specific regulators that control the production of one or a small number of closely related secondary metabolites define the bottom of this hierarchy. The genes that encode these pathway-specific regulators are often located within or close to the antibiotic gene clusters that they regulate (Chater and Bibb, 1997). The next level is the global regulators that control both morphological development and secondary metabolite production. In *S. clavuligerus*, mechanisms that are involved in either level of regulation are not completely understood. On top of this regulatory hierarchy are different kinds of signalling molecules, such as γ-butyrolactones, which serve to monitor both the environment and physiology of the cells, so that appropriate responses can be exerted.

1.4.1 SARPS

The *Streptomyces* Antibiotic Regulatory Proteins (SARPs) are pathway-specific regulators that control the biosynthesis of various antibiotics. The N-terminal end of SARPs resemble a DNA binding domain similar to the “winged

helix-turn-helix" DNA binding domain found in transcriptional regulators that belong to the OmpR family (Wietzorrek and Bibb, 1997). Since members of the OmpR family regulate transcription by binding to direct DNA repeats located in the promoter region, it was proposed that SARPs also control gene expression by binding to direct heptameric repeats located in the promoter region of the genes they regulate (Martinez-Hackert and Stock, 1997; Wietzorrek and Bibb, 1997). The ActII-ORF4 protein is a well characterized SARP that positively regulates the biosynthesis of actinorhodin (Act), an antibiotic produced by *S. coelicolor* (Fernandez-Moreno *et al*., 1991). Fernandez-Moreno *et al*. (1991) observed that Act was over-produced when extra copies of *act*II-ORF4 were introduced into *S. coelicolor* while Act production was abolished in an *act*II-ORF4 mutant. Electrophoretic Mobility Shift Assays (EMSA) and DNase I footprinting also showed that ActII-ORF4 was capable of binding specifically to imperfect repeated sequences found in the -35 region of the promoters of Act biosynthetic genes including *act*III, *act*VI-ORF1 and *act*VI-ORFA (Arias *et al*., 1999). CdaR, encoded by *cdaR* is also a SARP homologue that was shown to activate calcium-dependent-antibiotic (CDA) production in *S. coelicolor* (Ryding *et al*., 2002). Similarly, StrR, a SARP homologue encoded by *strR* in *S. griseus*, activated streptomycin production specifically (Retzlaff and Distler, 1995). This confirmed the role of SARPs in general as pathway-specific positive transcriptional regulators on antibiotic production in *Streptomyces* species.

The *ccaR* (Cephamycin and Clavulanic Acid Regulator) gene from the cephamycin C gene cluster of *S. clavuligerus* encodes a SARP called CcaR. It

regulates both the biosynthesis of cephamycin C and clavulanic acid as shown by Perez-Llarena *et al*. (1997a) who found that a *S. clavuligerus ccaR* mutant was incapable of producing any cephamycin C or clavulanic acid (Alexander and Jensen 1998; Perez-Llarena *et al*., 1997a). Perez-Llarena *et al*. (1997a) also observed that cephamycin C and clavulanic acid were over-produced when extra copies of *ccaR* on a plasmid were introduced into *S. clavuligerus*. Western analysis of the cell free extracts (CFEs) from a *S. clavuligerus ccaR* mutant showed that lysine 6-aminotransferase (LAT), isopenicillin N synthase (IPNS) and desacetoxycephalosporin C synthase (DAOCS), which are key enzymes involved in cephamycin C production, and CcaR were not produced (Alexander and Jensen, 1998). As a result, it was proposed that CcaR is an autoregulator that controls its own expression as well as controlling the transcription of the cephamycin C biosynthetic genes. Since *cefE*, encoding DAOCS, is transcribed as a polycistronic transcript with *cefD*, CcaR may regulate the upstream *cefD* promoter (Figure 1.3). This was proved as EMSA showed that CcaR can bind to the divergent *cefD-cmcI* and *ccaR* promoters (Santamarta *et al*., 2002). On the other hand, it is still unclear if CcaR directly regulates the *lat* promoter, which is responsible for for the expression of *lat* (encoding LAT), because contradictory results were reported from two different research groups. Kyung *et al*., (2001) showed that His-tagged CcaR from recombinant *E. coli* could bind to the -35 region of the *lat* promoter, by carrying out EMSA and DNase I footprinting analysis. However, Santamarata *et al*. (2002) showed that purified CcaR protein from *S. clavuligerus* was unable to bind to the *lat* promoter. Despite the unclear

role of CcaR in regulating the *lat* promoter, it is obvious that CcaR positively regulates cephamycin C biosynthesis by directly binding to at least some biosynthetic genes and controlling their transcription.

1.4.2 Other pathway specific transcriptional regulators

CcaR also controls clavulanic acid biosynthesis by direct binding to control the expression of another pathway-specific transcriptional regulator called ClaR (Clavulanic Acid Regulator), encoded by *claR* (Paradkar *et al*., 1998; Figure 1.3). Transcriptional analysis showed that *claR* was not transcribed in a *S. clavuligerus ccaR* mutant (Perez-Redondo *et al*., 1998). ClaR belongs to the LysR family and contains two helix-turn-helix DNA binding domains at both the amino and carboxyl termini. A *S. clavuligerus claR* mutant was incapable of producing clavulanic acid while it retained the ability to produce cephamycin C and 5*S* clavams. Also, clavulanic acid production was increased by three-fold when multicopy plasmids carrying *claR* were introduced into *S. clavuligerus* (Perez-Redondo *et al*., 1998). This suggested that ClaR regulates the "late" steps responsible for clavulanic acid biosynthesis. This hypothesis was supported by the fact that expression of *oppA1*, *cad* and *cyp*, which are genes involved in converting clavaminic acid to clavulanic acid (Arulanantham *et al*., 2006; Jensen *et al*., 2004), was significantly reduced in the *S. clavuligerus claR* mutant (Perez-Redondo *et al*., 1998).

It is interesting that CcaR co-regulates both the biosynthesis of cephamycin C (β-lactam antibiotic) and clavulanic acid (β-lactamase inhibitor). It

was proposed that this type of regulation may actually reflect an evolutionary event that allows *S. clavuligerus* to adapt to the highly competitive environment in the soil (Ward and Hodgson, 1993).

1.4.3 Bald (*bld*) genes

Regulation mediated by pleiotropic regulators, which regulate both the morphological differentiation and secondary metabolite production, comes next in the hierarchy. The best characterized pleiotropic regulator gene is the *bldA* gene from *S. coelicolor*. A *S. coelicolor bldA* mutant was unable to form aerial mycelia or antibiotics (Merrick, 1976). *bld*A regulates both aerial mycelium formation and antibiotic production by encoding the only leucyl tRNA capable of translating the rare TTA codons. TTA codons are mainly found in genes that are involved in aerial mycelium formation and antibiotic production, including *ccaR* (Chater and Chandra, 2008; Leskiw *et al*., 1991; Trepanier *et al*., 2002). Although disrupting *bldA* in *S. clavuligerus* blocked aerial mycelium formation, surprisingly, it had no effect on β-lactam production (Trepanier *et al*., 2002). Trepanier *et al*. (2002) proposed that the TTA codon context has an important effect on regulation as all *bldA* dependent targets that resulted in a null phenotype were shown to contain TTA codons in the context of TTAC or TTAT. It was further proposed that *ccaR*, which carries a TTA codon in TTAG context, is not under *bldA* regulation and instead CcaR is mistranslated giving rise to functional protein in *bldA* mutants (Trepanier *et al*., 2002).

A *S. clavuligerus bldG* mutant was also unable to produce β-lactams and aerial mycelia (Bignell *et al*., 2005). Since BldG shows similarity to anti-anti-sigma factor proteins found in various *Bacillus* spp., *bldG* in *S. clavuligerus* is thought to encode an anti-anti-sigma factor that interacts with an anti-sigma factor that in turn regulates various sigma factors that control morphological development and secondary metabolite biosynthesis. The function of BldG was shown to be activated by phosphorylation (Bignell *et al*., 2003). In addition, *ccaR* transcription was blocked in a *S. clavuligerus bldG* mutant (Bignell *et al*., 2005). Therefore, it is apparent that BldG regulates β-lactam biosynthesis through CcaR. However, it is still unclear how BldG controls transcription of *ccaR*, whether directly or indirectly.

1.4.4 γ-butyrolactone regulators

Many *Streptomyces* species were shown to produce γ-butyrolactones, which are diffusible low molecular weight signalling compounds (Kholkov *et al*., 1967). γ-butyrolactones control gene expression by binding to their cognate receptor proteins, which in the absence of the γ-butyrolactones act as DNA-binding repressors that bind to conserved palindromic inverted repeats called autoregulatory elements (AREs) (Kinoshita *et al*., 1999). Once a γ-butyrolactone binds to the receptor protein, the complex is released from the DNA. Thus, gene expression occurs. γ-butyrolactones serve as *Streptomyces* hormones to regulate morphological differentiation and antibiotic production (Horinouchi and Beppu, 1992). A γ-butyrolactone receptor protein called ScaR (*S. clavuligerus* autoregulator receptor), which is encoded by *scaR*, was found in *S. clavuligerus*

(Kim *et al*., 2004). Sequence analysis of the upstream region of *ccaR* and *scaR* revealed the presence of ARE sequences. EMSAs showed that ScaR was capable of binding specifically to these two ARE sequences. This suggested ScaR autoregulates its own expression as well as controlling *ccaR* expression. Moreover, in a *scaR* mutant, the production of both clavulanic acid and cephamycin C increased significantly compared to the wild type. This indicated that ScaR is a repressor and exerts it effect by binding to the ARE sequence and preventing gene transcription (Santamarta *et al*., 2005). The same study also found a novel protein that is capable of binding to ARE sequences as shown by EMSA. Recently, this protein was isolated from *S. clavuligerus* and named AreB (Santamarta *et al*., 2007). AreB, which is encoded by *areB*, was identified as a regulatory protein of the IclR family. It was shown to autoregulate its own expression and is also involved in leucine biosynthesis and fatty acid catabolism. *areB* mutants show elevated cephamycin C and clavulanic acid production and more interestingly, binding of AreB to the ARE of *ccaR* requires an unknown small molecule other than γ-butyrolactone (Santamarta *et al*., 2007). As a result, AreB controls primary metabolism and when induced by some as yet unidentified signals, regulates secondary metabolite production, simultaneously.

1.4.5 The stringent response

The "stringent response" is another system that was shown to be involved in controlling morphological differentiation and secondary metabolite production in *Streptomyces* species. Under amino acid starvation conditions, cellular levels of highly phosphorylated guanine nucleotide (p)ppGpp increase. Accumulation of

(p)ppGpp was shown to initiate morphological differentiation and antibiotic production in *Streptomyces* sp. MA406-A-1 (Ochi, 1986). Similarly, when *relA*, which encodes the ppGpp synthetase in *S. coelicolor*, was knocked out, the mutant was delayed in morphological differentiation and incapable of producing actinorhodin and undecylprodigiosin (Chakraburtty and Bibb, 1997). It was further demonstrated that (p)ppGpp induced transcription of *actII*-ORF4 (Hesketh *et al*., 2007). Two homologues of *relA* (*relA* and *rhs*) were isolated from *S. clavuligerus* and mutants of *relA* were unable to synthesize (p)ppGpp (Jin *et al*., 2004). Although mutations in *relA* impaired aerial mycelium formation and sporulation, contradicting results were obtained in regard to antibiotic production, where Jin *et al.* (2004) showed *relA* mutants were unable to produce either cephamycin C or clavulanic acid but Gomez-Escribano *et al*. (2008) showed overproduction of these compounds. As a result, it is still unclear at this point about the role of "stringent response" in *S. clavuligerus* antibiotic production.

1.4.6 Two-component regulatory systems

Two-component regulatory systems (TCSs) have been identified in a wide range of organisms. In its simplest form, the system involves one sensor kinase and one response regulator. Sensor kinases sense and respond to stimuli by undergoing autophosphorylation at a conserved histidine residue. The phosphate is then transferred to a conserved aspartate residue of the response regulator, which can then activate transcription of target genes. The complete genome sequence of *S. coelicolor* revealed a large number of TCSs, as 84 genes encoding sensor kinases and 79 genes encoding response regulators were identified. Most

of the sensor kinase genes are located beside a response regulator gene, presumably forming a cognate pair (Bentley *et al*., 2002; Hutchings *et al*., 2004). Although the majority of these systems have not been studied and the stimuli recognized by these systems remain largely unknown (Hutchings *et al*., 2004), this still reflected the complexity of the regulatory networks in *S. coelicolor* and presumably in other *Streptomyces* spp., which are essential for survival in the drastically changeable soil environment.

Among the TCSs that are present in *S. coelicolor*, the AbsA1/A2 system is the most studied. The *absA* locus, which encodes the sensor kinase AbsA1 and the response regulator AbsA2, is located within the CDA biosynthetic cluster and was shown to be pleotropic in that it controls not only the biosynthesis of CDA, but also actinorhodin, undecylprodigiosin and methylenomycin, the four well-studied antibiotics produced by *S. coelicolor* (Adamidis *et al*., 1990; Brain *et al*., 1996). Transcript analysis showed that disrupting *absA2* led to higher transcript levels of *act*II-ORF4 and *redD*, which encode the pathway-specific activators in undecylprodigiosin biosynthesis (Aceti and Champness, 1998). Recent work further indicated that AbsA2 binds specifically to the promoter regions of *act*II-ORF4, *cdaR* and *redZ* (a transcriptional activator of *redD*) and binding was enhanced when AbsA2 was phosphorylated (McKenzie and Nodwell 2007). Although the signal recognized by AbsA1 is not known, the AbsA two-component system negatively regulates antibiotic biosynthesis by repressing transcription of pathway-specific activators.

It is well known that the presence of inorganic phosphate in the environment represses secondary metabolite production in a wide range of bacteria. In *S. lividans* and *S. coelicolor*, this regulation is mediated through the PhoR/PhoP two-component system. Deletion mutants of *S. lividans* lacking either PhoP (the response regulator) or both PhoR (the sensor kinase) and PhoP, overproduced actinorhodin and undecylprodigiosin while production of PhoA, an extracellular alkaline phosphatase encoded by *phoA*, was depressed (Sola-Landa *et al*., 2003). This indicated that PhoP positively regulates PhoA production while it negatively controls antibiotic production. It was proposed that under phosphate starvation, PhoR undergoes autophosphorylation and then transfers its phosphate molecule to PhoP. Phosphorylated PhoP can then exert its regulation, and this was confirmed as phosphorylated PhoP induced expression of *phoA* (Martin, 2004). In the *E. coli* and *B. subtilis* PhoR/PhoP system, PhoP~P activates transcription of target genes by binding to consensus phosphate boxes (PHO boxes) located in the promoter regions (Martin, 2004). Recent work revealed that PhoP~P represses *afsS* transcription by binding to the PHO box located in its promoter region. AfsS, encoded by *afsS*, was shown to induce actinorhodin and undecylprodigiosin production (Floriano and Bibb, 1996; Martin and Liras, 2010; Santos-Beneit *et al*., 2009; Vogtli *et al*., 1994). Interestingly, although actinorhodin and undecylprodigiosin are under phosphate control in *S. coelicolor*, overproduction of these antibiotics was not observed in a deletion mutant in *phoP* (Santos-Beneit *et al*., 2009). This again reflected the idea that production of antibiotics is under the control of extensive inter-connected regulatory networks.

As mentioned before, the *snk*/*res1*/*res2* atypical two-component system is located in the paralogue gene cluster of *S. clavuligerus*, and was shown to affect 5*S* clavam biosynthesis (Zelyas, 2007; Figure 1.7). It is hypothesized that this TCS controls 5*S* clavam biosynthesis through controlling transcription of *c7p*, which encodes a putative pathway-specific transcriptional activator.

The regulatory systems described above form part of the complex regulatory network controlling antibiotic production, but many more regulators and systems may well be involved that have not yet been identified. With more information being collected, a complete picture of how various regulatory circuits, which govern morphological differentiation, secondary metabolite production and nutrient utilization, are inter-connected to ensure proper timing of gene expression will be revealed.

1.5 Thesis objective

Although two copies of *ceaS* genes, *ceaS1* and *ceaS2*, exist in *S. clavuligerus*, mutants in *ceaS2* are severely impaired, and in some cases unable, to produce clavulanic acid and 5*S* clavams (Tahlan *et al*., 2004a). This drastic effect from disrupting *ceaS2* suggested that cross regulation may exist between *ceaS2* and *ceaS1*. Therefore, one main objective of this thesis was to characterize the relationship between these two genes. In addition, the close proximity of the enzymatic genes and regulatory genes (*snk*/*res1*/*res2* two-component system and *c7p* that encodes a transcriptional regulator) in the paralogue gene cluster (Figure 1.5) and their apparent effect on 5*S* clavam production suggested that the

regulatory proteins they encode control expression of genes that are involved in the "late" steps of 5*S* clavam biosynthesis. Studies were carried out to identify the genes that are regulated by C7P and/or the two-component system. Identified genes were further examined to assess if they are directly controlled by these regulatory proteins. Finally, each component of the two-component system was further characterized and the phosphorelay mechanism between these proteins was analyzed.

Chapter 2

Materials and Methods

2. Materials and Methods

2.1 Materials

Restriction endonucleases were purchased from Roche (Laval, QC) or New England Biolabs Ltd. (NEB) (Mississauga, ON). Oligonucleotide primers used were synthesized by Integrated DNA Technologies, Inc. (IDT) (Coralville, IA).

Ampicillin (amp), kanamycin (kan), chloramphenicol (cam), penicillin G (PenG) and thiostrepton (tsr) were purchased from Sigma-Aldrich Ltd. (Oakville, ON). Apramycin (apr) was purchased from Provel Division Eli Lilly Canada Inc. (Scarborough, ON). Dimethylsulfoxide (DMSO), lysozyme, isopropyl-β-D-thiogalactopyranoside (IPTG) and 5-bromo-4-chloro-3-β-D-galactopyranoside (X-gal) were purchased from Sigma-Aldrich. [γ-^{32}P] ATP was purchased from PerkinElmer, Inc. (Waltham, MA).

Bacto™ agar, Bacto™ yeast extract, Bacto™ tryptone, soluble starch, ISP-4 medium, Trypticase Soy Broth (TSB) and malt extract were all purchased from Difco Laboratories (Detroit, MI). All other chemicals used in this study were of reagent grade.

PCR tubes (0.2 ml and 0.5 ml) and microcentrifuge tubes (1.5 ml) were purchased from Axygen Inc. (Union city, CA). Aerosol Resistant Tips (ART®10, 20, 100 and 1000) were purchased from Molecular BioProducts, San Diego, CA.

All electrophoresis equipment was purchased from Bio-Rad laboratories Ltd. (Mississauga, ON). Other materials and enzymes used in this study are described along with their use in corresponding sections.

2.2 Bacterial strains and plasmids

Escherichia coli and *Streptomyces clavuligerus* strains used in this study are listed in Table 2.1 and 2.2 respectively. Plasmid vectors used are listed in Table 2.3.

2.3 Centrifugation and culture harvesting

All large scale centrifugations were carried out at 4^{o}C with a Beckman Model J2-21 centrifuge. *E. coli* cultures were harvested at 5,000 rpm with a JA-20 rotor when culture volume was 2-50 ml; otherwise, a JA-14 rotor was used for large volumes. A Clinical centrifuge (International Equipment, Needham, MA) at speed setting 7 was used to harvest *S. clavuligerus* cultures in 15 ml screw cap polypropylene tubes (Corning Lifesciences, Lowell, MA). Microcentrifugations were typically carried out at 14,000 rpm at 21^{o}C with an Eppendorf 5415 C microcentrifuge (Brinkmann Instruments Inc., Mississauga, ON). Exceptions are stated in corresponding sections.

2.4 *E. coli* procedures

2.4.1 Culture media and growth conditions for *E. coli*

E. coli strains were grown in Lennox broth (LB) [1% (w/v) tryptone, 0.5% (w/v) yeast extract, and 0.5% (w/v) NaCl; in some cases, 0.1% (w/v) glucose was

Table 2.1. *E. coli* strains used in this study.

Strains	Description	Reference or source
BL21(DE3)	Carries the bacteriophage T7 RNA polymerase encoded on its chromosome, used for expression of proteins at high levels under the control of the T7 promoter	Stratagene
DH5α	General cloning host	Gibco BRL
ET12567/pUZ8002	Methylation-deficient host, expresses transfer functions from pUZ8002, used for inter-generic conjugation from *E. coli* to *Streptomyces*	Kieser *et a*l., 2000
One Shot® TOP10	Host for TOPO™ vectors, used for TA cloning of PCR products	Invitrogen

Table 2.2. *S. clavuligerus* strains used in this study.

Strain	Description	Reference or Source
NRRL 3585	Wild type strain capable of producing cephamycin C, clavulanic acid and 5*S* clavams	Northern Regional Research Laboratory, Peoria, Ill. USA
bls1::tsr	*bls1* insertional disruption mutant	Tahlan, 2004
bls1::tsr/*bls2*::apra	*bls1*/*bls2* double mutant	Tahlan, 2004
bls2::apra	*bls2* insertional disruption mutant	Jensen, 2000
ceaS2::apra	*ceaS2* insertional disruption mutant	Jensen *et al*., 2000
ceaS2-Fs	*ceaS2* frame shift mutant	Tahlan, 2004
Δ*c7p*::apra	Mutant strain with *c7p* replaced by a REDIRECT©-apra cassette	Tahlan, 2007
Δ*ceaS1*::apra	Mutant strain with *ceaS1* replaced by a REDIRECT©-apra cassette	Tahlan, 2004
Δ*ceaS1*::apra/*ceaS2*-Fs	*ceaS1*/*ceaS2* double mutant	Tahlan, 2004
Δ*ceaS2*-IF	*ceaS2* in frame deletion mutant	Tahlan, 2005

Table 2.2. (Continued)

Strain	Description	Reference or Source
Δ*ceaS2*::apra	Mutant strain with *ceaS2* replaced by a REDIRECT©-apra cassette	Tahlan, 2005
Δ*ceaS2*-C	*ceaS2* in frame deletion mutant carrying pSET152-5.3	Tahlan, 2005
Δ*ceaS2*-C2-9	*ceaS2* in frame deletion mutant carrying pSET152-2-9	Tahlan, 2005
Δ*ceaS2*-P	*ceaS2* in frame deletion mutant containing pSET152	Tahlan, 2005
Δ*res1*::apra	Mutant strain with *res1* replaced by a REDIRECT©-apra cassette	Zelyas, 2007
Δ*res2*::apra	Mutant strain with *res2* replaced by a REDIRECT©-apra cassette	Zelyas, 2007
Δ*snk* IF	*snk* in frame deletion mutant	Zelyas, 2007

Table.2.3. *E. coli* and *Streptomyces* plasmids used in this study.

Plasmid	Antibiotic Marker	Description	Reference or Source
***E. coli* plasmids**			
pCR®2.1-TOPO®	Ampicillin, Kanamycin	Phagemid for TA-cloning of PCR products	Invitrogen
pDA504	Ampicillin	*E. coli* cloning vector, pSL1180 derivative with a 1.1 kb *Bcl*I fragment carrying *tsr* inserted	Alexander, 1998
pUC119	Ampicillin	Phagemid cloning vector	Vieira & Messing, 1987
pUC119-*snk-c7p*	Ampicillin	pUC119 derivative with *c7p* and upstream region including 3' end of *snk* inserted	This study
pUC119-*c7p*-complete	Ampicillin	pUC119 derivative with *c7p* inserted	This study
pET-9c-*ceaS1*	Kanamycin	Protein expression vector, pET-9c derivative with *ceaS1* inserted	S. Jensen, University of Alberta
pET-24a-*ceaS2*	Kanamycin	Protein expression vector, pET-9c derivative with *ceaS2* inserted	C. Schofield, Oxford university
pET-19b	Ampicillin, Chloramphenicol	Protein expression vector conferring an N-terminal 10X His-tag	Novagen

Table.2.3. (Continued).

Plasmid	Antibiotic Marker	Description	Reference or Source
pET-19b-*c7p*	Ampicillin, Chloramphenicol	pET-19b derivative with *c7p* inserted as an *Nde*I/*Hind*III fragment	This study
pET-19b-*res1*	Ampicillin, Chloramphenicol	pET-19b derivative with *res1* inserted as an *Nde*I/*Bam*HI fragment	Zelyas, 2007
pET-19b-*res1*-SD	Ampicillin, Chloramphenicol	pET-19b derivative with mutated version of *res*1 inserted as an *Nde*I/*BamH*I fragment	This study
pMAL-C5X	Ampicillin	Protein expression vector, expresses maltose-binding protein fusion proteins	New England Biolabs
pMAL-*snk*	Ampicillin	pMAL-C5X derivative with *snk* inserted as a *Nde*I/*BamH*I fragment	This study
pMAL-*res1*	Ampicillin	pMAL-C5X derivative with *res1* inserted as a *Nde*I/*BamH*I fragment	This study
pMAL-*res2*	Ampicillin	pMAL-C5X derivative with *res2* inserted as a *Nde*I/*BamH*I fragment	This study
pT7-7His	Ampicillin	Protein expression vector, pT7-7 derivative conferring a C-terminal 7x His-tag	J. Manchak, University of Alberta

Table.2.3. (Continued).

Plasmid	Antibiotic Marker	Description	Reference or Source
pT7-7His-*res2*	Ampicillin	pT7-7His derivative with *res2* inserted as an *Nde*I/*BamH*I fragment from TOPO-*res2*	Zelyas, 2007
pT7-7His-*res2*-SD	Ampicillin	pT7-7His derivative with mutated version of *res*2 inserted as an *Nde*I/*BamH*I fragment from TOPO-*res*2-SD	This study
pT7-7His-*snk*	Ampicillin	pT7-7His derivative with *snk* inserted as an *Nde*I/*BamH*I fragment from TOPO-*snk*	Zelyas, 2007
pT7-7His-*snk*-SD	Ampicillin	pT7-7His derivative with mutated version of *snk* inserted as an *Nde*I/*BamH*I fragment from TOPO-*snk*-SD	This study
TOPO-*c7p*	Ampicillin, Kanamycin	pCR®2.1-TOPO® derivative with 585 bp 5' end of *c7p* inserted	S. Jensen, University of Alberta
TOPO-*res1*-SD	Ampicillin, Kanamycin	pCR®2.1-TOPO® derivative with mutated version of *res*1 inserted, amplified by two step site-directed mutagenesis	This study

Table.2.3. (Continued).

Plasmid	Antibiotic Marker	Description	Reference or Source
TOPO-*res2*-SD	Ampicillin, Kanamycin	pCR®2.1-TOPO® derivative with mutated version of *res2* inserted, amplified by two step site-directed mutagenesis	This study
TOPO-*snk*-SD	Ampicillin, Kanamycin	pCR®2.1-TOPO® derivative with mutated version of *snk* inserted, amplified by two step site-directed mutagenesis	This study
***E. coli-Streptomyces* shuttle plasmids**			
pSET152	Apramycin	*E. coli* cloning vector, conjugates and integrates into *att* site of *Streptomyces* chromosome	Northern Regional Research Laboratory, Peoria, III. USA
pSET152-5.3	Apramycin	pSET152 derivative with a 5.3kb *Bam*HI/*Xba*I fragment carrying *ceaS*2 and upstream region from pBB5.3AB inserted	Tahlan, 2005
pSET152-*orf*2-9	Apramycin	pSET152 derivative with a DNA fragment carrying *ceaS2* to *cad* inserted	Tahlan, 2005

Table.2.3. (Continued).

Plasmid	Antibiotic Marker	Description	Reference or Source
pSET152-*snk-c7p*	Apramycin	pSET152 derivative with *c7p* and upstream region inserted as a *Eco*RI/*HinD*III fragment	S. Jensen, University of Alberta
pIJ8660	Apramycin	Promoterless EGFP reporter plasmid	Sun *et al*., 1999
pSET-*ceaS1*	Apramycin	pSET152 derivative with the 2.37 kb *Bam*HI/*Eco*RI fragment encompassing the *ceaS1* promoter from pTO6-*ceaS1* cloned upstream of the *egfp* gene	Tahlan, 2004

added] at 37ºC on a Cell Production Roller Drum (Bellco Biotechnology, Vineland, NJ) or a G-24 Environmental incubator shaker (New Brunswick Scientific Co., Edison, NJ). Solid LB medium with 1.5% agar (LBA) was used to maintain plate cultures. Antibiotic-resistant strains of *E. coli* were grown in LB or LBA supplemented with ampicillin (100 µg/ml), kanamycin (50 µg/ml), apramycin (50 µg/ml), or chloramphenicol (25 µg/ml).

2.4.2 Storage of *E. coli* strains

All *E. coli* strains were maintained as frozen glycerol stocks. One milliliter amounts of *E. coli* cultures that were grown for 16 hours in LB were harvested by microcentrifugation. Supernatants were removed by aspiration and cell pellets were then resuspended in 500 µl of sterile 20% glycerol and stored at -80^{o}C.

2.4.3 Isolation of *E. coli* plasmid DNA

Plasmid DNA was primarily isolated from *E. coli* by using the alkaline lysis method as described by Sambrook *et al*. (1989). Occasionally, a QIAprep Spin Miniprep Kit was used to purify plasmid DNA by following the manufacturer's protocol (Qiagen, Mississauga, ON).

2.4.4 Electroporation of DNA into electrocompetent *E. coli*

All electrocompetent cells used in this study were prepared by previous graduate students and were stored at -80^{o}C (Zelyas, 2007). Prior to electroporation, competent cells (40 µl) were slowly thawed on ice, after which 0.5 to 5 µl of DNA were added. Electroporation was carried out by placing the

mixture in a 4°C 2 mm gap Disposable Electroporation Cuvette (Molecular BioProducts) and pulsed using the Bio-Rad GenePulser II device set to 200 Ω, 25 μF and 2.5 kV. Immediately after the pulsing, 955 μl of 4°C LB was added and the cell suspension was transferred to a 1.5 ml microcentrifuge tube and incubated at 37ºC for one hour for cell recovery. Aliquots of 100 μl and 900 μl (reduced to a smaller volume by removing most of the supernatant after microcentrifugation) were plated onto LB agar. If blue/white screening was used to detect insert containing clones, 100 mM of IPTG and 40 μg/ml of X-gal were added along with appropriate antibiotics to the agar plates.

2.5 *Streptomyces* procedures

2.5.1 Culture media and growth conditions for *S. clavuligerus*

S. clavuligerus strains were grown on MYM [0.4% (w/v) maltose, 0.4% (w/v) yeast extract, 1% (w/v) malt extract, and 1.8% (w/v) agar] (Stuttard, 1982) or ISP-4 plates at 28ºC. Antibiotic-resistant strains of *S. clavuligerus* were grown in media supplemented with apramycin (25 μg/ml), kanamycin (50 μg/ml), or thiostrepton (5 μg/ml).

2.5.2 Storage of *S. clavuligerus* strains

All *S. clavuligerus* strains used in this study were maintained as frozen spore stocks. Various strains were grown on ISP-4 medium for 7-14 days. Cell biomass on plates was then scraped and transferred into 1 ml of 20% sterile glycerol. Spore and mycelia mixtures were then placed into a Branasonic 42-sonication bath (Branson cleaning equipment Co., Shelton, CN) for 1 minute to

resuspend spores into the solution. Mixtures were then filtered through sterile non-absorbent cotton wool to remove mycelia and stored at -80^{o}C.

2.5.3 Introduction of DNA into *S. clavuligerus*

Plasmid DNA was introduced into *S. clavuligerus* by inter-generic conjugation following the procedure as described by Kieser *et al*. (2000). *E. coli* ET12567/pUZ8002 carrying the plasmid DNA to be transferred was grown for 16 hours in LB at 37ºC. One hundred microliters of the culture was used to inoculate 10 ml of LB. This larger culture was grown at 37ºC until it reached an OD_{600} of ~0.4 - 0.6. Cells were then harvested, washed twice with 10 ml of 1/2 strength LB to remove antibiotics added in the culture medium and resuspended in ~600 µl of residual LB. *S. clavuligerus* spores (100 µl) were harvested in a microcentrifuge and then resuspended in 500 µl of LB and heat-shocked at 50ºC for 10 minutes. After cooling to room temperature, heat-shocked spores were combined with 500 µl of the washed *E. coli* cell suspension. The mixture was microcentrifuged again and most of the supernatant was removed. The pellet of the spore and *E. coli* cell mixture was resuspended in the residual fluid and spread onto AS-1 medium plates [0.1% (w/v) yeast extract, 0.02% (w/v) L-alanine, 0.02% (w/v) L-arginine, 0.05% (w/v) L-asparagine, 0.5% (w/v) soluble starch, 0.25% (w/v) NaCl, 1% (w/v) Na_2SO_4, and 2% (w/v) agar (pH 7.5)] (Baltz, 1980) supplemented with 10 mM $MgCl_2$ and incubated at 28ºC for 16-20 hours. The plates were then overlaid with 1 ml of water containing appropriate antibiotics to select for the transferred plasmid and 0.5 mg of nalidixic acid (to obtain a final concentration of 20 µg/ml in the plate). After 7-10 days of growth at 28ºC, *S. clavuligerus* exconjugant

colonies that appeared were patched onto MYM plates (Stuttard, 1982) containing appropriate antibiotics for further growth.

2.5.4 Fermentation of *S. clavuligerus*

S. clavuligerus strains were grown in production media to determine clavulanic acid and 5*S* clavam production. Twenty microliters (~10^8 spores) of spore stocks were used to inoculate 25 ml of TSBS seed medium [3% (w/v) trypticase soy broth and 1% (w/v) soluble starch] and incubated at 28ºC and ~250 rpm in a Model G-25 rotary shaker (New Brunswick Scientific Co.). After 40 hours of growth, TSBS seed cultures (at 2% v/v) were used to inoculate 100 ml of complex Soy medium [15 g/l soy flour, 47 g/l soluble starch, 0.1 g/l KH_2PO_4, and 0.2 g/l $FeSO_4 \cdot 7H_2O$, pH6.8] (Salowe *et al*. 1990) or defined starch asparagine (SA) medium [10 g/l soluble starch, 2 g/l asparagine, 21 g/l MOPS, 0.6 g/l $MgSO_4.7H_2O$, 4.4 g/l K_2HPO_4 and 1 ml of trace element solution (0.13% $CaCl_2.3H_2O$, 0.1% $FeSO_4.7H_2O$, 0.1% $MnCl_2.4H_2O$ and 0.1% $ZnSO_4.7H_2O$), pH 6.8] (Salowe *et al*., 1990). Cultures were harvested after 48, 72 and 96 hours of growth by centrifugation and the culture supernatants obtained were used for antibiotic production analysis. Cells pellets were used for RNA isolation (section 2.5.5) or cell-free extract preparations as described in section 2.5.6.

2.5.5 RNA isolation

S. clavuligerus RNA used in this study was initially isolated by using the modified version of the Kirby *et al*. (1967) method as described by Kieser *et al*. (2000). RNeasy Protect Bacteria Midi kit (Qiagen) was later used for RNA

isolation as one of the chemicals used in the Kirby's mix was no longer available. Liquid cultures from section 2.5.4 were harvested by filtering through a Whatman #1 filter paper. For solid media, cultures were harvested by scraping mycelia that had grown on cellophane discs placed on the surface of agar plates. When using the modified Kirby method, cultures harvested were transferred into 4^{o}C universal bottles containing ~14 g of glass beads and 5 ml of double strength Kirby's mix [2% (w/v) sodium tri-isopropyl naphthalene sulphonate, 12% (w/v) sodium 4-amino salicylate and 12% (v/v) neutral phenol buffered in Tris-HCl (pH8.0)]. The bottles were vortexed vigorously for a total of 2 minutes, interchanging between 30 seconds on ice and 30 seconds of vortexing to keep the cultures' temperature at 4^{o}C. Five milliliters of phenol/chloroform/IAA was added and vortexed for another 1 minute as described above. Samples were then stored frozen at -20^{o}C until all samples were harvested and ready for downstream processing.

Culture slurries were transferred to 10 ml polypropylene tubes and centrifuged at 8,000 rpm for 5 minutes at 4^{o}C. The aqueous layer was transferred to a fresh 10 ml polypropylene tube containing 5 ml of phenol/chloroform/IAA. Samples were then vortexed for 30 seconds and centrifuged at 8,000 rpm for 5 minutes at 4^{o}C. Phenol/chloroform extraction was repeated until there was no visible material at the interface. Total nucleic acids were precipitated by adding 1/10 volume of 3M NaOAC and 1 volume of isopropanol and stored at -80^{o}C for 16 hours. Samples were centrifuged at 8,000 rpm for 10 minutes and pellets obtained were rinsed with 98% ethanol, air dried and dissolved in 450 µl of H_20.

Chromosomal DNA present in the samples was removed by adding 7.5 µl of RNase-free DNase I (Roche) and 1/10 volume of 10 x DNase buffer provided [400 mM Tris-HCl (Ph 7.9), 100 mM NaCl, 60 mM $MgCl_2$, 10 mM $CaCl_2$] and incubated at 21^{o}C for 30 minutes. The samples were then extracted with phenol/chloroform and precipitated with 3M NaOAC and isopropanol as described above, for 1 hour. Pellets were washed with 80% ethanol, air dried and redissolved in 450 µl of H_2O. The entire DNaseI digestion procedure was repeated to ensure chromosomal DNA was removed. Finally, the samples were extracted twice with phenol/chloroform/IAA, followed by one chloroform extraction and then precipitated with 3M NaOAC and isopropanol as described above. The pellets were rinsed with 100 µl of 80% ethanol, air dried and redissolved in 100 µl of H_2O.

When using the RNeasy protect Bacteria midi kit, 5 ml of cultures were first added to 10 ml of RNAprotect bacteria reagent to stabilize RNA inside the cells. RNA was then isolated by following the manufacturer's protocol (Qiagen). Before eluting RNA from the spin column, on-column DNase digestion was carried out by adding 160 µl of DNase I diluted in RDD buffer supplied (Qiagen) to the column and incubated at 21^{o}C for 15 minutes. Columns were then washed twice with RPE buffer provided and RNA was eluted with 150 µl of H_2O.

Before the RNA preparations were precipitated in isopropanol for storage at -80^{o}C, two samples were taken in order to determine the RNA quality and quantity.

2.5.6 Cell-free extract preparation

Cell-free extracts of various *S. clavuligerus* strains were prepared for Western analysis. Five milliliters of *S. clavuligerus* cultures that were grown in liquid Soy and SA media for 48 and 72 hours were harvested by centrifugation and resuspended in 1 ml of lysis buffer [50 mM Tris-HCl (pH 7.4), 2 mM EDTA, 0.1% Triton X-100, 0.15 mg/ml lysozyme]. Cell suspensions were incubated at 37^{o}C for 20 minutes and then sonicated 5 times for 15 seconds each time on a setting of 15% with a 1/8" (3.175 mm) diameter microtip connected to the Model 500 Dismembrator (Fisher Scientific, Ottawa, ON). Cell debris was separated from the soluble protein fraction by microcentrifugation for 10 minutes at 4^{o}C. Resulting supernatants were then aliquoted into 100 µl fractions and stored at -80^{o}C for future analysis.

2.6 Determination of antibiotic production

2.6.1 Clavulanic acid bioassay

A disc diffusion assay using *Klebsiella pneumoniae* ATCC 15380 as the indicator organism was used to detect the presence of clavulanic acid in culture supernatants from various *S. clavuligerus* strains (Mosher *et al*. 1999). For each assay, two bioassay plates containing 150 ml TSB agar were inoculated with 250 µl of glycerol stock of the indicator organism. One of the two plates also contained 6 µg/ml of penicillin G. Paper discs were placed onto the TSB agar surface and 20 µl of *S. clavuligerus* culture supernatants were dispensed onto the discs. Plates were then incubated for 16 hours at 37ºC and the diameter of the

inhibition zones produced was measured and compared between the two plates. Inhibition zones formed on plates with penicillin G were attributed to the presence of clavulanic acid while the inhibition zones of the same sample formed on the plate without penicillin G were due to factors other than clavulanic acid.

2.6.2 High performance liquid chromatography

High performance liquid chromatography (HPLC) was used to determine and quantify the amounts of clavulanic acid and 5*S* clavams present in *S. clavuligerus* culture filtrates (Foulstone and Reading, 1982; Paradkar and Jensen, 1995). Culture supernatants were microcentrifuged for 5 minutes to remove mycelia and insoluble material. For each culture supernatant, two 20 µl aliquots were taken and transferred to fresh microcentrifuge tubes and diluted with 80 µl of milliQ water. One of the two aliquots was imidazole-derivatized by adding 25 µl of 25% (w/v) imidazole (pH 6.8). For the other set, 25 µl of MilliQ water was added. These underivatized samples served as a control to subtract background absorbance that was not related to clavam compounds. Samples were then incubated at 21^{o}C for 15 minutes and microcentrifuged for 5 minutes to sediment any insoluble material. For each sample, 100 µl was transferred to polypropylene spring inserts (Fisher Scientific) which were then placed into HPLC screw neck vials.

Fifty microliters of each sample was injected into a Phenomenex® Bondclone 10µ C18 (100 x 800 mm 10 micron) column (Phenomenex, Torrance, CA) by using an automated Waters 2690 Separations Module. Absorbance

spectrum was determined with a Waters 996 Photodiode Array Detector (Waters, Milford, MA). Samples were analyzed by isocratic elution at a flow rate of 2 ml/minute. The mobile phase was composed of 100 mM NaH_2PO_4 (pH 3.68, adjusted with glacial acetic acid) + 6% (v/v) methanol. Each run was 15 minutes in length and derivatized clavam compounds were detected by measuring the absorbance at 311 nm. Data obtained were processed and analyzed with the Waters Millenium^{32} Software (version 3.20; Waters, Milford, MA).

2.7 DNA methods

2.7.1 DNA quantification

Purified DNA was quantified by using the NanoDrop® ND-1000 Spectrophotometer (NanoDrop Technologies, Inc., Wilmington, DE.). In addition to concentration, A_{260}:A_{280} ratio of each sample was also provided by the machine and was used to assess the purity of DNA samples. Oligonucleotide primers were quantified by measuring A_{260} with the UNICAM UV/Vis Spectrophotometer UV3 (ATI Unicam, Cambridge, UK).

2.7.2 Digestion and ligation reactions

Restriction digests were carried out according to manufacturer's recommendations (NEB and Roche). For standard subcloning, DNA was digested with appropriate restriction enzymes for 2 hours. To prevent self-annealing, vector DNA digested with a single restriction enzyme was 5' end dephosphorylated after restriction digestion. Two units of shrimp alkaline phosphatase (SAP) (NEB) was added to the reaction and incubated at 37^{o}C for 15

minutes. SAP was then inactivated by heating at 65°C for 15 minutes. Restriction enzymes were then inactivated by phenol/chloroform extraction and DNA was recovered either by ethanol precipitation or purified from agarose gels after fractionation by electrophoresis (Section 2.3.5). Ligation reactions were set up according to manufacturer's suggestions. In general, reactions were 10 to 30 µl in volume with up to 1 µg of digested DNA, and 20 U of T4 ligase prepared in the ligation buffer provided (NEB). The entire mixture was incubated at 16°C for 16 hours before electroporating (section 2.4.4) into appropriate host strains. Typically, an insert to vector molar ratio of 3:1 was used when vector DNA and insert DNA were similar in length, otherwise, a molar ratio of 1:1 was used.

PCR products were cloned using pCR®2.1-TOPO® kits according to the manufacturer's instructions (Invitrogen Inc., Burlington, ON). Briefly, 4 µl of PCR product was mixed with 1 µl of the salt solution provided and 1µl of pCR®2.1-TOPO® vector. The mixture was incubated at 21°C for 5 minutes. Two microliters of the cloning reaction mixture was then mixed into a vial of thawed One Shot® TOP10 *E. coli* chemically competent cells and incubated on ice for 5 minutes. Cells were heat-shocked for 30 seconds at 42°C followed by addition of 250 µl of SOC medium. Cells were then recovered and plated as described in section 2.4.4.

2.7.3 Polymerase chain reaction

DNA fragments used for cloning and used as DNA probes for electrophoretic mobility shift assays (EMSA) were produced by polymerase chain

reaction (PCR). PCRs were carried out using the Expand high fidelity PCR system when the accuracy of the PCR product amplified was important. Reactions were set up based on manufacturer's recommendation (Roche). Each reaction was 50 µl in volume and contained 100-500 ng of plasmid DNA as template, 200 µM of each dNTP, 5-15 pmol of each primer, 5% DMSO, 2.6 U of enzyme and 1/10 volume of 10 x buffer with 1.5 mM $MgCl_2$ supplied. In cases where fidelity of the enzyme was less of a concern, 2.5 U of Taq DNA polymerase (supplied by the Fermentation Service Unit, Department of Biological Sciences, University of Alberta) and 1 x Taq buffer [50 mM Tris (pH9.0), 1.5 mM $MgCl_2$, 0.4 mM β-mercaptoethanol, 0.1 mg/ml BSA, 10 mM NH_2SO_4 and 0.2 mM of each dNTP] were used. Reactions were carried out in thin-walled 0.2 ml PCR tubes in a TGradient thermocycler (Biometra, Goettingen, Germany), equipped with a heated lid. The following cycling conditions were used: an initial denaturation step for 2 minute at 96ºC, followed by 25-30 cycles of 96ºC for 30-60 seconds, 55-65ºC for 30 seconds, and 72ºC for 45 seconds-120 seconds. A final elongation step was carried out at 72ºC for 5 minutes. All oligonucleotides primers used in this study are listed in Table 2.4.

2.7.4 Agarose gel electrophoresis

DNA fragments were subjected to electrophoresis on 0.8, 1 or 1.5 % (w/v) agarose gels in 1 x TAE buffer system [40 mM Tris-Acetate and 1 mM EDTA (pH 8.0)]. All gels were stained in ~2.0 µg/ml ethidium bromide in distilled water for 15 minutes before they were exposed to UV light and photographed. DNA samples were combined with 5 x loading buffer [60% (w/v) sucrose, 100 mM

Table 2.4. Oligonucleotide primers used in this study.

Primer	Sequence (5'-3') [a]	Use
ANW 48	GGGGCAGGACCGGGTGGAAC	Forward primer to amplify promoter region of *c6p* for EMSA
ANW 49	GCCCGTGTCCCGTTCCTCCG	Reverse primer to amplify promoter region of *c6p* for EMSA
ANW 50	CGCCCAGACAGCCCAGGACGG	Forward primer to amplify intergenic region between *c7p* and *snk* for EMSA
ANW 51	CTGGGAAGTGCGTCGCGGAGAGTC	Reverse primer to amplify intergenic region between *c7p* and *snk* for EMSA
ANW 52	CCGTGGAGAACCCGCAGCGTC	Forward primer to amplify intergenic region between *c7p* and *snk* for EMSA
ANW 53	CCGCCCGCTCCTCGACGATCT	Reverse primer to amplify intergenic region between *c7p* and *snk* for EMSA
ANW 54	TCGGGCGGAGAGCGGGACATA	Forward primer to amplify intergenic region between *cas1* and *cvm1* for EMSA
ANW 55	TGGAAAGGGCGGCGGTGTTGG	Reverse primer to amplify intergenic region between *cas1* and *cvm1* for EMSA

Table 2.4. (Continued).

Primer	Sequence (5'-3') [a]	Use
ANW 56	TCCGCCGTTCTCCCCCGTTCC	Forward primer to amplify intergenic region between *cas1* and *cvm1* for EMSA
ANW 57	CGCGCAGCTCGGGGCCGTAC	Reverse primer to amplify intergenic region between *cas1* and *cvm1* for EMSA
ANW 58	CGACCGTTGGCAGATAGAAGAGAA	Forward primer to amplify intergenic region between *cvm5* and *cvm6* for EMSA
ANW 59	GTCGGGAGCGCGCGGAGATTG	Reverse primer to amplify intergenic region between *cvm5* and *cvm6* for EMSA
bls1 forward	TCCTGAACGGACGGTTCGC	Forward primer for *bls1* RT-PCR
bls1 reverse	AGGGCAGTTCCCTGACGAGTT	Reverse primer for *bls1* RT-PCR
CAN169	CGGCTGCTGGAACGCTATGACCT	Forward primer for *bls2* RT-PCR
CAN170	CCGCCGGAGAGCACCACCAA	Reverse primer for *bls2* RT-PCR
c7p RT-forward	GGTGATCATGCTGGAGGACATGGA	Forward primer for *c7p* RT-PCR
c7p RT-reverse	ATCACACGCCGTTCGCAACT	Reverse primer for *c7p* RT-PCR
ceaS1-RT-For	GCGCAGTCCGAGTCGTAC	Forward primer for *ceaS1* RT-PCR

Table 2.4. (Continued).

Primer	Sequence (5'-3') [a]	Use
ceaS1-RT-Rev	TTGGCGGTGTAGGTGGTGAC	Reverse primer for *ceaS1* RT-PCR
ceaS2-RT-For	AGGCCGCGTCGATTCTCTTC	Forward primer for *ceaS2* RT-PCR
ceaS2-RT-Rev	CGGCGGGTTGGGGACGGT	Reverse primer for *ceaS2* RT-PCR
cvm5 RT-forward	TTTCGAGGTCTCCAACAACCCGATCA	Forward primer for *cvm5* RT-PCR
cvm5 RT-reverse	TTGATGATCTCCCAGTGCTCCTCGAA	Reverse primer for *cvm5* RT-PCR
cvm6p RT-forward	ACCATCAGCAACGACAAGGCCATC	Forward primer for *c6p* RT-PCR
cvm6p RT-reverse	ACCTCGTCCAGGATCAGCAGGAT	Reverse primer for *c6p* RT-PCR
hrdB RT-forward	ATTCCGCCAACCCAGTGGAAGAATG	Forward primer for *hrdB* RT-PCR
hrdB RT-reverse	TCCTTCTTGGACGCGGTCTTCTTG	Reverse primer for *hrdB* RT-PCR
M13 Forward	GTAAAACGACGGCCAG	Universal forward primer for sequencing in pCR®2.1-TOPO® vector
M13 Reverse	CAGGAAACAGCTATGAC	Universal reverse primer for sequencing in pCR®2.1-TOPO® vector

Table 2.4. (Continued).

Primer	Sequence (5'-3') [a]	Use
orfA RT-forward	CGCAAGCCCAGCCTGAATCTTT	Forward primer for *orfA* RT-PCR
orfA RT-reverse	GTAAGAACTCGACCTCGTAGCCGAA	Reverse primer for *orfA* RT-PCR
res1 RT-forward	ATGGTGCGTTGCCTGATCGT	Forward primer for *res1* RT-PCR
res1 RT-reverse	ACAGCGACATCTTGGGCAGGAAA	Reverse primer for *res1* RT-PCR
res1-pfwd	CATATGGCGGCCGGGGAGGCGCACTG	Forward primer for cloning of *res1* used in two-step site-directed mutagenesis
res1-prev	GGATCCCCTTTCTGGAGGCCCAGTAGC	Reverse primer for cloning of *res1* used in two-step site-directed mutagenesis
res1 site-directed-For	GTGGCGCTGGTGG**C**CCTCGACCTCGG	Forward primer for cloning of *res1* used in two-step site-directed mutagenesis
res1 site-directed-Rev	CCGAGGTCGAGG**G**CCACCAGCGCCAC	Reverse primer for cloning of *res1* used in two-step site-directed mutagenesis
res2 RT-forward	AGGGCATCGGATACCTGCTGAA	Forward primer for *res2* RT-PCR
res2 RT-reverse	CCAGAAAGGTGATCACGGCGAGTA	Reverse primer for *res2* RT-PCR

Table 2.4. (Continued).

Primer	Sequence (5'-3') [a]	Use
res2-pfwd	CATATGAGGGTAGTACTGGCCGAGGAC	Forward primer for cloning of *res2* used in two-step site-directed mutagenesis
res2-prev	GGATCCCTGGGCCTCCAGAAAGGTGATC	Reverse primer for cloning of *res2* used in two-step site-directed mutagenesis
res2 site-directed-For	CTGGTGATCGTGG**C**CATCCGGATGCCG	Forward primer for cloning of *res2* used in two-step site-directed mutagenesis
res2 site-directed-Rev	CGGCATCCGGATGG**C**CACGATCACCAG	Reverse primer for cloning of *res2* used in two-step site-directed mutagenesis
snk RT-forward	GTGATGATGGCGATCTCGCTGAC	Forward primer for *snk* RT-PCR
snk RT-reverse	TACCTGGATACCGGCGGGAAA	Reverse primer for *snk* RT-PCR
snk seqFor2	AACACCCAGGCACGTGTGGA	Reverse primer for sequencing internal region of *snk*
snk seqRev2	GGTCTGGATGTCGAGCCGGA	Forward primer for sequencing internal region of *snk*
snk-pfwd	CATATGTCGTGCGAACAGATCGTC	Forward primer for cloning of *snk* used in two-step site-directed mutagenesis

Table 2.4. (Continued).

Primer	Sequence (5'-3') [a]	Use
snk-prev2	GGCCGGGATCCGTCGGTGTGCTC	Reverse primer for cloning of *snk* used in two-step site-directed mutagenesis
snk site-directed-For	GAACGCGACCTG**GC**CGACGGCCCCCAAC	Forward primer for cloning of s*nk* used in two-step site-directed mutagenesis
snk site-directed-Rev	GTTGGGGGCCGTCG**GC**CAGGTCGCGTTC	Reverse primer for cloning of *snk* used in two-step site-directed mutagenesis

[a] Engineered restriction sites are underlined and non homologous nucleotides incorporated into the primers used for site-directed mutagenesis are shown in bold letters.

EDTA, 0.25% (w/v) bromophenol blue, 0.25% (w/v) ficoll orange, and 0.25% (w/v) xylene cyanol] to aid in loading and to visualize migration of DNA in the gel. Lambda phage DNA digested with *Bst*II or *Pst*I was used as the molecular weight marker. When size of the DNA fragment was crucial, GeneRuler 100 bp or 1 kb DNA ladder were used (Ferrnentas, Burlington, ON).

2.7.5 DNA purification from agarose gels

DNA fragments generated by PCR or restriction digestions were separated on agarose gels. After electrophoresis, gels were stained with ethidium bromide and DNA bands were visualized by exposing to UV light. A small block of agarose gel containing the desired fragment of DNA was excised with a razor and transferred into a 1.5 ml microcentrifuge tube. DNA was then purified from the agarose gel by using the QIAquick Gel Extraction Kit (Qiagen).

2.7.6 Polyacrylamide gel electrophoresis

Polyacrylamide gel electrophoresis was used to examine DNA fragments of less than 500 bp. DNA samples were combined with loading buffer and electrophoresed on 6% polyacrylamide gels (37.5:1, acrylamide:N,N'-methylene bisacrylamide), at 100Vfor 1.5 hours, using a 1 x TBE buffer system [10.8 g/l Tris base, 5.5 g/l boric acid and 2 mM EDTA (pH 8.0)]. GeneRuler 1 kb DNA ladder (Fermentas) and λ-*Pst*I were used as molecular weight standards. Gels were then stained with ethidium bromide and DNA bands were visualized by exposing to UV light.

2.7.7 DNA purification from polyacrylamide gels

DNA fragments used for EMSA were purified from polyacrylamide gels by using the "Crush and Soak" method as described in Sambrook *et al*. (1989). Samples were electrophoresed and visualized as described in section 2.7.6. The desired DNA band was excised and transferred to a 1.5 ml microcentrifuge tube, crushed with a small pestle and soaked in elution buffer [0.5M ammonium acetate, 10 mM magnesium acetate, 1 mM EDTA (pH8.0) and 0.1% (w/v) SDS] for 16 hours at 37^{o}C. The solution was then filtered to remove any residual polyacrylamide. DNA was ethanol precipitated twice, washed in 70% ethanol and resuspened in 10 µl H_2O.

2.7.8 DNA labelling

PCR probes for EMSA were 5' end-labelled by using T4 polynucleotide kinase (Roche). Fifty pmol or 200 ng of DNA was combined with 5 µl of [γ-^{32}P] ATP, 20 U of kinase enzyme and 1 µl of 10 x kinase buffer [0.5 M Tris-HCl (pH 9.5), 1 mM spermidine, 100 mM $MgCl_2$, 1 mM EDTA and 50 mM DTT) in a total volume of 10 µl. Reaction mixtures were incubated at 37^{o}C for 30 minutes (15 minutes after each 1 µl of kinase enzyme was added). Once the reaction was complete, labelled DNA was separated from unincorporated labelled nucleotides by ethanol precipitation and resuspended in 10 µl of 1/5 diluted TE buffer.

2.7.9 DNA sequencing

DNA sequencing was carried out by using the BigDye Terminator v3.1 Cycle Sequencing Kit (Applied Biosystems, Foster city, USA). Each reaction mixture (20 µl) contained 100-200 ng of PCR products or 400 ng of plasmid DNA

as the template DNA. Five picomoles of primer, 2 µl of BigDye premix and 6 µl of dilution buffer [200 mM Tris (pH9.0) and 5 mM $MgCl_2$] along with DMSO to give a final concentration of 5% were added to the reaction tube and subjected to the following cycling conditions: 30 cycles of 96 ºC for 30 seconds and 60 ºC for 2 minutes. Once the cycling was complete, the entire contents was transferred to a fresh 1.5 ml microcentrifuge tube with 2 µl of sodium acetate/EDTA buffer added. After mixing, 80 µl of 95% (v/v) ethanol was added. The tube was vortexed and incubated on ice for 15 minutes and then microcentrifuged for 15 minutes. DNA pellets were washed with 500 µl of 70% ethanol, air dried for 5 minutes and then sent to the Molecular Biology Service Unit (Department of Biological Sciences, University of Alberta), where the sequence information was determined.

2.8 RNA methods

2.8.1 RNA quantification

Purified RNA was quantified by using the NanoDrop® ND-1000 Spectrophotometer. Quality of RNA samples was determined by the A_{260}:A_{280} ratio provided by the machine as well as agarose gel electrophoresis (section 2.7.4).

2.8.2 Reverse transcriptase polymerase chain reaction

Reverse transcriptase-polymerase chain reaction (RT-PCR) was carried out to determine transcription profiles of various *S. clavuligerus* strains. First strand cDNA synthesis in two-step RT-PCR was carried out by using Superscript

III (SSIII) reverse transcriptase (Invitrogen). Reactions were set up according to manufacturer's suggestions with the following changes: 1 µg of total RNA, 5% DMSO and 0.5µl of SSIII (200 U/µl) were used in all RT reactions. The second step PCR reactions were set up as described in section 2.7.3 except that 10 µl of RT product from above and 25 pmol of each primer were used. When all components were added to the reaction tube, the mixture was aliquoted into two 25 µl volumes; one was subjected to 25 cycles of amplification and the other one subjected to 30 cycles of amplification. Negative control reactions were set up by repeating the experiment with the same RNA preparations but without carrying out the RT step, to confirm that the results obtained were not due to chromosomal DNA contamination. Amplification of the RT product of *hrdB*, which encodes a constitutively expressed sigma factor, was also carried out to assess the quality and quantity of each RNA preparation.

2.9 Protein methods

2.9.1 Protein quantification

Protein concentration of each sample used in this study was measured by using the Bio-Rad protein assay (Bio-Rad), which is based on the protein-dye binding assay as described by Bradford (1976). A standard curve was constructed with bovine gamma globulin and A_{595} of each sample was determined by using the UNICAM UV/Vis Spectrophotometer UV3.

2.9.2 SDS-Polyacrylamide gel electrophoresis

Protein samples were analyzed through discontinuous SDS-polyacrylamide gels except for EMSAs, for which non-denaturing continuous gels were used. Gels were cast by using the Mini-PROTEAN 3 apparatus (Bio-Rad) and the stacking gels were composed of 4% (v/v) acrylamide:N,N'-methylene bisacrylamide (37.5:1), 125 mM Tris-HCl (pH 6.8), 0.1% (w/v) SDS, 0.1% (v/v) TEMED, and 0.05% (w/v) ammonium persulfate. Resolving gels were composed of 8-15% (v/v) acrylamide:N,N'-methylene bisacrylamide (37.5:1), 375 mM Tris-HCl (pH 8.8), 0.1% (w/v) SDS, 0.05% (v/v) TEMED, and 0.5% (w/v) ammonium persulfate. Gels were run in 1 x running buffer (14.34 g/l glycine, 3.03 g/l Tris base and 1 g/l SDS) at 200 V for 1 hour at 4^{o}C. Protein samples were combined with 5 x sample buffer [62.5 mM Tris-HCl (pH 6.8), 10% (v/v) glycerol, 2 % (w/v) SDS, 720 mM β-mercaptoethanol, and 0.00125% (w/v) bromophenol blue] and heated at 95ºC for 4 minutes before loading.

After electrophoresis, gels were stained with Phast Coomassie stain [0.1% (w/v) PhastGel Blue R Stain, 30% (v/v) methanol, and 10% (v/v) glacial acetic acid] for at least one hour and then destained overnight in 30% (v/v) methanol and 10% (v/v) glacial acetic acid. After destaining, gels were soaked in 10% (v/v) glacial acetic acid and 5% (v/v) glycerol and then preserved in BioDesignGelWrap (BioDesign Inc., Carmel, NY).

2.9.3 Overproduction of CeaS1 and CeaS2

E. coli BL21 (DE3) carrying pET-9c-*ceaS1* or pET-24a-*ceaS*2 was used to inoculate 2.5 ml of LB medium. Cultures were incubated at 37^{o}C for 16 hours and

0.5 ml was used to inoculate 25 ml of LB. These larger cultures were incubated at 37^{o}C until OD_{600} reached ~0.6. At this point, 0.5 mM IPTG was added and cultures were further incubated at 37^{o}C for 4 hours to induce protein expression. Cells were then harvested and disrupted as described in section 2.5.6. Since proteins were insoluble and present as inclusion bodies, samples were microcentrifuged and supernatant was decanted. Pellets were resuspended in 1 ml of 50 mM Tris (pH 8.0) and stored at -80^{o}C and were used as protein standards for Western analysis.

2.9.4 Overproduction of Snk-His_7 and Res2-His_7

E. coli BL21 (DE3) carrying pT7-7His-*snk* or pT7-7His-*res2* plasmid was grown for 16 hours in 10 ml of LB medium at 37^{o}C. The entire culture was used to inoculate 200 ml of LB and then incubated at 37^{o}C until OD_{600} reached ~0.6. At this point, 0.4 mM of IPTG was added and further incubated at 37^{o}C for ~5 hours to induce protein expression. Cultures were harvested by centrifugation at 5,000 rpm for 20 minutes. Culture supernatants were poured off and cell pellets were stored for 16 hours at -20^{o}C.

The same procedure described above was used to over express the mutated version of Snk-His_7 and Res2-His_7 except that *E. coli* BL21 (DE3) carrying pT7-7His-*snk*-SD or pT7-7His-*res2*-SD was used.

2.9.5 Overproduction of His_{10}-Res1, His_{10}-Res1-SD and His_{10}-C7P

A similar procedure as described above was used to over express His_{10}-Res1, His_{10}-Res1-SD and His_{10}-C7P by *E. coli* BL21 (DE3) carrying pET-19B-

res1, pET-19B-*res1*-SD and pET-19B-*c7p* respectively, but with the following changes. To induce protein expression, 1 mM IPTG was added to the medium once the culture OD_{600} reached ~0.6. During induction, these cultures were incubated at 21^{o}C for ~7 hours and harvested by centrifugation at 5,000 rpm for 20 minutes. Cell pellets were stored overnight at -20^{o}C.

2.9.6 Overproduction of MBP-Res1 and MBP-Res2

MBP-Res1 and MBP-Res2 fusion protein were over expressed using a similar procedure as described above with *E. coli* BL21 (DE3) carrying pMal-*res1* or pMal-*res2*. LB medium was supplemented with glucose (2 g/l) to inhibit amylase production by the *E. coli* host strain to prevent degradation of the amylose resin that was used in downstream process to purify fusion proteins (NEB). To induce protein expression, 0.3 mM of IPTG was added to the medium once the culture OD_{600} reached ~0.5. These cultures were further incubated at 37^{o}C for 2 hours and harvested by centrifugation at 5,000 rpm for 20 minutes. Cell pellets were resuspended in 5 ml of column buffer [20 mM Tris-HCL (pH7.4), 200 mM NaCl, 1 mM EDTA and 1 mM DTT] and stored overnight at -20^{o}C.

2.9.7 Purification of His-tagged proteins

To purify the His-tagged proteins from *E. coli* cells, pellets were first thawed on ice for 10 minutes and resuspended in 5 ml of lysis buffer (50 mM NaH_2PO_4, 300 mM NaCl, 10 mM imidazole, pH8.0) supplemented with 1 mg/ml of lysozyme. Cell suspensions were incubated on ice for 30 minutes and then

sonicated 6 x 15 seconds on setting of 25% with a ¼" (6.35 mm) diameter microtip. Samples were centrifuged at 9,000 rpm for 20 minutes to remove insoluble cell debris and clarified cell lysates were transferred to 15 ml polypropylene tubes.

One milliliter of 50% nickel-nitrilotriacetic acid (Ni-NTA) resin slurry (Qiagen) was added to the supernatants and incubated on ice on a rotary shaker for 60 minutes to facilitate the binding of His-tagged proteins to the resin. The mixture was then loaded into a column, which was made by filling a 5 ml syringe with non-absorbent cotton wool. The mixture was washed twice with 4 ml of wash buffer [50 mM NaH_2PO_4, 300 mM NaCl, and 20 mM imidazole (pH 8.0)]. Bound His-tagged proteins were eluted from the resin with 0.5 ml fractions of elution buffer (50 mM NaH_2PO_4, 300 mM NaCl, 50-250 mM imidazole, pH8.0). Fractions collected were analyzed by SDS-PAGE (Section 2.9.2) and those carrying the desired protein were pooled and concentrated down to ~50 µl by centrifugation with Amicon® Centricon®-10 concentrators (Millipore, Billerica, MA) at 6,500 rpm at 4ºC. The concentrated solution was adjusted to ~500 µl with protein storage buffer [10 mM Tris-HCl (pH 8.0), 0.1% CHAPS, 0.1 mM DTT, 0.1 mM EDTA, 0.3 M NaCl, and 30% glycerol] and aliquoted into 50 µl fractions and stored at -80^{o}C.

2.9.8 Purification of MBP fusion protein

Cell suspensions stored at -20^{o}C (Section 2.9.6) were thawed on ice for 10 minutes and then sonicated 6 times for 15 seconds on a setting of 25% with a ¼"

(6.35 mm) diameter microtip. Crude cell lysates were centrifuged at 9,000 rpm for 20 minutes to remove insoluble materials. MBP fusion proteins were then purified according to the manufacturer's recommendations (NEB). Clarified cell lysates were diluted 1:6 with column buffer (as described in section 2.9.6) and loaded onto columns. Prior to loading, 1 ml of amylose resin (NEB) was poured into a column (set up as described above) and washed with 5 ml of column buffer. After loading, resin was washed with 12 ml of column buffer to remove unbound proteins. Bound MBP fusion protein was eluted with column buffer supplemented with 10 mM maltose. Ten 1 ml fractions were collected and analysed by SDS-PAGE. Identified fractions that contained the desired protein were pooled together and subjected to the same treatment as described above and stored at -80^{o}C for future analysis.

Maltose present in the elution buffer must be removed in order to carry out some of the assays performed in this study. For those procedures, the desired protein was further purified by FPLC through an anion exchange column. Fractions identified from above were first pooled and diluted 1:3 with buffer [20 mM Tris-HCl (pH 7.8) and 10% glycerol] then loaded onto a HiLoad 26/10 Q Sepharose High Performance column (GE healthcare Bio-Sciences, Uppsala, Sweden). The column was washed with 1 column volume of washing buffer [20 mM Tris-HCl (pH 7.8), 50 mM NaCl, 0.1 mM DTT and 10% glycerol] and eluted with elution buffer (washing buffer with increasing concentration of NaCl, up to 2M). A_{280} of collected fractions was monitored to follow protein elution and fractions that might contain the desired protein were analyzed by SDS-PAGE.

Identified fractions were pooled and subjected to the same treatment as described in section 2.9.7 and stored at -80^{o}C for future analysis.

2.9.9 *In vitro* phosphorylation assays

In vitro phosphorylation assays were carried out to determine the phosphorylation status of various proteins. Each reaction mixture composed of 2 µM of Snk-His$_7$ protein and 6 µM of His$_{10}$-Res1 or Res2-His$_7$ protein. However, when all 3 proteins were present in the same reaction mixture, only 3 µM of His$_{10}$-Res1 and Res2-His$_7$ were used. In addition to appropriate protein amounts, each 20 µl reaction also contained 4 µl of 5 x kinase buffer [50 mM Tris-HCl (pH 8.0), 2 mM DTT, 50 mM KCl, 0.1 mM $MgCl_2$ and 10% (v/v) glycerol], 60 µM ATP and 2 µCi [γ-^{32}P] ATP. Kinase reactions were carried out at 30ºC for 30 minutes. Reactions were stopped by placing the reaction tubes on ice and adding 5 µl of 5 x SDS-PAGE sample buffer. The entire mixtures were then run into 15% polyacrylamide gels. The resulting gels were dried with a Model 583 Gel Dryer (Bio-Rad) for 45 minutes at 80^{o}C and exposed to a BAS cassette 4043 phosphor screen (Fujifilm, Tokyo, Japan) for 16 hours. The image was developed in an Image Reader FLA-5000 phosphorimager (Fujiflim, Tokyo, Japan).

2.9.10 Phospho-transfer assays

MBP-Res1 was first phosphorylated with Snk-His$_7$ as described above in a 500 µl reaction mixture. A total of 450 µl of amylose resin resuspended in 1 x kinase buffer was then added to the reaction tube and incubated on ice. After 15 minutes, reaction tubes were microcentrifuged for 2 minutes. Supernatant was

decanted and pelleted resins were washed 4 times with 800 µl 1 x kinase buffer. Bound phosphorylated MBP-Res1 was then eluted from the resin by adding 150 µl of kinase buffer supplemented with 1 mM maltose and incubated on ice for 15 minutes. The mixture was then subjected to microcentrifugation and supernatant containing phosphorylated MBP-Res1 was transferred to a fresh 1.5 ml microcentrifuge tube. Kinase reactions were then set up by mixing 15 µl of phosphorylated MBP-Res1 with Res2-His_7 (final concentration, 6 µM; volume adjusted to 20 µl with 1 x kinase buffer) and incubated at 30^{o}C for 30 minutes.

MBP-Res2 was phosphorylated with Snk-His_7 as described above in a 250 µl reaction mixture. A total of 250 µl (two 125 µl volumes) of Ni-NTA resin slurry resuspended in 1 x kinase buffer was added. After each addition, the reaction tube was incubated at 4 ^{o}C for 10 minutes and then microcentrifuged for 1 minute to sediment the Ni-NTA resin, whereupon the supernatant containing phosphorylated MBP-Res2 was transferred to a fresh 1.5 ml microcentrifuge tube. Kinase reactions were then set up by mixing 15 µl of phosphorylated MBP-Res2 with His_{10}-Res1 (final concentration, 6 µM; volume adjusted to 20 µl with 1 x kinase buffer) and incubated at 30^{o}C for 30 minutes.

Once the kinase reactions from above were complete, reaction tubes were placed on ice and combined with 5 µl of SDS-PAGE sample buffer. The entire reaction mixtures were loaded onto 12% polyacrylamide gels. Resulting gels were dried and exposed for 16 hours to a phosphor screen. Images were developed as described above.

2.9.11 *In vitro* dephosphorylation assays

Twelve microliters of the supernatant containing phosphorylated MBP-Res2 purified from section 2.9.10 was added to His_{10}-Res1 (final concentration, 6 μM; adjusted to 20 μl with kinase buffer). The 20 μl reaction mixture was incubated at 30°C for 1, 5, 20, 60, or 300 minutes, and the reaction was stopped by adding 5 μl of SDS-PAGE sample buffer. The reaction products were resolved on a 12% polyacrylamide gel. Resulting gels were dried and images were obtained as described in section 2.9.9.

2.9.12 Western analysis

Ten micrograms of cell-free extract protein from each test strain was subjected to Western analysis. Each sample was combined with SDS-PAGE sample buffer and heated at 95^{o}C for 4 minutes and subjected to SDS-PAGE (section 2.9.2). After electrophoresis, separated proteins were transferred to Hybond-P PVDF membranes (Amersham) at 4 ^{o}C in transfer buffer composed of 25 mM Tris (pH8.3), 192 mM glycine and 20% methanol. Transfers were carried out at 30V for 16 hours by using the mini-Trans-Blot apparatus (Bio-Rad). PVDF membranes were first pre-wetted by soaking in methanol and then equilibrating in transfer buffer for at least 15 minutes. Gels with the separated proteins were also equilibrated in transfer buffer for 15 minutes prior to transfer.

Protocols and reagents from the ECL Western blotting analysis system were used to detect proteins of interest (Amersham BioSciences, Uppsala, Sweden) with minor changes as stated below. Membranes were rinsed with wash

buffer [0.02 M Tris-HCl (pH 7.6), 0.14 M NaCl and 0.1% Tween 20] and blocked overnight at 4^{o}C with blocking buffer (10% non-fat dried milk in wash buffer). Primary antibody was added at a dilution of 1/5,000 to 1/15,000 in 25ml of blocking buffer and incubated at 21^{o}C for 1 hour on an orbital shaker. Primary polyclonal antibodies were obtained from rabbits injected with proteins purified by SDS-PAGE, using standard methods as described by Sambrook *et al*. (1989). Horseradish peroxidise-linked anti-rabbit IgG isolated from donkey, as provided in the kit was added at a dilution of 1/10,000 to 1/15,000 in 25 ml blocking buffer and incubated at 21^{o}C for 1 hour. The blot was rinsed and washed 1 x 15 minutes and 3 x 5 minutes with wash buffer after incubation with each antibody.

Six milliliters of the supplied detection reagent was dispensed onto the blot and incubated at 21^{o}C for 1 minute. Excess reagent was drained off and the blot was wrapped in Saran wrap and exposed to Kodak BioMax light X-ray film (GE Healthcare) for 10 to 20 minutes. Films were then developed by using the Fuji RGII X-ray film processor (Fuji Photo Film Co., Tokyo).

2.10 DNA-Protein interactions

2.10.1 Electrophoretic mobility shift assays

Electrophoretic mobility shift assays were carried out to determine the ability of Res2 or C7P to bind DNA. DNA fragments of potential targets as determined by RT-PCR were generated by PCR, purified from polyacrylamide gels by the “crush and soak” method and ^{32}P end-labelled (section 2.8.2, 2.7.3, 2.7.6, 2.7.7 and 2.7.8, respectively). Reactions were set up in a total volume of 20

µl by mixing 20 fmol of each labelled fragment with 0-100 pmol of purified protein in a buffer containing 10 mM Tris-HCl (pH 8.0), 1 mM DTT, 10% glycerol, 150 mM NaCl and 1 µg of poly d(I-C). Binding reactions were carried out at 21^{o}C for ~25 minutes. Reaction products were then separated on 1.5% glycerol containing 6-10% non-denaturing polyacrylamide gels (37.5:1 acrylamide:N,N'-methylene bisacrylamide) in 1 x Tris-glycine buffer system (3.03 g/l Tris base, 14.3 g/l glycine, 0.39 g/l EDTA, pH 8.3). Before the samples were loaded, gels were pre-run at 200V for ~1 hour. Electrophoresis was then carried out at 120-150V for ~30 minutes at 4^{o}C to separate bound and free DNA probes. Gels were then dried for 45 minutes, placed on phosphor screen and exposed for 16 hours. The images were developed in an Image Reader FLA-5000 phosphorimager.

Control reactions were also carried out by setting up reaction mixtures as described above, but with 5 and 50 x molar excess of unlabelled DNA probe added to the binding reactions for specific competition. For non-specific competition, 5 and 50 x molar excess of unlabeled non-specific DNA (a 350 bp *hrdB* fragment amplified by using primers *hrdB* RT-forward and *hrdB* RT-reverse and *S. clavuligerus* genomic DNA as the template) were added to the binding reactions.

2.11 Confocal Microscopy

S. clavuligerus strains carrying the *egfp* reporter construct were grown in TSBS for 40 hours and 500 µl of the resulting cultures were then used to inoculate

25 ml of Soy medium. After 48 h of growth, 1ml of the cultures were harvested by microcentrifugation, and then washed once with an equal volume of acetonitrile and twice with dH_2O. The washed cells were resuspended in 500 µl of 40% glycerol and 10 µl amounts were loaded onto a microscope slide and mounted with a microscope cover slip. The edges of the cover slips were sealed with clear nail polish before observation.

Confocal microscopy was carried out using a Leica DM IRB Inverted microscope. An argon laser with 50-52% attenuation was used to provide excitation at 488 nm and EGFP excitation was detected between 500 nm to 520 nm. Corresponding Differential Interference Contrast (DIC) images were also obtained.

2.12 Software and web sources used for analysis

GeneTools version 2.0 (BioTools Inc., Edmonton, AB) was used to identify restriction sites within DNA sequences. Lasergene version 7.1 (DNASTAR Inc., Madison, WI) was used for sequence editing, alignment and to locate restriction sites. It was also used to calculate the molecular weight of various proteins. Similarity searches were performed by using the BLAST program (Altschul *et al*. 1990; Gish and States, 1993) available at the National Institute for Biotechnology Information (http://www.ncbi.nlm.nih.gov/BLAST/). OligoAnalyzer version 3.1 (IDT) was used to design and analyze oligonucleotide primers.

Chapter 3

Results

3. Results

3.1 Analysis of the regulation of *ceaS* involved in clavam biosynthesis

Carboxyethylarginine synthase (CeaS), which is encoded by *ceaS1* and *ceaS2*, catalyzes the first reaction involved in clavam production. Since first enzymes of biosynthetic pathways are typically subjected to tight regulation, CeaS is a likely control point for regulating production of clavulanic acid and 5*S* clavams in *S. clavuligerus*.

In a previous study, a *ceaS2* mutant constructed by inserting an apramycin resistance gene cassette into *ceaS2* (*ceaS2*::apra) was found to be severely compromised in clavam biosynthesis (Jensen *et al*., 2000). As *ceaS2*, *bls2* and *pah2* are transcribed together as a polycistronic transcript (Paradkar and Jensen, 1995), it was initially proposed that the severe phenotype was due to the insertion of the *apr* gene cassette, which could have polar effects on transcription of the downstream genes. As a result, a new *ceaS2* mutant was prepared by replacing the *apr* gene cassette in *ceaS2*::apra with a frame shift mutation (*ceaS2*-Fs) to alleviate polar effects (Tahlan, 2005). However, a similar phenotype was observed and so it was proposed that, either polarity still remains an issue, or that the truncated form of CeaS2 produced may interfere with other biosynthetic enzymes, thus affecting production of clavam metabolites. Therefore, Δ*ceaS2*::apra was constructed by replacing the entire *ceaS2* gene with the *apr* gene cassette to eliminate the possibility of production of truncated CeaS2 protein. In view of the fact that the *apr* gene cassette may still exert polar effects on downstream genes,

Δ*ceaS2* in-frame (IF) was also prepared by removing the gene cassette and thus leaving just an unmarked in-frame deletion. This Δ*ceaS2*-IF mutant was expected to have the least potential to cause polar effects on expression of downstream *bls2* and *pah2*. Nonetheless, all four *ceaS2* mutants: Δ*ceaS2*-IF, Δ*ceaS2*::apra, *ceaS2*-Fs and *ceaS2*::apra were still severely compromised or incapable of producing clavulanic acid (Table 3.1) or 5*S* clavams (data not shown). This is unexpected because both CeaS1 and CeaS2 catalyze the same reaction and disruption of *ceaS2* would be expected to leave the functional copy of *ceaS1* to support *S. clavuligerus* to continue synthesizing clavulanic acid. Moreover, since *ceaS2*, *pah2* and *cas2* are genes involved in the early steps of clavam biosynthesis, by disrupting *ceaS2*, we would expect *ceaS2* mutants to have a phenotype similar to those of *pah2* or *cas2* mutants, where reduced levels but not a complete loss of clavulanic acid production, was observed (Jensen *et al*., 2000).

This much more severe phenotype of the *ceaS2* mutants suggested that cross regulation is taking place between *ceaS1* and *ceaS2*. As a first step in understanding how *ceaS* may regulate clavam biosynthesis, a study was undertaken to investigate the potential cross regulation between *ceaS1* and *ceaS2* and to determine if disrupting *ceaS2* caused a polar effect and influenced transcription of downstream genes.

3.1.1 Overproduction of CeaS1 and CeaS2

CeaS1 and CeaS2 proteins were required for use as protein markers for subsequent Western analyses and were over produced as described in section

Table 3.1. Bioassay using *Klebsiella pneumonia* ATCC 15380 as the indicator organism to detect clavulanic acid production by various *S. clavuligerus* mutants after 48 hours of growth in Soy or SA media.

Strain	**Clavulanic acid production in Soy medium (in µg/ml)**	**Clavulanic acid production in SA medium (in µg/ml)**
Wild type	158	53
Δ*ceaS2*-IF	0	0
Δ*ceaS2*::apra	13	0
ceaS2-Fs	0	0
ceaS2::apra	0	0
Δ*ceaS1*::apra	128	30
Δ*ceaS2*-C	0	0
Δ*ceaS2*-C2-9	73	36.5
bls2::apra	24	0
bls1::tsr	106	25
Δ*ceaS1*::apra/*ceaS2*-Fs	0	0
Double *bls*	0	0

2.9.3. Sixteen hour cultures of *E. coli* BL21(DE3) carrying pET-9c-*ceaS1* or pET-24a-*ceaS2* (Table 2.3) were used to inoculate 25 ml of TSBS medium. Once the culture OD_{600} reached ~0.6, expression of *ceaS1* and *ceaS2*, as driven by a T7 promoter, was initiated by adding 0.5 mM IPTG to the cultures to induce production of T7 RNA polymerase, and incubating at 37^{o}C for 4-6 hours. After induction, cells were harvested, frozen overnight, lysed with lysozyme and sonicated to release the overproduced protein. Crude lysates were centrifuged to sediment insoluble cell matter. Since induction of wild type CeaS proteins resulted in the production of insoluble inclusion bodies localized in the cytoplasm (Figure 3.1.1 and observation under microscope, data not shown), the insoluble protein fraction was stored at -80^{o}C and used for later studies.

3.1.2 Cross reaction of anti-CeaS2 antibody with CeaS1 protein

As mentioned in Section 3.1.1, CeaS1 and CeaS2 obtained through high level expression in *E. coli* were insoluble. The optimum amount used for each Western analysis was therefore determined empirically. In addition, only anti-CeaS2 antibody was available for use in these studies. As sequence comparison revealed a high similarity between CeaS1 and CeaS2 (67% identity, 80% similarity) (Tahlan, 2005), Western analysis was carried out to determine if anti-CeaS2 antibody can cross react with CeaS1 protein. Single protein bands corresponding to CeaS2 and CeaS1 (Figure 3.1.2) were observed on the developed x-ray film in the most diluted samples when cell-free extracts (CFEs) from the CeaS2 and CeaS1 overproducing *E. coli* strains were examined. This

Figure 3.1.1. Overproduction of CeaS1 and CeaS2 from *E. coli* BL21(DE3) carrying pET9c-*ceaS1* and pET24a-*ceaS2*, respectively. Samples were analyzed by SDS-PAGE with the use of precast PhastGel Gradient 8-25% and proteins were visualized by staining with Coomassie blue. (A) soluble protein fractions. (B) insoluble cell matter.

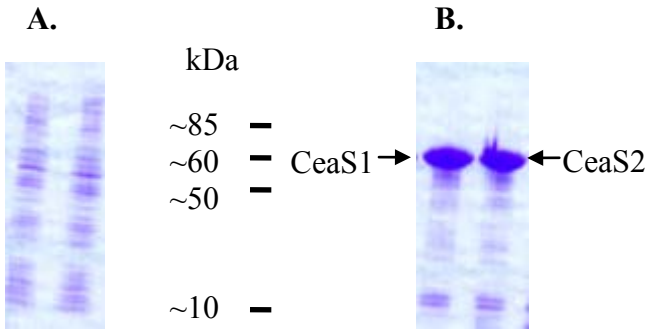
A.
B.
kDa
~85
~60
~50
~10
CeaS1
CeaS2

Figure 3.1.2. Western analysis of CeaS1 and CeaS2. Cell-free extracts were isolated from *E. coli* BL21(DE3) carrying (A) pET-24a-*ceaS2* or (B) pET-9c-*ceaS1*. Series of dilutions of CFE were electrophoresed on 8% SDS-PAG to determine the optimal amount to use as a protein standard for subsequent Western analyses. Samples were separated on 8% SDS-PAG and transferred to PVDF membranes. Membranes were then incubated with rabbit anti-CeaS2 polyclonal antibodies, followed by incubation with horseradish peroxidase-conjugated, donkey anti-rabbit secondary antibodies. The membranes were exposed to x-ray film for 5-10 minutes after treatment with enhanced chemiluminescence reagents.

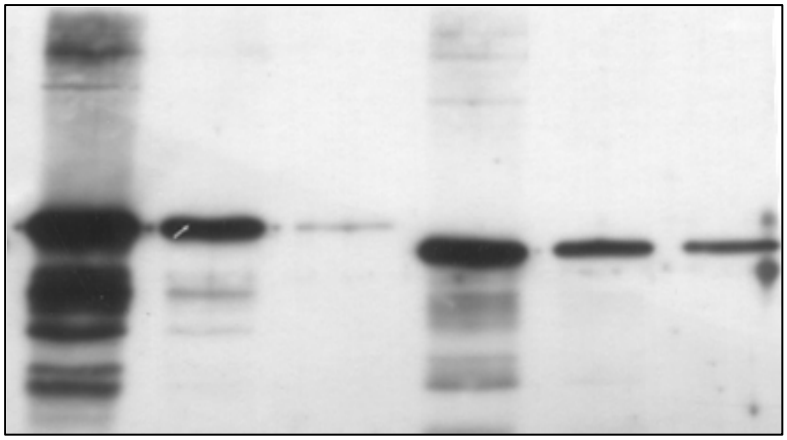
A.
CeaS2
1:50
1:100
1:200
B.
C eaS1
1:50
1:100
1:200

indicated that both proteins can be detected by anti-CeaS2 antibody. For subsequent Western analyses, 5 µl of the appropriately diluted CFEs were used as the protein standard. In addition, under the electrophoresis conditions used, when the gels were electrophoresed until the bromophenol blue indicator present in the SDS-PAGE sample buffer ran completely off the gel, CeaS1 could be resolved from CeaS2, despite the fact that they are very similar in molecular weight (59 and 61 kDA, respectively).

3.1.3 Western analyses to detect CeaS1 and CeaS2 production

To investigate the unexpected observation that *ceaS2* mutants cannot produce clavam metabolites, Western analyses using CeaS-specific polyclonal antibodies were carried out to examine CeaS1 production in these mutants. CFEs from wild type *S. clavuligerus*, Δ*ceaS2*-IF, Δ*ceaS2*::apra, *ceaS2*-Fs, *ceaS2*::apra, Δ*ceaS1*::apra and Δ*ceaS1*::apra/*ceaS2*-Fs mutants (Table 2.2) were obtained after growth for 48 and 72 hours in Soy and SA media. Proteins were then separated on 8% SDS-PAG and transferred to PVDF membranes.

After overnight transfer, the membranes were first incubated with rabbit anti-CeaS antibody at 1:15,000 dilution and then incubated with 1:15,000 diluted horseradish peroxidase-conjugated, donkey anti-rabbit secondary antibodies. The membranes were exposed to x-ray film for 5-10 minutes after treatment with enhanced chemiluminescence reagents.

Protein bands representing CeaS2 and CeaS1 were observed when CFE of wild type *S. clavuligerus* grown in Soy medium was subjected to Western analysis, but only the CeaS2 band was observed in CFE from cells grown in SA medium (Figure 3.1.3). This is in consistent with findings from previous studies that *ceaS1* is regulated differently from *ceaS2* and is not transcribed in SA medium (Tahlan *et al*., 2004). As expected, the protein band corresponding to CeaS2 could not be observed when CFEs of the four *ceaS2* mutants grown in Soy or SA media were subjected to analysis (Figure 3.1.4). Surprisingly, the protein band representing CeaS1 was also not observed in these mutants when grown in Soy medium (Figure 3.1.4). This indicated that all of the *ceaS2* mutants mentioned above were unable to produce CeaS1 even though the *ceaS1* gene was still intact. This profile is similar to the phenotype observed from a *ceaS1*/*ceaS2* double mutant (Figure 3.1.4). On the other hand, the CeaS2 band was observed on the developed x-ray film when CFEs of the Δ*ceaS1*::apra mutant that was grown in Soy and SA media were subjected to Western analysis indicating that disrupting *ceaS1* has no effect on *ceaS2* expression (Figure 3.1.5).

When CFE of WT *S. clavuligerus* grown in Soy medium was subjected to Western analysis, a protein band of unknown identity was observed between the CeaS2 and CeaS1 bands (Figure 3.1.3). Since this band was also present in a *ceaS1* mutant (Figure 3.1.5), but it was not observed in *ceaS2* or *ceaS1/ceaS2* double mutants (Figure 3.1.4), this band is believed to be an alternatively processed, or degradation product of CeaS2. In order to minimize protein degradation, a cocktail of protease inhibitors was added when preparing CFEs

Figure 3.1.3. Western analysis of CeaS using cell-free extracts isolated from wild type *S. clavuligerus* grown either in liquid complex soy (Soy) or defined starch asparagine (SA) medium. Ten microgram amounts of total cellular protein were separated on 8% SDS-PAG and transferred to PVDF membranes. Equal volume (5 µl) of diluted CeaS1 and CeaS2 overproducing *E. coli* CFEs were mixed and used as the protein standard. Membranes were then incubated with rabbit anti-CeaS2 polyclonal antibodies, followed by incubation with horseradish peroxidase-conjugated, donkey anti-rabbit secondary antibodies. The membranes were exposed to x-ray film for 5-10 minutes after treatment with enhanced chemiluminescence reagents.

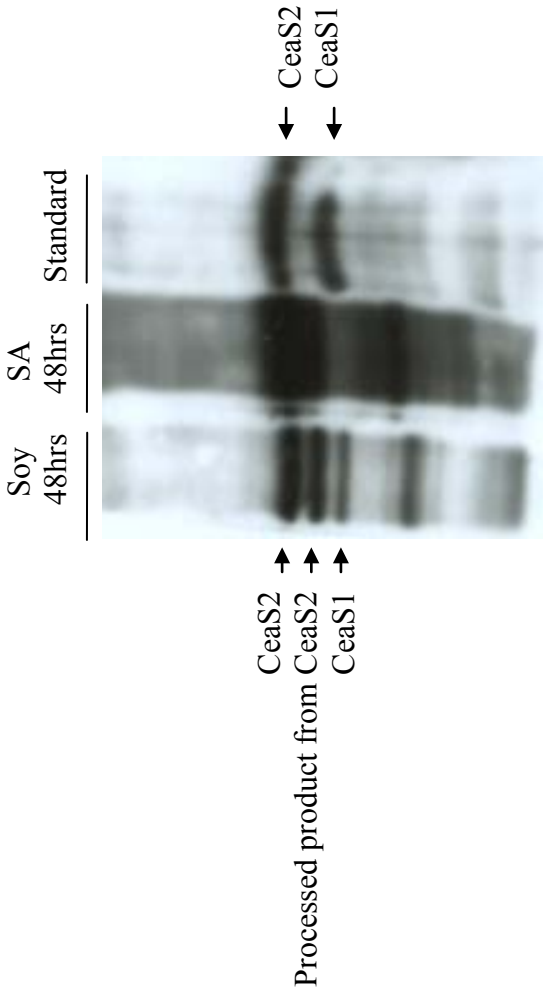
CeaS2
CeaS1
Soy 48hrs
SA 48hrs
Standard
CeaS2
Processed product from CeaS2
CeaS1

Figure 3.1.4. Western analysis of CeaS in *ceaS2* mutant strains and *ceaS1*/*ceaS2* double mutant. Cell-free extracts were isolated from Soy or SA grown cultures of (A) Δ*ceaS2*-IF, (B) Δ*ceaS2*::apra, (C) *ceaS2*-Fs, (D) *ceaS2*::apra and (E) Δ*ceaS1*::apra/*ceaS2*-Fs. Ten microgram amounts of total cellular protein were separated on 8% SDS-PAG and transferred to PVDF membranes. Membranes were then incubated with anti-CeaS2 polyclonal antibodies from rabbit, followed by incubation with horseradish peroxidase-conjugated, donkey anti-rabbit secondary antibodies. The membranes were exposed to x-ray film for 5-10 minutes after treatment with enhanced chemiluminescence reagents.

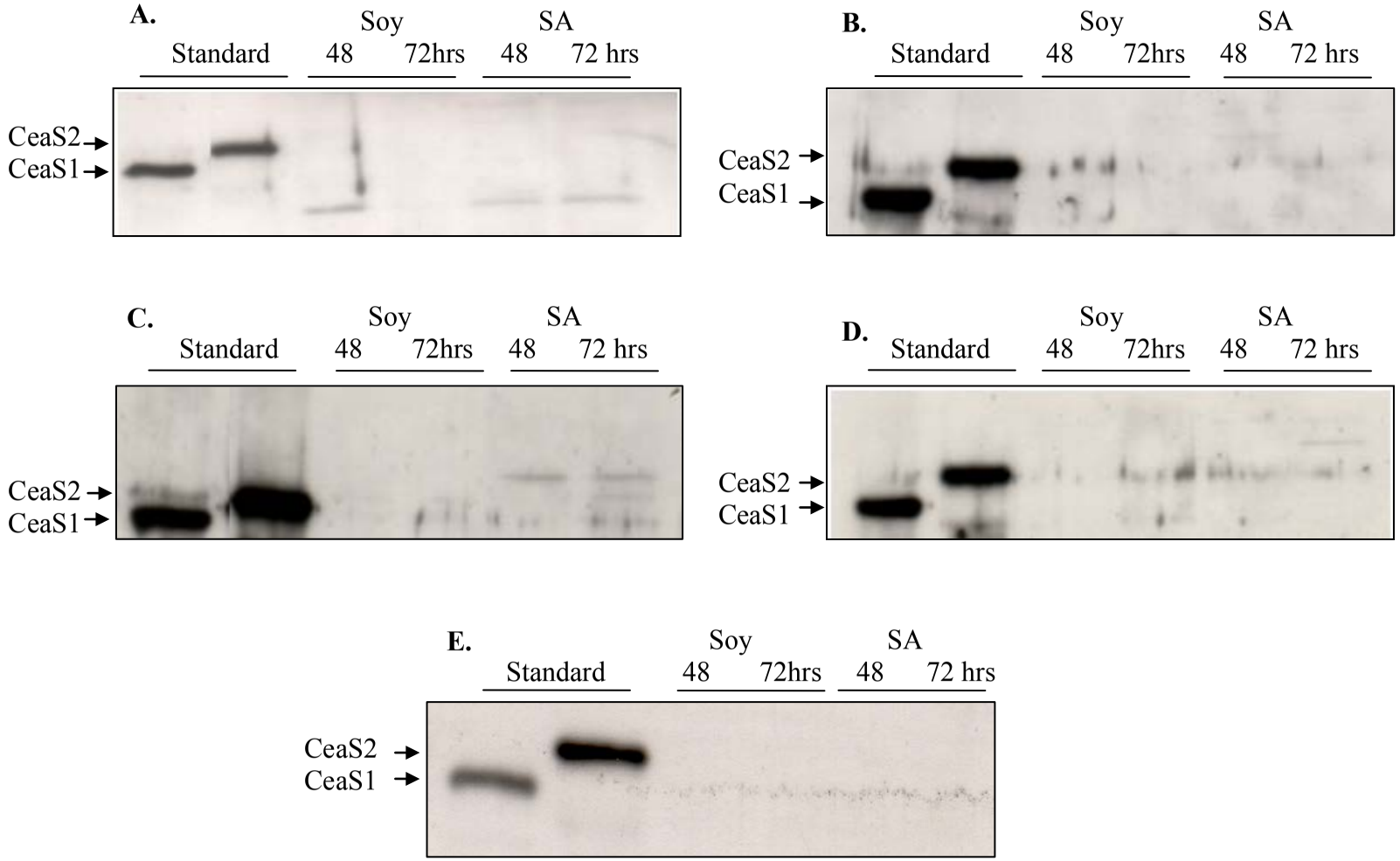
A.
Soy
SA
Standard
48
72hrs
48
72 hrs
CeaS2
CeaS1
B.
Soy
SA
Standard
48
72hrs
48
72 hrs
CeaS2
CeaS1
C.
Soy
SA
Standard
48
72hrs
48
72 hrs
CeaS2
CeaS1
D.
Soy
SA
Standard
48
72hrs
48
72 hrs
CeaS2
CeaS1
E.
Soy
SA
Standard
48
72hrs
48
72 hrs
CeaS2
CeaS1

Figure 3.1.5. Western analysis of CeaS in *ceaS1* mutant strains. Cell-free extracts were isolated from Soy or defined SA grown cultures of Δ*ceaS1*::apra. Ten microgram amounts of total cellular protein were separated on 8% SDS-PAG and transferred to PVDF membranes. Membranes were incubated with anti-CeaS2 polyclonal antibodies obtained from rabbit, followed by incubation with horseradish peroxidise-conjugated, donkey anti-rabbit secondary antibodies. After being treated with enhanced chemiluminescence reagents, membrane was exposed to x-ray film for 5-10 minutes.

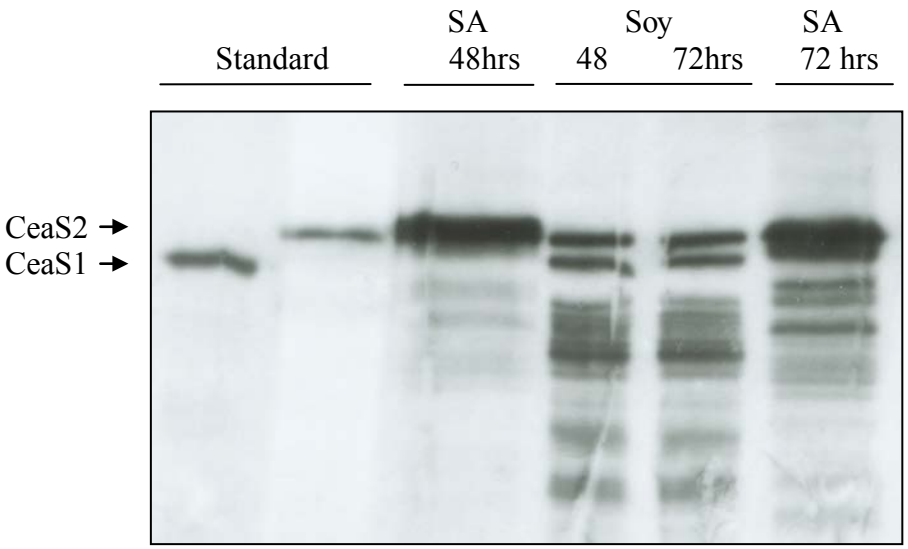
Standard
SA
48hrs
Soy
48
72hrs
SA
72 hrs
CeaS2
CeaS1

from the various strains. However, no significant improvement was found. As mentioned before, CeaS catalyzes the first reaction in the clavam production pathway, and first enzymes are typical control points for biosynthetic pathways, it might have an intrinsically high turn-over rate. As a result, degraded CeaS may already be present in the cells when samples were taken at 48 and 72 hours post inoculation into the production media.

Overall, the results obtained from Western analyses correspond with the observation that clavulanic acid production was abolished, as determined by clavulanic acid bioassay (Table.3.1), in all of the various *ceaS2* mutants, as neither CeaS1 nor CeaS2, which catalyze the first reaction involved in clavam biosynthesis, were produced.

To examine this effect further, cell free extracts from Δ*ceaS2*-C and Δ*ceaS2*-C2-9 (Table 2.2), which represent the Δ*ceaS2*-IF mutant carrying a copy of *ceaS2* alone or an ~11kb DNA fragment carrying all of the early genes required for clavulanic acid biosynthesis including *ceaS2* and flanking regions, respectively, were subjected to Western analysis using the same conditions as described above. Although the protein band corresponding to CeaS2 could now be observed in both complemented strains growing either in Soy or SA medium, the CeaS1 protein band was still missing (Figure 3.1.6). Furthermore, clavulanic acid bioassays indicated that only the latter construct (the ~11kb DNA fragment) restored clavulanic acid production despite the restoration of CeaS2 production in both strains (Table 3.1).

Figure 3.1.6. Western analysis of CeaS in complemented *ceaS2* mutants. Cell-free extracts were isolated from Soy or SA grown cultures of (A) Δ*ceaS2*-C and (B) Δ*ceaS2*-C2-9. Ten microgram amounts of total cellular protein were separated by electrophoresis on 8% SDS-PAG and transferred to PVDF membrane. Membranes were incubated with rabbit anti-CeaS2 polyclonal antibodies and then incubated with horseradish peroxidase-conjugated, donkey anti-rabbit secondary antibodies. After being treated with enhanced chemiluminescence reagents, membranes were exposed to x-ray film for 5-10 minutes.

A.

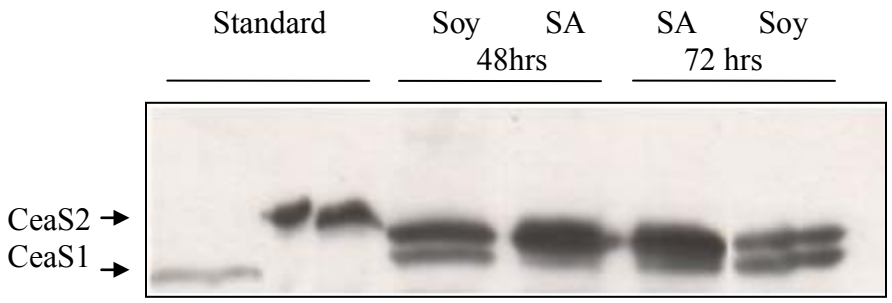
Standard
Soy
SA
48hrs
SA
Soy
72 hrs
CeaS2
CeaS1

B.

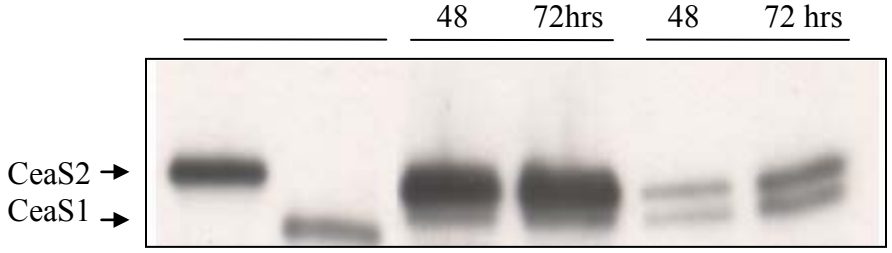
Standard
SA
48
72hrs
Soy
48
72 hrs
CeaS2
CeaS1

3.1.4 Western analyses to detect Bls1 and Bls2 production

To investigate if disrupting *ceaS2* affected transcription of the downstream genes, Western analyses using Bls2-specific polyclonal antibodies were carried out to examine Bls2 production in the four *ceaS2* mutants. CFEs from wild type *S. clavuligerus*, Δ*ceaS2*-IF, Δ*ceaS2*::apra, *ceaS2*-Fs, *ceaS2*::apra, Δ*ceaS1*::apra, *bls1*::neo, *bls2*::apra and *bls1*::neo/*bls2*::apra double mutants (Table 2.2), obtained after growth for 48 and 72 hours in Soy and SA media, were separated on 8% SDS-PAG and transferred to PVDF membranes.

After overnight transfer, the membranes were first incubated with rabbit anti-Bls2 antibody at 1:5,000 dilution and then incubated with 1:10,000 diluted horseradish peroxidase-conjugated, donkey anti-rabbit secondary antibodies. The membranes were exposed to x-ray film for 15-20 minutes after treatment with enhanced chemiluminescence reagents.

When CFE of WT *S. clavuligerus* grown in Soy or SA media was subjected to Western analysis, a protein band corresponding to Bls2 was observed (Figure 3.1.7). The protein appeared to have a slightly lower molecular weight compared to the standard Bls2 protein (54.5 kDA), as the band migrated further down on the gel. This is presumably due to the 6 x His-tag attached to the Bls2 protein standard (Figure 3.1.7). Unlike the situation for CeaS1 and CeaS2, electrophoresis conditions could not be found that would allow separation of Bls1 (55 kDA) from Bls2. When CFE of *bls1*::neo grown in Soy or SA media was subjected to Western analysis,

Figure 3.1.7. Western analysis of Bls in wild type *S. clavuligerus* and *bls* mutants. Cell-free extracts were isolated from Soy or SA grown cultures of (A) WT *S. clavuligerus*, (B) *bls1*::neo, (C) *bls1*::tsr/*bls2*::apra and (D) *bls2*::apra mutants. Ten microgram amounts of total cellular protein were separated by electrophoresis on 8% SDS-PAG and transferred to PVDF membranes. Twenty nanograms of purified His-tagged Bls2 was used as the protein standard. Membranes were incubated with rabbit anti-Bls2 polyclonal antibodies and then incubated with horseradish peroxidase-conjugated, donkey anti-rabbit secondary antibodies. After being treated with enhanced chemiluminescence reagents, membranes were exposed to x-ray film for 15-20 minutes.

A.

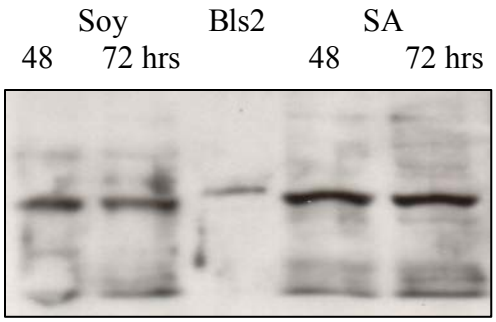
Soy
Bls2
SA
48
72 hrs
48
72 hrs

B.

C.

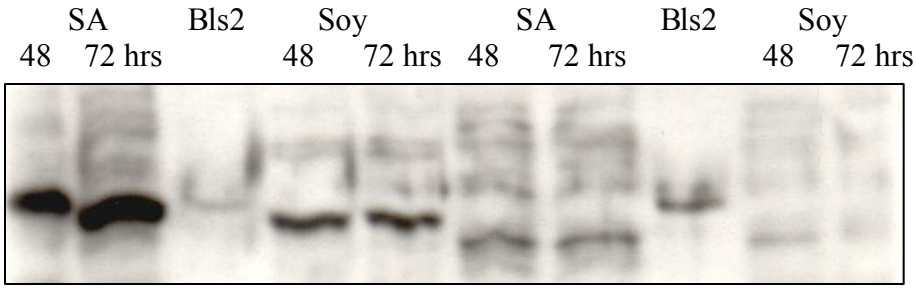
SA
Bls2
Soy
SA
Bls2
Soy
48
72 hrs
48
72 hrs
48
72 hrs
48
72 hrs

D.


Soy
Bls2
SA
48
72 hrs
48
72 hrs

the protein band corresponding to Bls2 was also observed (Figure 3.1.7). However, when CFE of the *bls2*::apra, grown in Soy or SA media, was subjected to Western analysis using the same conditions, no band corresponding to Bls1 was observed, and gels resembled those seen when CFE from *bls1/bls2* double mutants were analyzed. Only minor amounts of common cross reacting bands were observed from these two strains (Figure 3.1.7). Unfortunately, no Bls1 protein was available for use as a protein standard. These results were interpreted to mean that the Bls2-specific antibody did not recognize Bls1, although the possibility that mutation of *bls2* somehow blocked the expression of *bls1* could not be ruled out as Bls1 and Bls2 proteins show 49% identity, 59% similarity.

When CFEs of Δ*ceaS2*-IF, Δ*ceaS2*::apra, *ceaS2*-Fs and *ceaS2*::apra mutants, grown for 48 and 72 hours in Soy and SA media, were subjected to Western analysis, signals corresponding to Bls2 protein were not observed, indicating Bls2 was not produced in any of these mutants (Figure 3.1.8). In contrast, a protein band corresponding to Bls2 was observed when CFEs of the Δ*ceaS1*::apra mutant, grown in Soy or SA media, were subjected to analysis (Figure 3.1.8).

In addition to the inability to separate Bls1 from Bls2 and the uncertainty about whether the Bls2 antibodies were recognizing Bls1, Western analyses for Bls were also severely hampered by the quality of the anti-Bls antibodies available. The anti-Bls2 antibody generated a much weaker signal with high background noise compared to the anti-CeaS2 antibody. Although approaches

Figure 3.1.8. Western analysis of Bls in *ceaS2* mutants. Cell-free extracts were isolated from Soy or SA grown cultures of (A) Δ*ceaS2*-IF, (B) *ceaS2*::apra, (C) Δ*ceaS2*::apra and (D) *ceaS2*-Fs mutants. Extracts from the (E) Δ*ceaS1*::apra mutant were used as a positive control. Ten microgram amounts of total cellular protein were separated by electrophoresis on 8% SDS-PAG and transferred to PVDF membrane. Membranes were incubated with rabbit anti-Bls2 polyclonal antibodies and then incubated with horseradish peroxidase-conjugated, donkey anti-rabbit secondary antibodies. After being treated with enhanced chemiluminescence reagents, membranes were exposed to x-ray film for 15-20 minutes.

A.

Soy Bls2 SA
48 72 hrs 48 72 hrs

B. **C.**

Soy Bls2 SA Soy Bls2 SA
48 72 48 72 48 72 48 72 hrs

D. **E.**

Soy Bls2 SA Soy Bls2 SA
48 72 48 72 48 72 48 72 hrs

were undertaken to clean up the antiserum in order to reduce background noise and cross-reacting bands, none of these gave consistently improved quality. Similarly, different conditions (amounts of blocking agent and antibodies) were tested when developing the Western blot procedure, but again, no significant improvement was observed. The anti-Bls2 antibodies used were from a previous study in which they were prepared using purified Bls2 protein provided by C. Schofield, Oxford University. No expression constructs were available to prepare Bls1 or additional Bls2 protein or new anti-Bls antibodies, and so this aspect of the project was abandoned in favour of a RT-PCR approach.

3.1.5 Reverse transcriptase-PCR analysis

3.1.5.1 Effect of Δ*ceaS2*-IF mutation on *ceaS1* and *bls2* transcription

Reverse transcriptase PCR (RT-PCR) was carried out to investigate further if the impairment of CeaS1 production in the Δ*ceaS2*-IF mutant occurred at the transcriptional or translational level. It was also used to investigate whether polarity due to the 81-bp scar left by using the REDIRECT PCR targeting system to remove the *ceaS2* gene is still an issue in the Δ*ceaS2*-IF mutant, as determined by analyzing *bls2* transcript levels.

Total RNAs were isolated from WT *S. clavuligerus*, Δ*ceaS1*::apra and Δ*ceaS2*-IF mutants after growing for 48 hours in Soy liquid medium. Reverse primers (Table 2.4) were used to generate cDNA and then specific primer pairs (Table 2.4) were used to determine if the genes of interest were being transcribed in the mutant strains. The primer pairs ceaS1-RT-For/ceaS1-RT-Rev, ceaS2-RT-

For/ceaS2-RT-Rev, bls1 forward/bls1 reverse, CAN169/CAN170 (*bls2* specific primers) and hrdB RT-forward/hrdB RT-reverse were used for PCR amplification of 433-bp *ceaS1*, 452-bp *ceaS2*, 600-bp *bls1*, 443-bp *bls2* and 350-bp *hrdB* RT-PCR products, respectively. PCR reactions were carried out for 28 cycles and signal intensities were compared to WT *S. clavuligerus*. The *hrdB* gene encodes a constitutively expressed sigma factor in *Streptomyces* and its transcription level served as a control for RNA quality from different strains.

When RNA of WT *S. clavuligerus* isolated from Soy grown cultures was subjected to RT-PCR, DNA bands of the expected size representing *ceaS1*, *ceaS2*, *bls1* and *bls2* were observed (Figure 3.1.9). This indicated *ceaS1*, *ceaS2*, *bls1* and *bls2* were transcribed normally in the WT strain. When RNA of Δ*ceaS1*::apra was subjected to RT-PCR using the same conditions, only *ceaS2* and *bls2* transcripts were observed (Figure 3.1.9), thus indicating *ceaS1* and *bls1* were not transcribed in a *ceaS1* mutant. This was expected as previous studies showed that these two genes are transcribed together as a polycistronic transcript. Therefore, insertion of the *apr* gene cassette to disrupt *ceaS1* was expected to have a polar effect on the transcription of the *bls1* gene. Similarly, when RNA of the Δ*ceaS2*-IF mutant was analyzed by RT-PCR, signals from *ceaS2* were not detected, but nor were transcripts for *bls2* and *bls1*, and only a faint band corresponding to *ceaS1* was observed (Figure 3.1.9). This indicated that transcription of *bls2* was blocked in the Δ*ceaS2*-IF mutant despite its supposedly non-polar character. Furthermore, transcription of *ceaS1* and *bls1* was severely impaired or absent in the *ceaS2* mutant. On the other hand, all tested samples showed a similar level of *hrdB*

Figure 3.1.9. Assessment of transcript levels by RT-PCR. Transcripts examined were: *ceaS1* (lanes 1, 8 and 14), *ceaS2* (lanes 2, 9 and 15), *hrdB* (lanes 3, 10 and 16), *bls1* (lanes 4, 11 and 17) and *bls2* (lanes 5, 12 and 18). RNA from wild type (WT) *S.clavuligerus*, Δ*ceaS2*-IF and Δ*ceaS1*::apra mutants grown on liquid Soy medium for 48 hours were used as the template. PCR reactions were carried out for 28 cycles. Lane M, GeneRuler 100bp DNA ladder. Lanes 6, 13 and 19 represent negative controls for each RNA sample used; no reverse transcriptase was added.

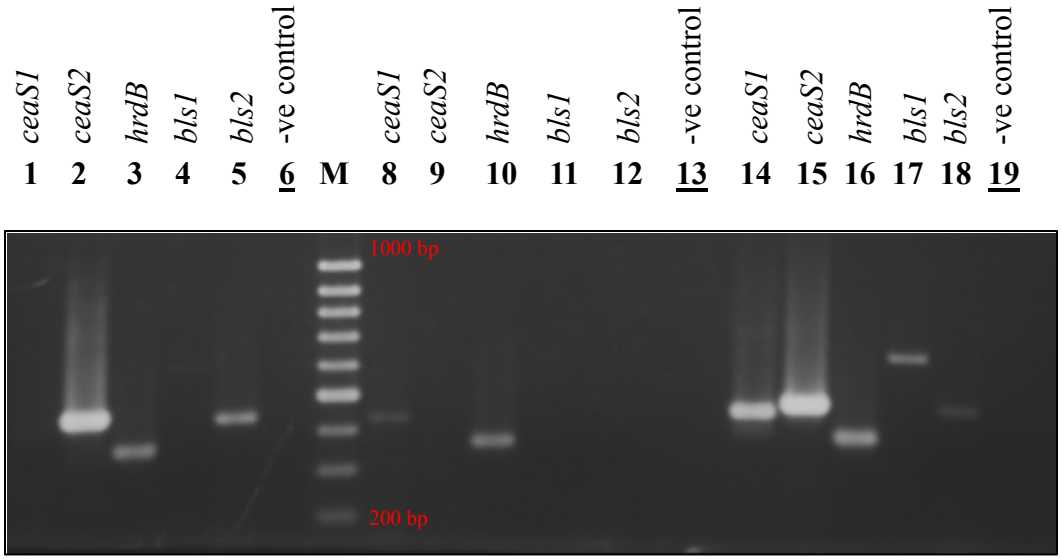
ceaS1 1
ceaS2 2
hrdB 3
bls1 4
bls2 5
-ve control 6
M
ceaS1 8
ceaS2 9
hrdB 10
bls1 11
bls2 12
-ve control 13
ceaS1 14
ceaS2 15
hrdB 16
bls1 17
bls2 18
-ve control 19
1000 bp
200 bp
ΔceaS1::apra
ΔceaS2 IF
WT S. clavuligerus

transcripts (Figure 3.1.9). RT-PCR analysis was repeated multiple times, and representative results are shown in Figure 3.1.9. The identities of the amplified PCR products, aside from product size, were also confirmed by sequencing and then compared to the known sequences of the corresponding genes (data not shown).

3.1.5.2 Investigation of transcription of other clavam biosynthetic genes in the Δ*ceaS2*-IF mutant by RT-PCR

Tight regulation of secondary metabolism is advantageous to the cell by conserving limited resources for other essential cell processes. Since *ceaS1* transcription was severely impaired and essentially all clavam production was abolished in a Δ*ceaS2*-IF mutant (Table 1.1 and 3.1), it was postulated that other 5*S* clavam-related biosynthetic genes in addition to *ceaS1* and its downstream genes, might also be regulated in a similar manner in the Δ*ceaS2*-IF mutant. Therefore, RT-PCR was undertaken to examine transcription of *cas1*, *cvm1*, *cvm5* from the clavam gene cluster (Figure 1.4) and *c6p*, *c7p*, *snk*, *res1*, *res2* and *orfA* from the paralogue gene cluster (Figure 1.5).

RNA used in this study was isolated from wild type *S. clavuligerus* and the Δ*ceaS2*-IF mutant after growing for 96 hours, in which 5*S* clavam production was at the maximal level, in Soy liquid medium. cDNA was first generated by using the reverse primers listed in Table 2.4. The primer pairs c7p RT-forward/c7p RT-reverse, ceaS1-RT-For/ceaS1-RT-Rev, ceaS2-RT-For/ceaS2-RT-Rev, cvm5 RT-forward/cvm5 RT-reverse, cvm6p RT-forward/cvm6p RT-reverse,

hrdB RT-forward/hrdB RT-reverse, orfA RT-forward/orfA RT-reverse, res1 RT-forward/res1 RT-reverse, res2 RT-forward/res2 RT-reverse and snk RT-forward/snk RT-reverse were then used for PCR amplification of 485-bp *c7p*, 433-bp *ceaS1*, 452-bp *ceaS2*, 303-bp *cvm*5, 512-bp *c6p*, 350-bp *hrdB*, 354-bp *orfA*, 312-bp *res1*, 339-bp *res2* and 339-bp *snk* RT-PCR products, respectively. PCR reactions were carried out for 25 and 30 cycles as a semi-quantitative measure to determine if transcription was completely blocked or changed to an altered level compared to WT *S. clavuligerus*. The *hrdB* transcription was again monitored as a quality control.

Bands corresponding to *cvm5*, *c6p* and *cas1* could not be observed in the Δ*ceaS2*-IF mutant (Figure 3.1.10 and 3.1.11). In contrast, transcripts of *orfA*, *snk*, *res1*, *res2* and *c7p* were detected (Figure 3.1.10, 3.1.11 and 3.1.12). Transcripts of all of these genes could be detected in WT *S. clavuligerus* (Figure 3.1.10, 3.1.11 and 3.1.12). This indicated that, in addition to *ceaS1*, the transcription of some other early *(cas1)* and late *(cvm5* and *c6p)* clavam biosynthetic genes is regulated by a common but as yet unknown mechanism, such that their transcription is blocked in *ceaS2* mutants. In contrast, transcription of the alanylclavam-specific gene, *orfA*, the elements of the two-component regulatory system, *snk, res1* and *res2*, and the pathway specific transcriptional regulator, *c7p*, are not controlled by this mechanism.

3.1.6 Promoter activity analysis by use of *egfp*

Figure 3.1.10. Assessment of *cvm5*, *c7p*, *c6p* and *hrdB* transcript levels by RT-PCR. For each gene under investigation, RNA from wild type (WT) *S. clavuligerus* (lanes 1, 6, 11 and 16), Δ*ceaS2*-IF (lanes 2, 7, 12 and 17), Δ*res2*::apra (lanes 3, 8, 13 and 18) and Δ*res1*::apra (lanes 4, 9, 14 and 19) mutants grown on liquid Soy medium for 96 hours were used as the template, respectively. (A) PCR reactions carried out for 25 cycles. (B) PCR reactions carried out for 30 cycles. Lane M, GeneRuler 100 bp DNA ladder.

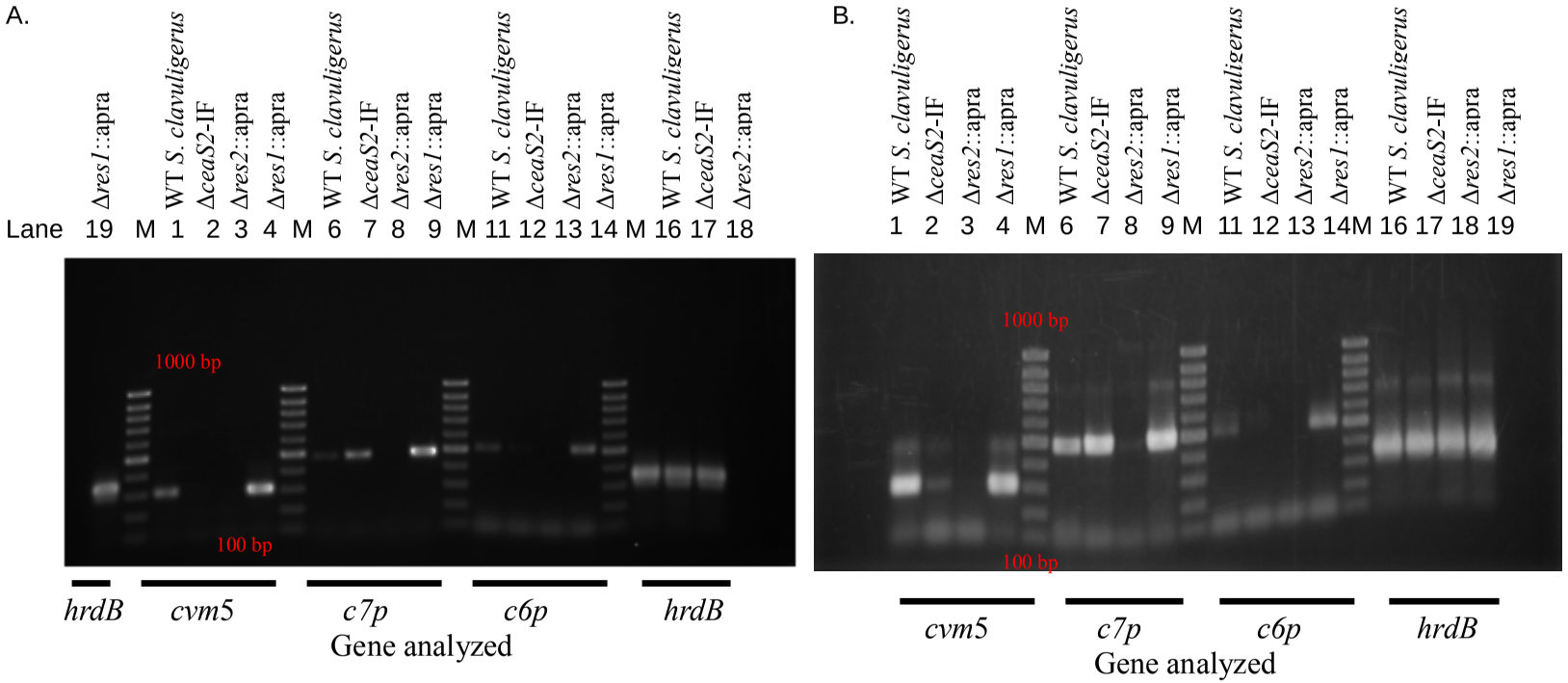
A.
Δres1::apra
WT S. clavuligerus
ΔceaS2-IF
Δres2::apra
Δres1::apra
WT S. clavuligerus
ΔceaS2-IF
Δres2::apra
Δres1::apra
WT S. clavuligerus
ΔceaS2-IF
Δres2::apra
Δres1::apra
WT S. clavuligerus
ΔceaS2-IF
Δres2::apra
Lane 19 M 1 2 3 4 M 6 7 8 9 M 11 12 13 14 M 16 17 18
1000 bp
100 bp
hrdB
cvm5
c7p
c6p
hrdB
Gene analyzed
B.
WT S. clavuligerus
ΔceaS2-IF
Δres2::apra
Δres1::apra
WT S. clavuligerus
ΔceaS2-IF
Δres2::apra
Δres1::apra
WT S. clavuligerus
ΔceaS2-IF
Δres2::apra
Δres1::apra
WT S. clavuligerus
ΔceaS2-IF
Δres2::apra
Δres1::apra
1 2 3 4 M 6 7 8 9 M 11 12 13 14M 16 17 18 19
1000 bp
100 bp
cvm5
c7p
c6p
hrdB
Gene analyzed

Figure 3.1.11. Assessment of *cas1*, *cvm1*, *res1* and *res2* transcript levels by RT-PCR. For each gene under investigation, RNA from WT *S. clavuligerus* (lanes 1, 6, 11 and 16), Δ*ceaS2*-IF (lanes 2, 7, 12 and 17), Δ*res2*::apra (lanes 3, 8, 13 and 18) and Δ*res1*::apra (lanes 4, 9, 14 and 19) mutants grown on liquid Soy medium for 96 hours were used as the template, respectively. (A) PCR reactions carried out for 25 cycles. (B) PCR reactions carried out for 30 cycles. Lane M, GeneRuler 100bp DNA ladder.

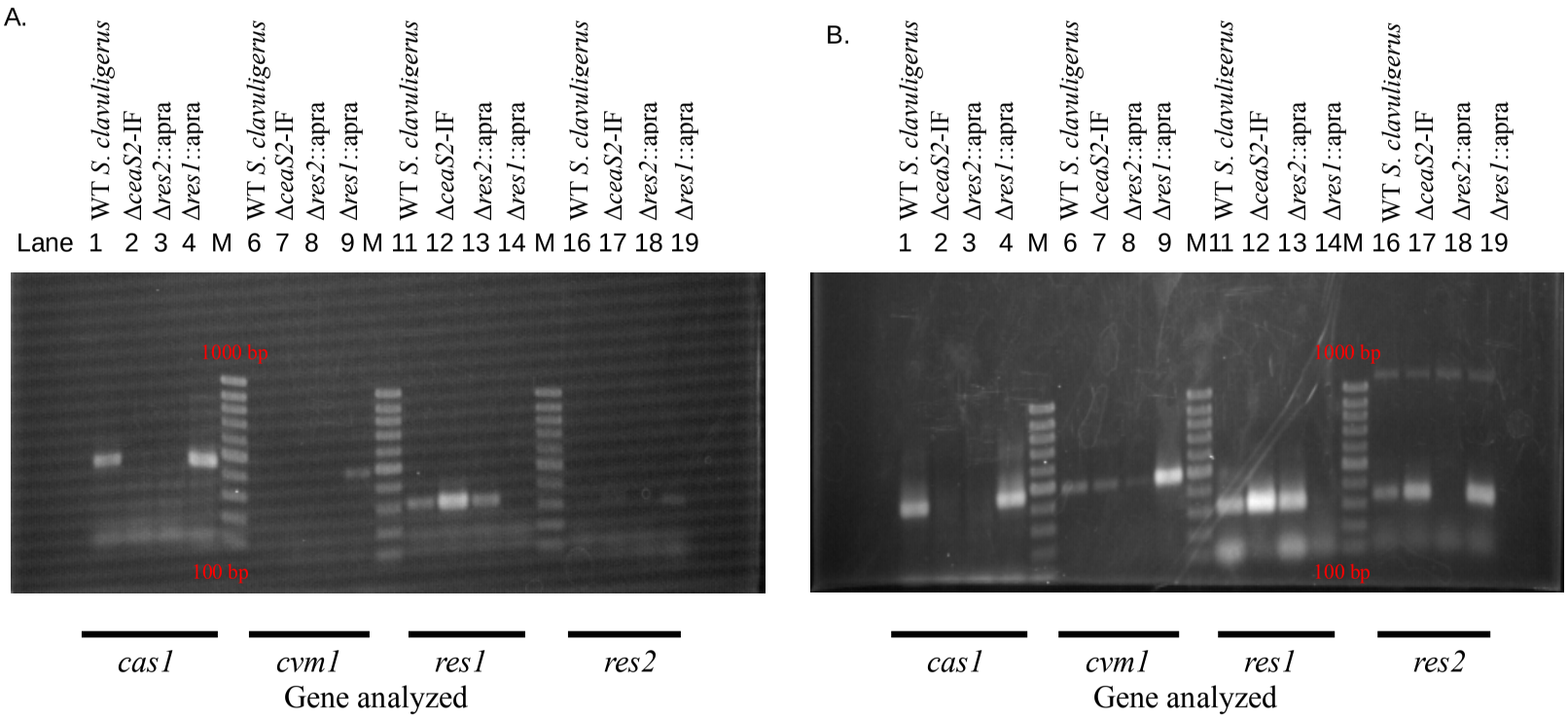
A.
WT S. clavuligerus
ΔceaS2-IF
Δres2::apra
Δres1::apra
Lane 1 2 3 4 M 6 7 8 9 M 11 12 13 14 M 16 17 18 19
1000 bp
100 bp
cas1
cvm1
res1
res2
Gene analyzed
B.
WT S. clavuligerus
ΔceaS2-IF
Δres2::apra
Δres1::apra
1 2 3 4 M 6 7 8 9 M11 12 13 14M 16 17 18 19
1000 bp
100 bp
cas1
cvm1
res1
res2
Gene analyzed

Figure 3.1.12. Assessment of *orfA*, *ceaS1*, *ceaS2* and *snk* transcript levels by RT-PCR. For each gene under investigation, RNA from WT *S. clavuligerus* (lanes 1, 6, 11 and 16), Δ*ceaS2*-IF (lanes 2, 7, 12 and17), Δ*res2*::apra (lanes 3, 8, 13 and 18) and Δ*res1*::apra (lanes 4, 9, 14 and 19) mutants grown on liquid Soy medium for 96 hours were used as the template, respectively. Lanes 21 to 24 represent negative controls for each RNA sample being used where no reverse transcriptase was added. (A) PCR reactions carried out for 25 cycles. (B) PCR reactions carried out for 30 cycles. Lane M, GeneRuler 100bp DNA ladder.

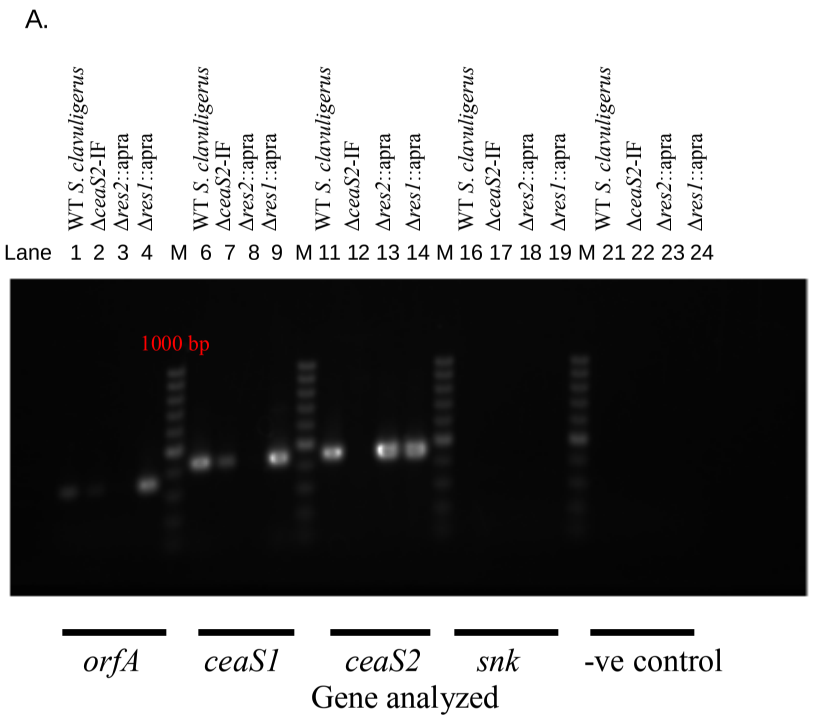
A.
WT S. clavuligerus
ΔceaS2-IF
Δres2::apra
Δres1::apra
Lane 1 2 3 4 M 6 7 8 9 M 11 12 13 14 M 16 17 18 19 M 21 22 23 24
1000 bp
orfA
ceaS1
ceaS2
snk
-ve control
Gene analyzed

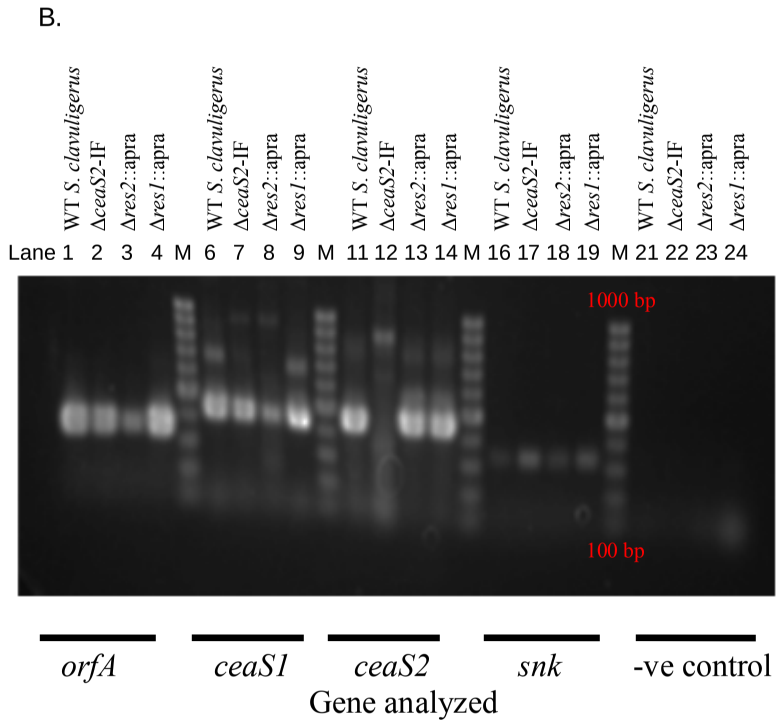
B.
WT S. clavuligerus
ΔceaS2-IF
Δres2::apra
Δres1::apra
Lane 1 2 3 4 M 6 7 8 9 M 11 12 13 14 M 16 17 18 19 M 21 22 23 24
1000 bp
100 bp
orfA
ceaS1
ceaS2
snk
-ve control
Gene analyzed

To confirm the original results obtained from RT-PCR that *ceaS1* was not transcribed efficiently in a Δ*ceaS2*-IF mutant, promoter activity of *ceaS1* was examined by using enhanced green fluorescence protein (EGFP) as a reporter. pSET-*ceaS1* carrying the promoter region of *ceaS1* coupled to a promoterless *egfp* gene previously constructed in the lab by K. Tahlan, was conjugated into the Δ*ceaS2*-IF mutant and WT *S. clavuligerus* strain, and integrated at the *attB* site on the chromosome. The resulting *S. clavuligerus* reporter strains were grown in liquid Soy medium for 48 hours. Mycelia were then harvested and analyzed by confocal microscopy to determine promoter activity by examining fluorescence due to EGFP production and excitation. Duplicates were setup for each reporter strain and fluorescence was observed when samples of WT *S. clavuligerus* carrying pSET-*ceaS1* were examined, but no fluorescence was observed from the Δ*ceaS2*-IF reporter strains (Figure 3.1.13). This indicated that the *ceaS1* promoter is not active in the Δ*ceaS2*-IF mutant.

3.1.7 Clavulanic acid production revisited

The studies described above employed cultures of *S. clavuligerus* strains grown in liquid Soy medium and showed that mutation of the *ceaS2* gene affected transcription of a large number of clavam biosynthesis related genes. However, when culture extracts of Δ*ceaS2*-IF mutants grown on solid Soy medium were obtained by the freeze and squeeze procedure and analyzed by HPLC, peaks corresponding to clavulanic acid and 5*S* clavams were detected and production of clavulanic acid was seen to be taking place at or near wild type levels (Figure 3.1.14). This unexpected production of clavam metabolites on solid medium when

Figure 3.1.13. Detection of *ceaS1* promoter activity in wild type and Δ*ceaS2* mutant strains of *S. clavuligerus* by using EGFP as a reporter. (A) Mycelia of WT *S. clavuligerus* carrying pSET-*ceaS1* reporter. (B) Mycelia of Δ*ceaS2*-IF carrying pSET-*ceaS1* reporter. Both reporter strains were grown in liquid Soy medium for 48 hours and then analyzed by confocal microscopy. Fluorescence images are shown in section 1. Differential interference contrast (DIC) images are shown in section 2.

A.

1

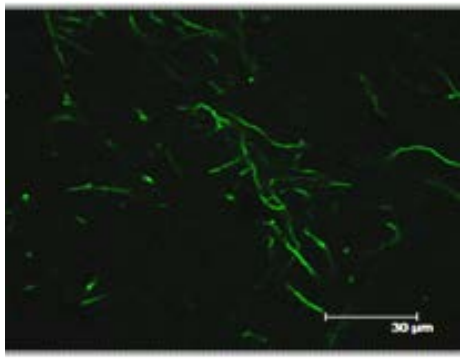

2

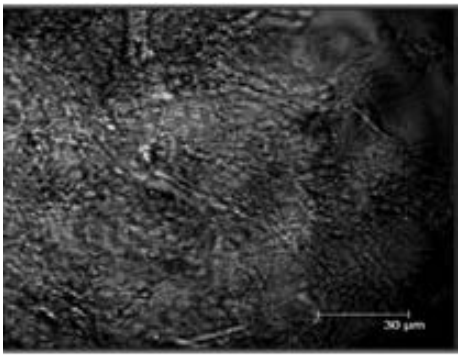

B.

1

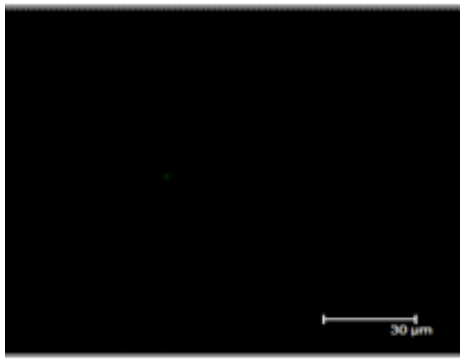

2

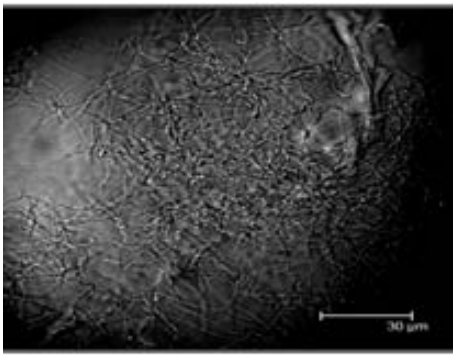

Figure 3.1.14. Clavam metabolites produced by *S. clavuligerus* and Δ*ceaS2*-IF mutants grown on solid Soy medium. Culture supernatants obtained by the freeze and squeeze procedure were diluted (1/5) and analyzed via HPLC. The peaks are as follows: AC: alanylclavam; C2C: clavam-2-carboxylate; 2HMC: 2-hydroxymethylclavam; CA: clavulanic acid.

Wild Type

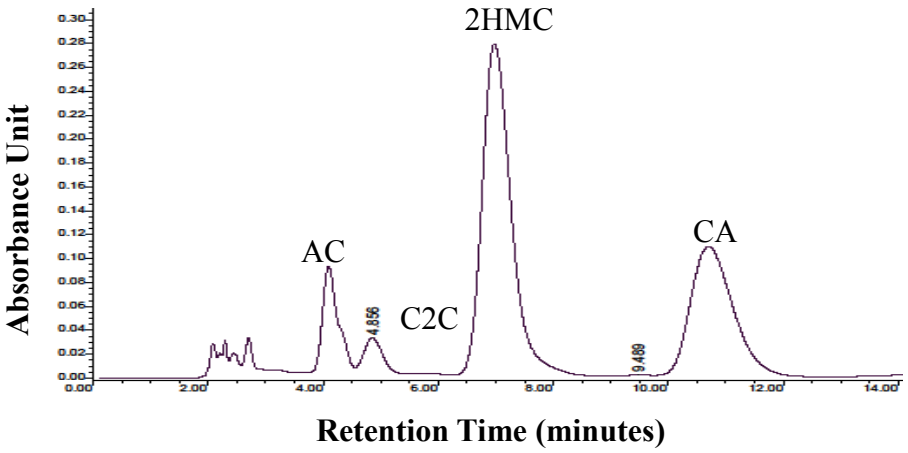

Δ*ceaS2*-IF

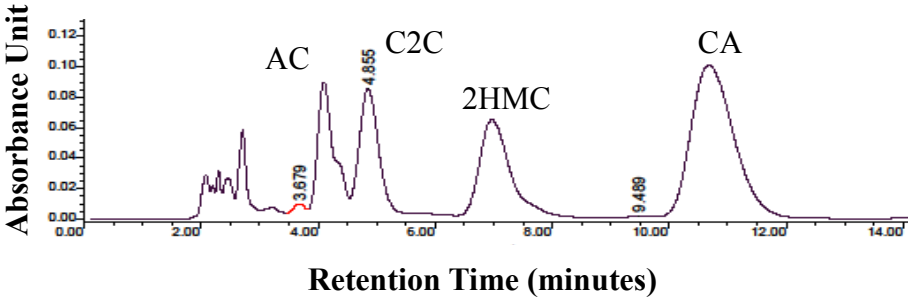

no production was seen on liquid medium suggested that the already complicated cross regulation between *ceaS2* and genes involved in clavam biosynthesis must require some additional unknown factors that are involved in sensing the physical nature of the surrounding environment. Under this scenario, it would be difficult to resolve and identify the factor(s) that may be involved. Therefore, the focus of this study was switched to investigate the regulatory elements that control the late steps of the 5*S* clavam biosynthetic pathway.

3.2 Analysis of the regulation of the late steps of 5*S* clavam biosynthesis

Previous studies have shown that a number of genes, including *cvm1*, *cvm2*, *cvm5* and *c6p*, encoding apparent biosynthetic enzymes, are specifically required for 5*S* clavam biosynthesis but not for clavulanic acid production (Tahlan *et al*., 2007; Zelyas, 2007). Furthermore, it has also been shown that disruption of *res2*, *snk* or *c7p*, encoding apparent regulatory proteins, abolished 5*S* clavam production (Zelyas, 2007). Due to the close proximity of these regulatory genes to 5*S* clavam biosynthetic enzyme genes (Figure 1.5), it was suspected that they may play a role in regulating expression of the genes responsible for 5*S* clavam production. Studies were therefore initiated to investigate how the transcriptional regulator, C7P, and the two-component system control 5*S* clavam production.

3.2.1 Phenotype of Δ*snk*-IF, Δ*res1*::apra, Δ*res2*::apra and Δ*c7p*::apra mutants

In view of the observation that growth medium type (solid agar plate versus liquid) had a tremendous and unanticipated effect on Δ*ceaS2*-IF mutant phenotype as described in section 3.1.8, it was first essential to examine the

clavam production profiles of Δ*snk*-IF, Δ*c7p*::apra, Δ*res2*::apra and Δ*res1*::apra mutant strains to ensure that their phenotypes did not depend on the physical form of the medium. Various mutant strains were grown on solid Soy medium for 7 to 10 days and culture extracts were obtained by using the freeze and squeeze procedure and analyzed by HPLC. Clavulanic acid was detected in the culture extracts from all of these mutants (Figure 3.2.1). Alanylclavam, clavam-2-carboxylate, 2-hydroxymethylclavam and 2-formyloxymethylclavam were not detected in extracts from Δ*snk*-IF, Δ*res2*::apra and Δ*c7p*::apra mutants while Δ*res1*::apra mutants still capable of producing clavam metabolites (Figure 3.1.14 and 3.2.1). Each of these mutants was shown to have the same phenotype as was observed previously when grown in liquid medium (Zelyas, 2007).

3.2.2 Transcript analysis by RT-PCR

Since Res2 and C7P, encoded by *res2* and *c7p* respectively, are apparent regulatory proteins, it was postulated that these two proteins may control the transcription of genes involved in 5*S* clavam production. RT-PCR was carried out to investigate this hypothesis. Analysis was carried out multiple times and representative results are shown in the following figures.

RNA used in this study was isolated from wild type *S. clavuligerus*, Δ*snk*-IF, Δ*c7p*::apra, Δ*res1*::apra and Δ*res2*::apra mutants after growing for 96 hours in Soy liquid medium. The reverse primers (Table 2.4) used to generate cDNA and specific primer pairs used to amplify RT-products were described previously 3.1.6.2, and listed in Table 2.4. PCR reactions were carried out for 25 and 30

Figure 3.2.1. Clavam metabolites produced by Δ*snk*-IF, Δ*res2*::apra, Δ*c7p*::apra and Δ*res1*::apra mutants grown on solid Soy medium. Culture supernatants obtained by the freeze and squeeze procedure were diluted (1/5) and analyzed via HPLC. The peaks are as follows: AC: alanylclavam; C2C: clavam-2-carboxylate; 2HMC: 2-hydroxymethylclavam; CA: clavulanic acid.

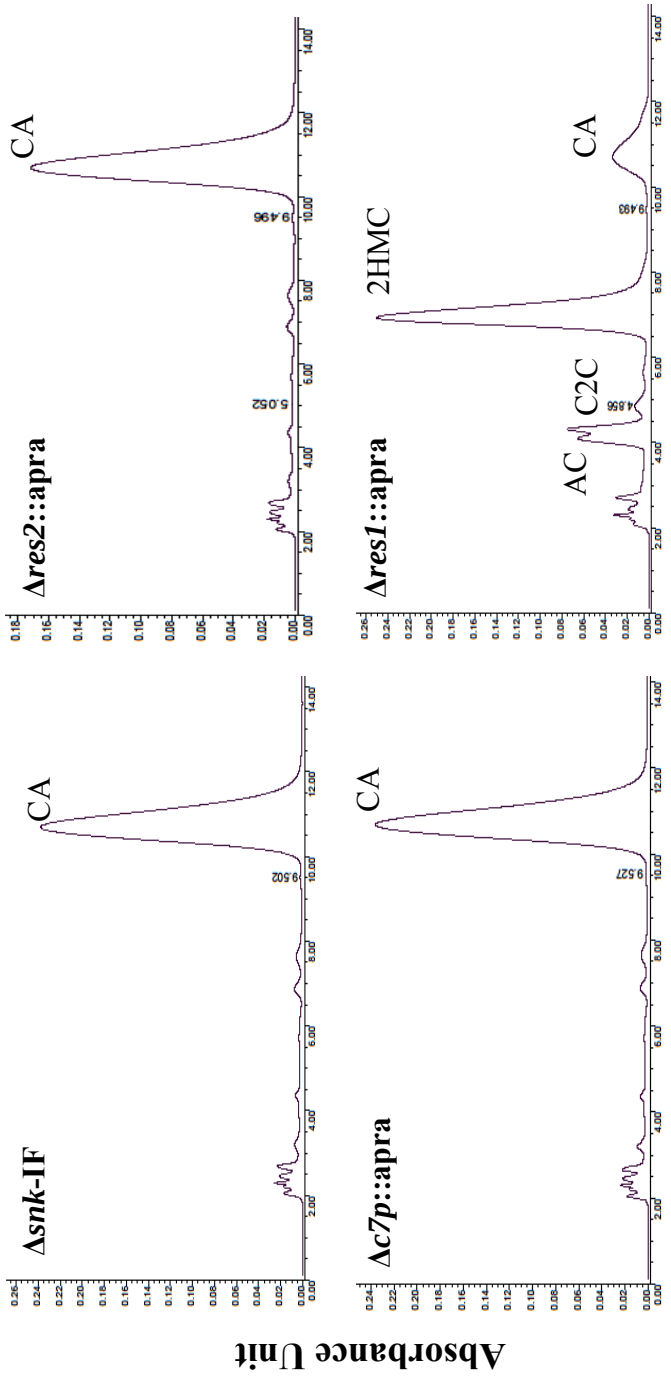
Δsnk-IF
CA
9.502
Δres2::apra
CA
9.496
5.052
Δc7p::apra
CA
9.527
Δres1::apra
2HMC
AC
C2C
4.856
CA
9.480
Absorbance Unit
Retention Time (minutes)

cycles as a semi-quantitative measure to determine if transcription was blocked or genes were transcribed at an altered level compared to WT *S. clavuligerus*. The *hrdB* transcription again served as a control.

Transcripts of *cvm1*, *cvm5*, *c7p* and *c6p*, which are all essential for 5*S* clavam biosynthesis, could not be detected, or were transcribed at greatly reduced levels, in Δ*snk*-IF or Δ*res2*::apra mutants as determined by RT-PCR (Figure 3.1.10, 3.1.11, 3.2.2 and 3.2.4). Interestingly, *cas1* transcripts were not detected in these mutants, suggesting that this two-component system also controls transcription of some of the early genes (Figure 3.1.11 and 3.2.2). Similarly, transcripts of *cvm1*, *cvm5* and *cas1* were not detected when RNA isolated from a Δ*c7p*::apra mutant was subjected RT-PCR (Figure 3.2.2). Transcription of *c7p* was abolished or reduced in *res2* and *snk* mutants, respectively, but transcription of *snk*, *res1* and *res2*, the genes of the two-component system, was not affected in a *c7p* mutant (Figure 3.1.10, 3.2.3 and 3.2.4). This indicated that the two-component system operates at a higher level in the regulatory hierarchy than C7P. *cvm1* and *orfA* transcripts were detected at elevated levels in a Δ*res1*::apra mutant (Figure 3.1.11 and 3.1.12). Despite the differences in transcription profiles from various strains, *hrdB* transcripts were detected at similar levels in all samples tested, thus validating the results obtained (Figure 3.1.10 and 3.2.2). Transcription profiles of various strains being tested in this study are summarized in Table 3.2.

3.2.3 Protein overproduction and purification

Figure 3.2.2. Assessment of *cas1*, *cvm5*, *cvm1* and *hrdB* transcript levels by RT-PCR. For each gene under investigation, RNA from Δ*ceaS1*::apra (lanes 1, 5, 9 and 13), Δ*c7p*::apra (lanes 2, 6, 10 and 14) and Δ*snk*-IF (lanes 3, 7, 11 and 15) mutants grown on liquid Soy medium for 96 hours were used as the template, respectively. Lanes 16 to 18 represents negative control for each RNA sample being used where no reverse transcriptase was added. (A) PCR reactions carried out for 25 cycles. (B) PCR reactions carried out for 30 cycles. Lane M, GeneRuler 100bp DNA ladder.

A.

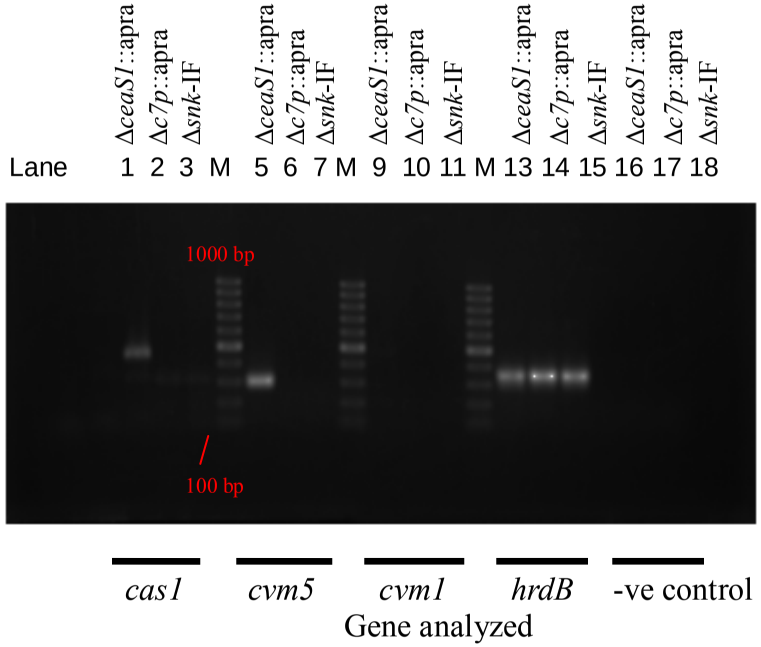
ΔceaS1::apra
Δc7p::apra
Δsnk-IF
Lane 1 2 3 M 5 6 7 M 9 10 11 M 13 14 15 16 17 18
1000 bp
100 bp
cas1
cvm5
cvm1
hrdB
-ve control
Gene analyzed

B.

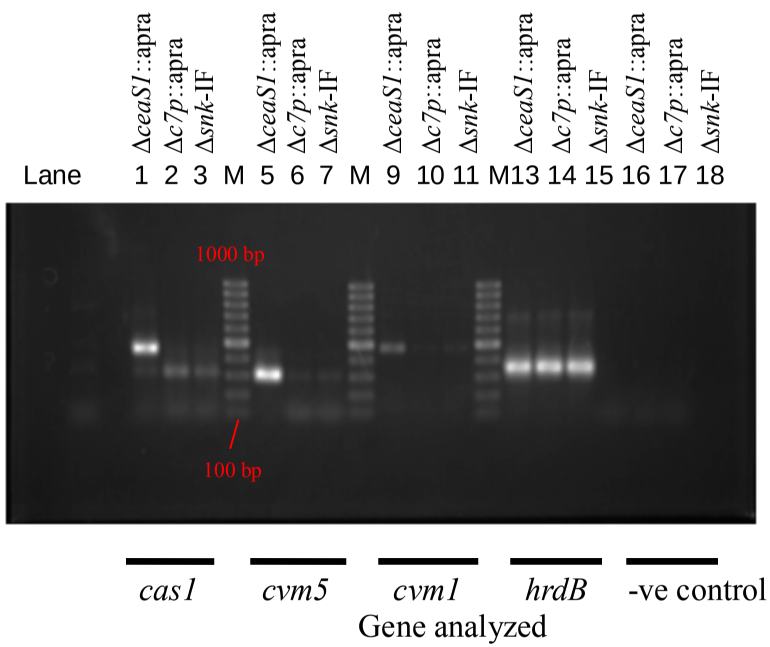
ΔceaS1::apra
Δc7p::apra
Δsnk-IF
Lane 1 2 3 M 5 6 7 M 9 10 11 M13 14 15 16 17 18
1000 bp
100 bp
cas1
cvm5
cvm1
hrdB
-ve control
Gene analyzed

Figure 3.2.3. Assessment of *res1, res2*, *snk* and *orfA* transcript levels by RT-PCR. For each gene under investigation, RNA from Δ*ceaS1*::apra (lanes 1, 5, 9 and 13), Δ*c7p*::apra (lanes 2, 6, 10 and 14) and Δ*snk*-IF (lanes 3, 7, 11 and 15) mutants grown on liquid Soy medium for 96 hours were used as the template, respectively. (A) PCR reactions carried out for 25 cycles. (B) PCR reactions carried out for 30 cycles. Lane M, GeneRuler 100bp DNA ladder.

A.

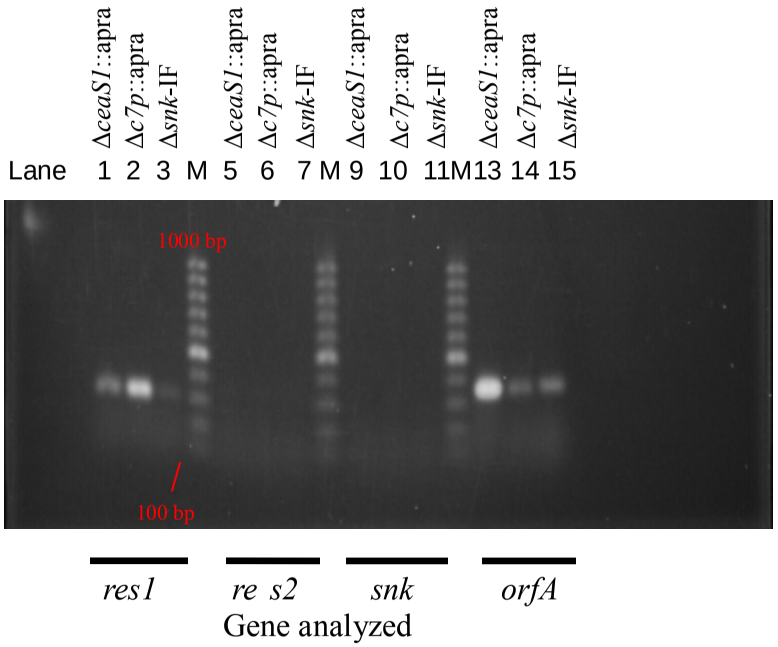
ΔceaS1::apra
Δc7p::apra
Δsnk-IF
Lane 1 2 3 M 5 6 7 M 9 10 11 M 13 14 15
1000 bp
100 bp
res1
re s2
snk
orfA
Gene analyzed

B.

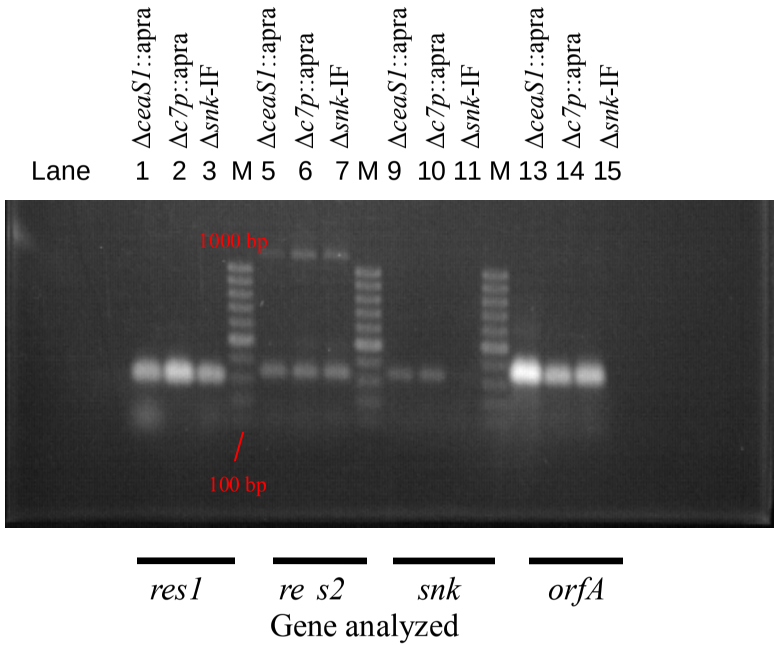
ΔceaS1::apra
Δc7p::apra
Δsnk-IF
Lane 1 2 3 M 5 6 7 M 9 10 11 M 13 14 15
1000 bp
100 bp
res1
re s2
snk
orfA
Gene analyzed

Figure 3.2.4. Assessment of *ceaS1*, *ceaS2*, *c6p* and *c7p* transcript levels by RT-PCR. For each gene under investigation, RNA from Δ*ceaS1*::apra (lanes 1, 5, 9 and 13), Δ*c7p*::apra (lanes 2, 6, 10 and 14) and Δ*snk*-IF (lanes 3, 7, 11 and 15) mutants grown on liquid Soy medium for 96 hours were used as the template, respectively. (A) PCR reactions carried out for 25 cycles. (B) PCR reactions carried out for 30 cycles. Lane M, GeneRuler 100bp DNA ladder.

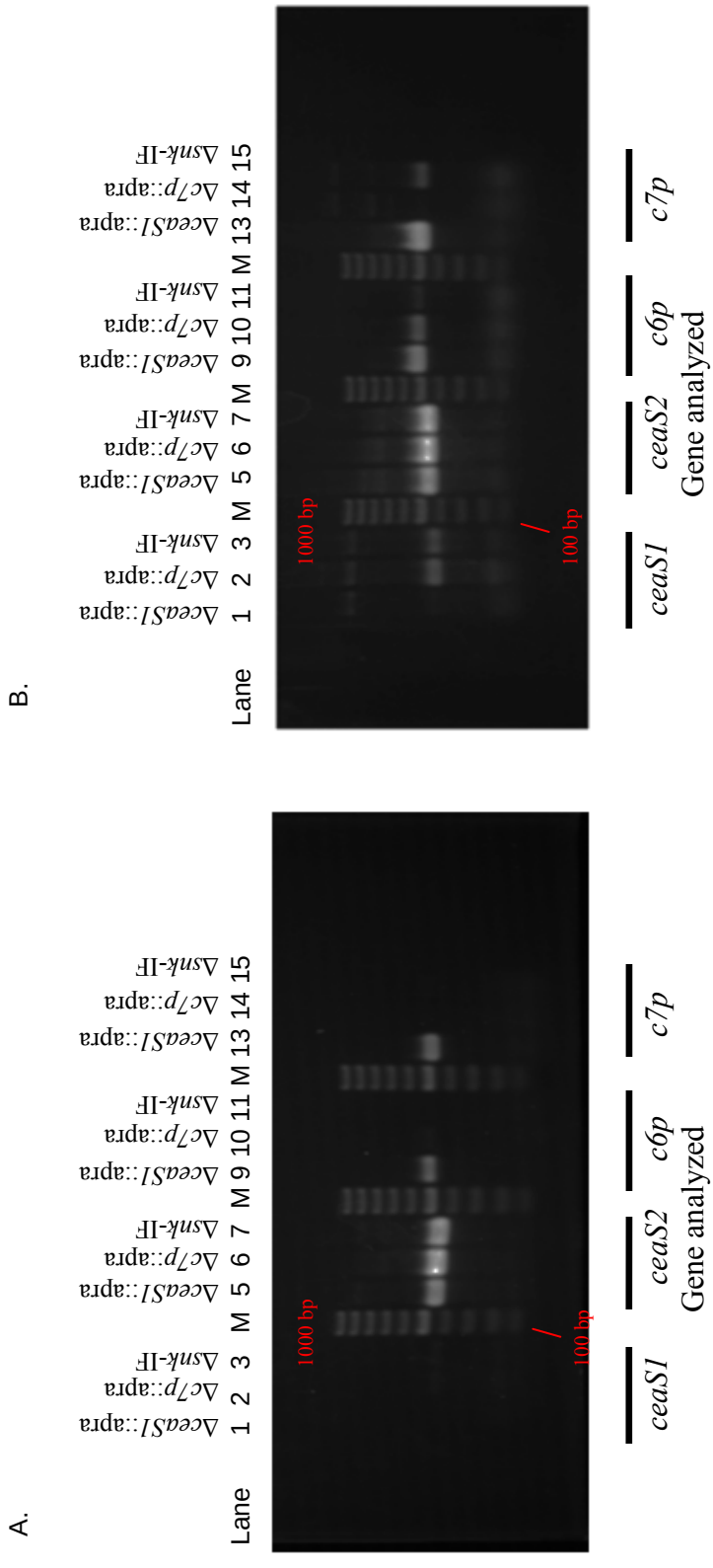
A.
B.
Lane
1 2 3 M 5 6 7 M 9 10 11 M 13 14 15
Δceas1::apra
Δc7p::apra
ΔsnkIF
1000 bp
100 bp
ceaS1
ceaS2
c6p
c7p
Gene analyzed

Table 3.2. Transcription profile of various *S. clavuligerus* strains as determined by RT-PCR.

Strain	*hrd*B	*orfA*	*ceaS1*	*ceaS2*	*snk*	*res1*	*res2*	*cvm1*	*cvm5*	*cas1*	*c6p*	*c7p*
Wild type *S.clavuligerus*	+	+	+	+	+	+	+	+	+	+	+	+
Δ*ceaS1*::apra	+	+	-	+	+	+	+	+	+	+	++	+
Δ*ceaS2*-IF	+	+	+ [a]	-	+	++	++	+	+/-	-	-	++
Δ*snk*-IF	+	+	+/-	+	-	+	+	+/-	-	-	+/-	+/-
Δ*res1*::apra	+	++	++	+	+	-	++	++	++	+	++	++
Δ*res2*::apra	+	+/-	+/-	+	+	+	-	+/-	-	-	-	-
Δ*c7p*::apra	+	+	+	+	+	++	+	+/-	-	-	+	-

-: transcripts could not be detected at 30 cycles
+: transcripts were detected at 30 cycles.
++: stronger signal was observed compared to WT *S. clavuligerus.*
+/-: transcripts could not be detected at 25 cycles and showed weaker signal compared to wild type *S. clavuligerus* at 30 cycles.
[a]: although *ceaS1* transcript was observed at 25 cycles in the Δ*ceaS2*-IF mutant, the signal is weaker than WT *S. clavuligerus*

BLAST analysis of the C7P and Res2 amino acid sequences predicted the presence of a DNA binding domain within each protein (data not shown). In order to carry out *in vitro* protein assays to examine if these two proteins bind DNA, it was necessary to obtain large quantities of Res2 and C7P proteins.

3.2.3.1 Res2-His_7 overproduction and purification

To obtain purified Res2, the *res2* coding sequence was cloned (by N. Zelyas) as an *Nde*I/*Bam*HI fragment upstream of a 7 x histidine tag in the *E. coli* protein expression plasmid, pT7-7His. Production of Res2-His_7 was driven by a T7 promoter and was induced by addition of 0.4 mM IPTG to activate expression of a T7 RNA polymerase-encoding gene, followed by incubation at 37^{o}C for 5 hours. Cells were harvested by centrifugation, stored frozen overnight and then treated with lysozyme and sonicated to release overproduced protein. The lysate was then centrifuged to remove cell debris and Res2-His_7 was purified from the soluble protein fraction.

Since overproduced Res2 carried a 7 x His-tag at the C-terminus, it was purified by combining the soluble protein fraction obtained from above with Ni-NTA resin under conditions where His-tagged protein binds to the resin and can thus be separated from the bulk proteins in the lysate. The entire mixture was incubated for one hour at 4ºC and after washing away unbound proteins, bound protein was eluted by using a gradient of imidazole. Each collected fraction was electrophoresed on a 12% SDS-PAG to identify fractions that contained the desired protein, which has an expected molecular weight of about 25 kDa (Figure

Figure 3.2.5. Purification of Res2-His_7 from *E. coli* BL21(DE3) carrying pT7-7His-*res2*. Protein samples were taken at different stages of the overproduction and purification processes and analyzed by SDS-PAGE. Proteins were visualized by staining with Coomassie blue. Lane M, PageRuler™ prestained Protein Ladder Plus molecular weight marker. Lane NI, non-induced total protein sample. Lane I, induced total protein sample. Lane CL, cleared lysate. Lane WT, wash-through. Numbers above lanes indicate the concentration of imidazole (in mM) used to elute the protein samples.

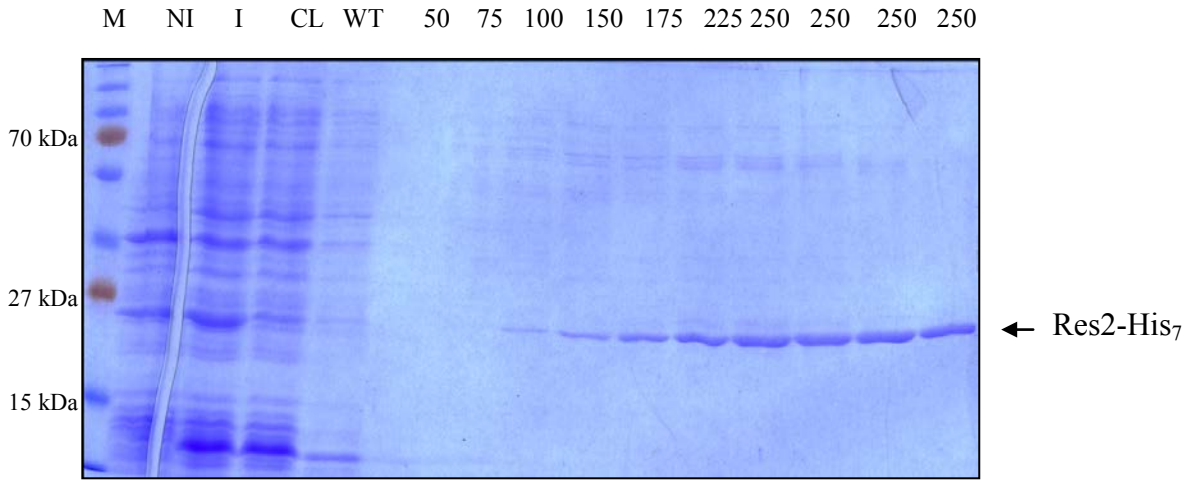
M NI I CL WT 50 75 100 150 175 225 250 250 250 250
70 kDa
27 kDa
15 kDa
Res2-His7

3.2.5). Fractions identified as containing Res2-His_7 were then pooled and concentrated using centrifugal concentrators with a molecular weight cutoff of 10 kDA, resuspended in protein storage buffer and stored at -80^{o}C.

3.2.3.2 Construction of a C7P overexpression vector

An *E. coli* strain expressing *c7p* was prepared in order to obtain C7P protein to assess C7P-DNA interactions. The strategy using plasmid pSET152-*snk*-*c7p* and TOPO-*c7p* (Table 2.3) to prepare this strain is outlined in Figure 3.2.6. pSET152-*snk*-*c7p* was originally constructed as a *S. clavuligerus* integrative plasmid used to complement *c7p* mutants. In order to clone the *c7p* gene into the protein expression vector pET19b as an *Nde*I/*Hin*dIII fragment, a 585 bp fragment encompassing the 5' end of *c7p* with a *Nde*I restriction site engineered at the start codon was amplified by PCR and cloned into pCR®2.1-TOPO® to obtain TOPO-*c7p* (by S. E. Jensen). pSET152-*snk*-*c7p* was digested with *EcoR*I and *Xba*I and the desired *snk*-*c7p* fragment was cloned into pUC119 to obtain pUC119-*snk*-*c7p* (by S. E. Jensen). TOPO-*c7p* was digested with *EcoR*I and *BstX*I and the DNA fragment corresponding to the 5' end of *c7p* with the engineered *Nde*I site was gel purified after electrophoresis on 1% agarose gel (Figure 3.2.7). The desired fragment was then ligated with gel purified pUC119-*snk*-*c7p* after *EcoR*I/*BstX*I double digestion (Figure 3.2.7) to obtain pUC119-*c7p*-complete. The entire coding sequence of *c7p* was then cloned into the *E. coli* protein expression plasmid pET-19b as an *Nde*I/*Hind*III fragment, resulting in the construction of pET-19b-*c7p*. The insertion and ligation of the correct fragment was confirmed by using restriction analysis.

Figure 3.2.6. Schematic of the process leading to the construction of pET-19b-*c7p*. Restriction sites utilized in the process are shown in the diagrams.

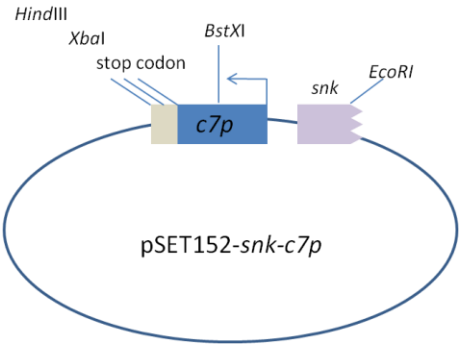

*EcoR*I/*Xba*I digestion

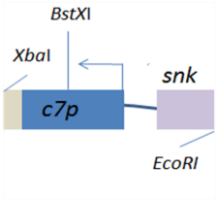

Ligation with *Xba*I/*EcoR*I digested pUC119

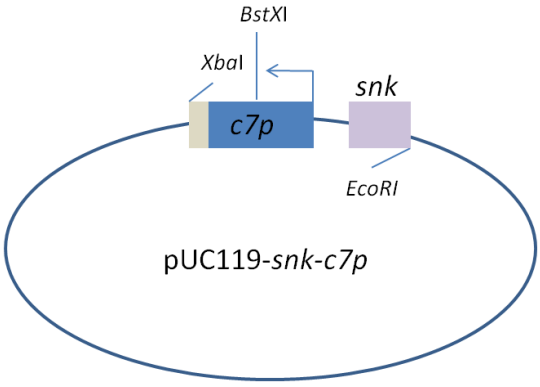

Figure 3.2.6. (Continued). Schematic of the process leading to the construction of pET-19b-*c7p*. Restriction sites utilized in the process are shown in the diagrams.

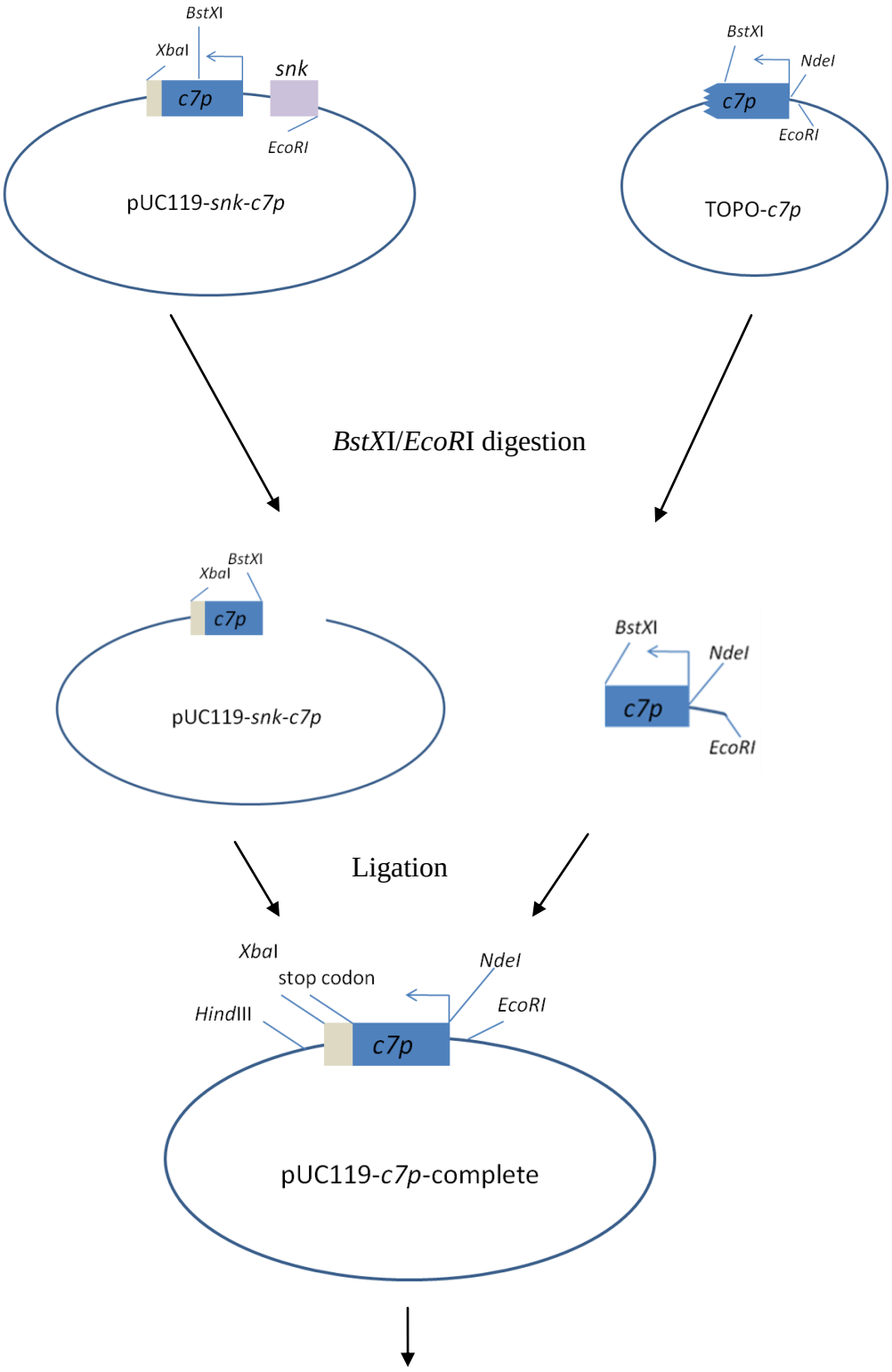

Cloned into pET19b as *Nde*I/*Hind*III fragment to obtain pET-19b-*c7p*

Figure 3.2.7. DNA fragments used to construct the *c7p* expression vector. Lane M, λ *BstE*II DNA marker. Lane 1, uncut pUC119-*snk*-*c7p*. Lane 2, pUC119-*snk*-*c7p* digested with *BstX*I. Lane 3, pUC119-*snk*-*c7p* digested with *EcoR*I and *BstX*I. Lane 4, purified ~585bp fragment encompassing the 5' end of *c7p*.

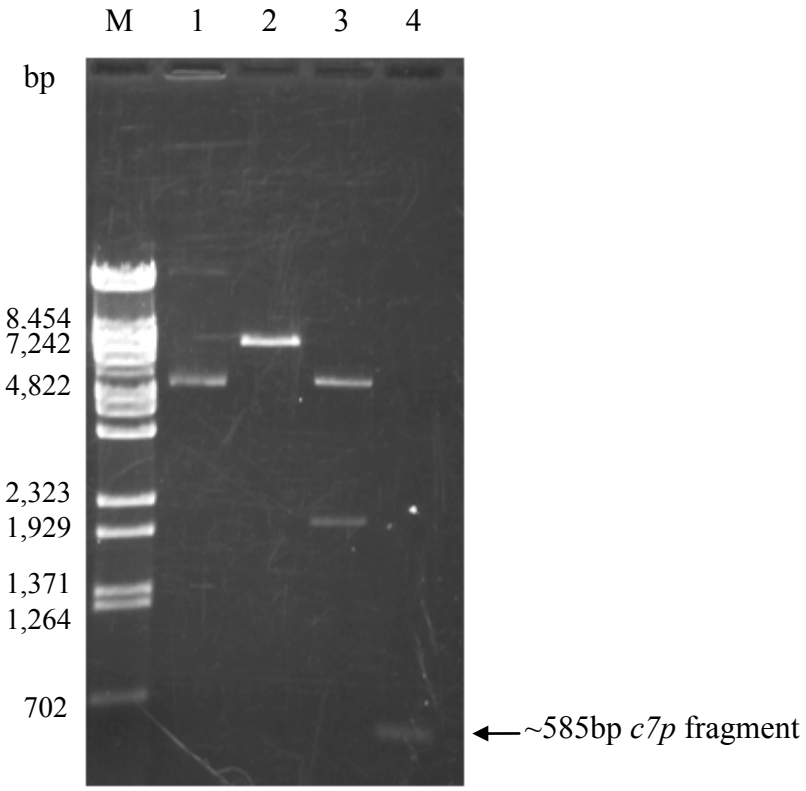
M
1
2
3
4
bp
8,454
7,242
4,822
2,323
1,929
1,371
1,264
702
~585bp c7p fragment

DNA fragments corresponding to the ~2.45 kb *c7p* gene and the ~5.72 kb pET-19b plasmid vector were observed after *Nde*I/*Hind*III restriction digestion (Figure 3.2.8). This plasmid was then transformed into *E. coli* DH5α for long term storage and subsequently into BL21(DE3) for expression.

3.2.3.3 His_{10}-C7P overproduction and purification

The *c7p* coding sequence was positioned in-frame downstream of a 10 x histidine tag in pET-19b. Production of His_{10}-C7P was driven by a T7 promoter and was initiated by addition of 1 mM IPTG, which induced production of T7 RNA polymerase, followed by incubation for 7 hours at 21°C. Cells were harvested, frozen overnight and then treated to release overproduced protein as described in Section 2.9.5. The lysate was then centrifuged to remove cell debris and His_{10}-C7P was purified from the soluble protein fraction.

His_{10}-C7P was purified by combining the soluble protein fraction with Ni-NTA resin and incubated for an hour at 4ºC. Protein was eluted from the washed resin by using a gradient of imidazole and each collected fraction was electrophoresed on 8% SDS-PAG to identify fractions that contained the desired protein. A high purity preparation of His_{10}-C7P could not be obtained as multiple protein bands, beside the expected 89 kDa protein band, were observed on the gel when stained with Coomassie Blue (Figure 3.2.9). This indicated that the conditions used were not optimal for C7P production. Despite various attempts to improve C7P production, which included changing the expression temperature from 21°C to 15°C or 37°C, changing the amount of IPTG added (from 1 mM to

Figure 3.2.8. Restriction analysis of pET-19b-*c7p* protein expression vector. Lane M, λ *BstE*II DNA marker. Lane 1, uncut pET-19b-*c7p*. Lane 2, pET-19b-*c7p* digested with *Nde*I/*Hind*III.

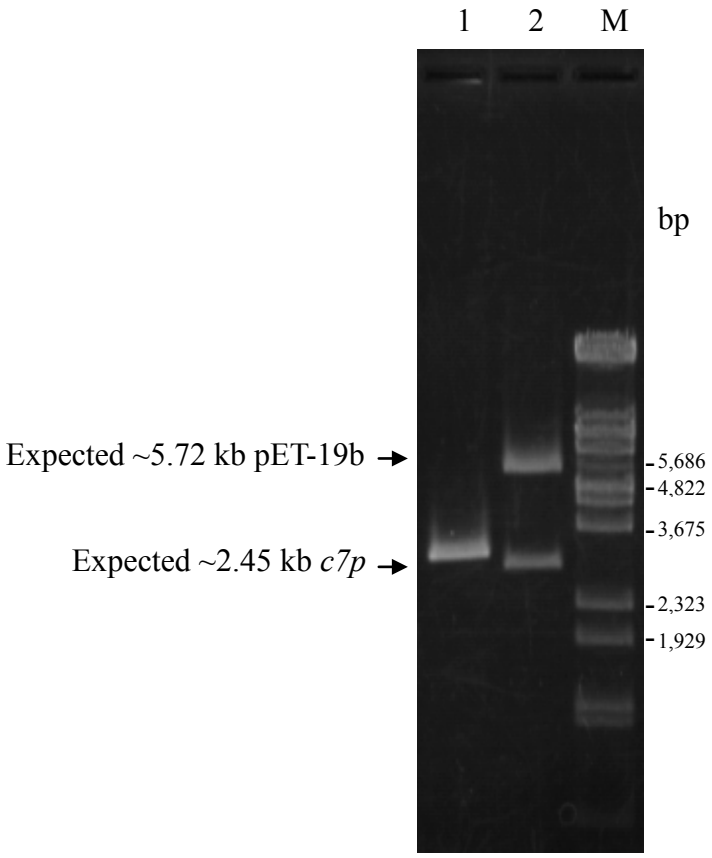
1
2
M
bp
Expected ~5.72 kb pET-19b
Expected ~2.45 kb c7p
5,686
4,822
3,675
2,323
1,929

Figure 3.2.9. Purification of His_{10}-C7P from *E. coli* BL21(DE3) carrying pET-19b-*c7p*. Protein samples were taken at different stages of the overexpression and purification processes and analyzed by SDS-PAGE. Proteins were visualized by staining with Coomassie blue. Lane M, PageRuler™ prestained Protein Ladder Plus molecular weight marker. Lane I, induced total protein sample. Lane CL, cleared lysate. Lane WT, wash-through. The number above each lane indicates the concentration of imidazole (in mM) used to elute the protein samples.

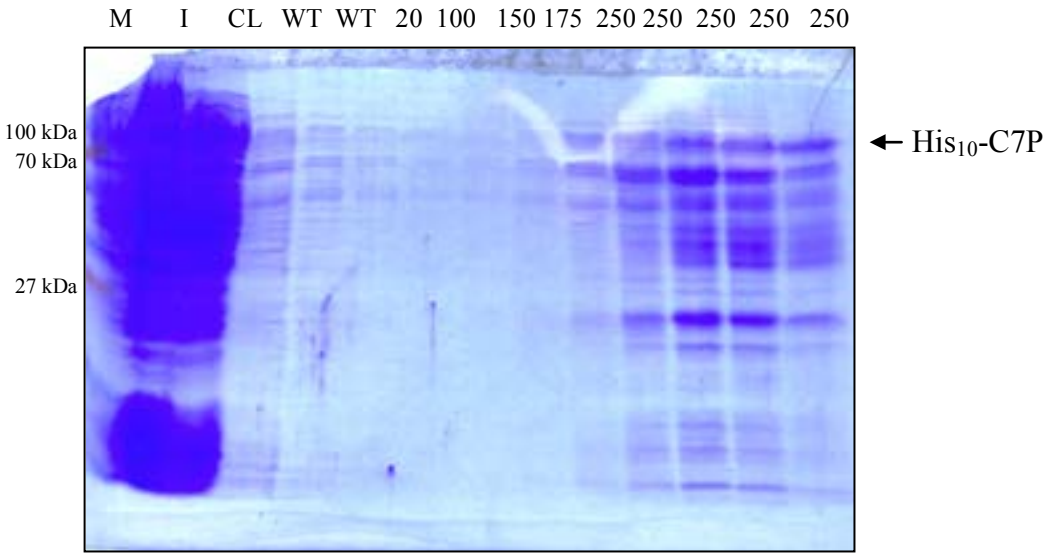
M
I
CL
WT
WT
20
100
150
175
250
250
250
250
250
100 kDa
70 kDa
27 kDa
His10-C7P

0.4 mM) to induce protein production and addition of protease inhibitors to inhibit protein degradation, similar expression patterns were observed (data not shown). It is possible that C7P, as a transcriptional regulator, is not stable and has a high turnover rate to ensure a dynamic response. C7P might have started to degrade once produced in BL21(DE3) even before lysis of the cells. Therefore, fractions containing the desired protein from the initial expression were concentrated using centrifugal concentrators to give a preparation enriched in His_{10}-C7P, and stored at -80^{o}C for future use after resuspending in protein storage buffer.

3.2.4 Protein-DNA interactions

Protein-sequence analysis of C7P and Res2 indicated that these two proteins have DNA-binding domains, which suggests they may exert their effects by binding to promoter regions of their targets. Electrophoretic mobility shift assays (EMSAs) were carried out to investigate this hypothesis. All EMSA work described below was carried out multiple times with various condition changes and the best results are shown in the following figures.

3.2.4.1 Analysis of Res2-DNA interactions by EMSA

Once Res2-His_7 was purified (Section 3.2.3.1), EMSAs were carried out to determine the ability of Res2 to bind to putative promoter regions of genes identified as potential targets from RT-PCR analyses (Section 3.2.2). Since the promoter regions of the potential targets have not been identified, a variety of DNA fragments, which covered the entire intergenic region between these genes as illustrated in Figure 3.2.10, were used to assess binding ability of Res2.

Figure 3.2.10. DNA probes for electrophoretic mobility shift assays of various targets identified by RT-PCR. Primer pairs used to generate each probe are listed to the right of its name along with the probe size in bp. Figures not drawn to scale.

Probes for Electrophoretic Mobility Shift Assays

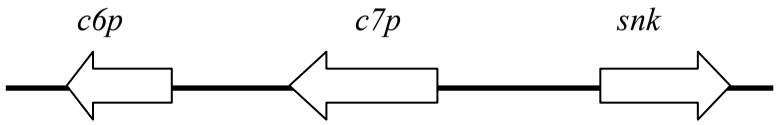

	Primers	Size (bp)
PCR1	ANW 48/49	408
PCR2	ANW 50/51	319
PCR3	ANW 52/53	406

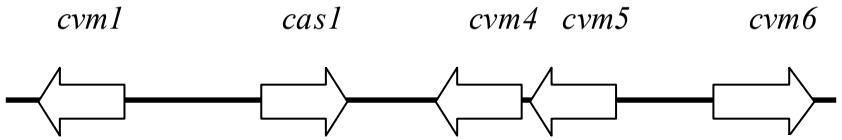

	Primers	Size (bp)
PCR4	ANW 58/59	347
PCR5	ANW 54/55	245
PCR6	ANW 56/57	454

Purified Res2-His_7 (100 pmol) was incubated with each ^{32}P end-labeled DNA probe, which had been amplified by PCR using cosmid pCEC018, pEC020 or p5N14E10 as the template, and purified by the "crush and soak" method (Section 2.7.7). Reactions were carried out in the presence of excess poly d(I-C) as non-specific DNA competitor. The reaction mixtures were electrophoresed on 8% non-denaturing PAG to determine whether or not there were DNA-protein complexes. Except for the samples containing PCR3, which is a region upstream of both of *c7p* and *snk*, shifting of the probes was not observed in other samples (Figure 3.2.11). This indicated a possible Res2-DNA complex formation with DNA fragment PCR 3 and suggested that Res2 binds and controls transcription of *c7p* and/or *snk*. Although the probe was clearly shifted, the protein-DNA complex was trapped in the loading well suggesting that either a very large protein-DNA complex was formed or the conditions used were not optimal for Res2 binding. Attempts were made to improve the shifting quality. This included varying the protein and DNA concentrations, changing the buffer and running conditions. However, none of the changes helped significantly to resolve the situation.

3.2.4.2 Analysis of C7P-DNA interaction by EMSA

C7P was also subjected to EMSA to determine its ability to bind to the DNA fragments described previously (Figure 3.2.10). The binding reaction mixtures were electrophoresed on a 6% non-denaturing PAG to determine the presence of a DNA-protein complex. A shifted band was observed when DNA fragment PCR 6, which is the region upstream of *cvm1* and *cas1* (Fig 3.2.12), was incubated with His_{10}-C7P in the binding reaction. Moreover, addition of 50-fold

Figure 3.2.11. Analysis of binding of Res2-His_7 to promoter regions of genes in the clavam and paralogue gene clusters. DNA probe used corresponds to intergenic regions between *c7p* and *c6p* (PCR1), *snk* and *c7p* (PCR2, 3), *cvm5* and *cvm6* (PCR4), and *cvm1* and *cas1* (PCR5 and 6). Reactions were set up in a total volume of 20 µl by mixing 20 fmol of each ^{32}P end- labeled fragment with 100 pmol of purified Res2-His_7 protein in binding buffer containing 10 mM Tris-HCl (pH 8.0), 1 mM DTT, 10% glycerol, 150 mM NaCl and 1 µg of poly d(I-C). Binding reactions were carried out at 21^{o}C for 25 minutes. Samples were separated on 1.5% glycerol-containing 8% non-denaturing PAG in 1X Tris-glycine buffer. Gels were dried for 45 minutes, placed on a phosphor screen and exposed for 16 hours. *Data in these figures were obtained by Annie Wong.*

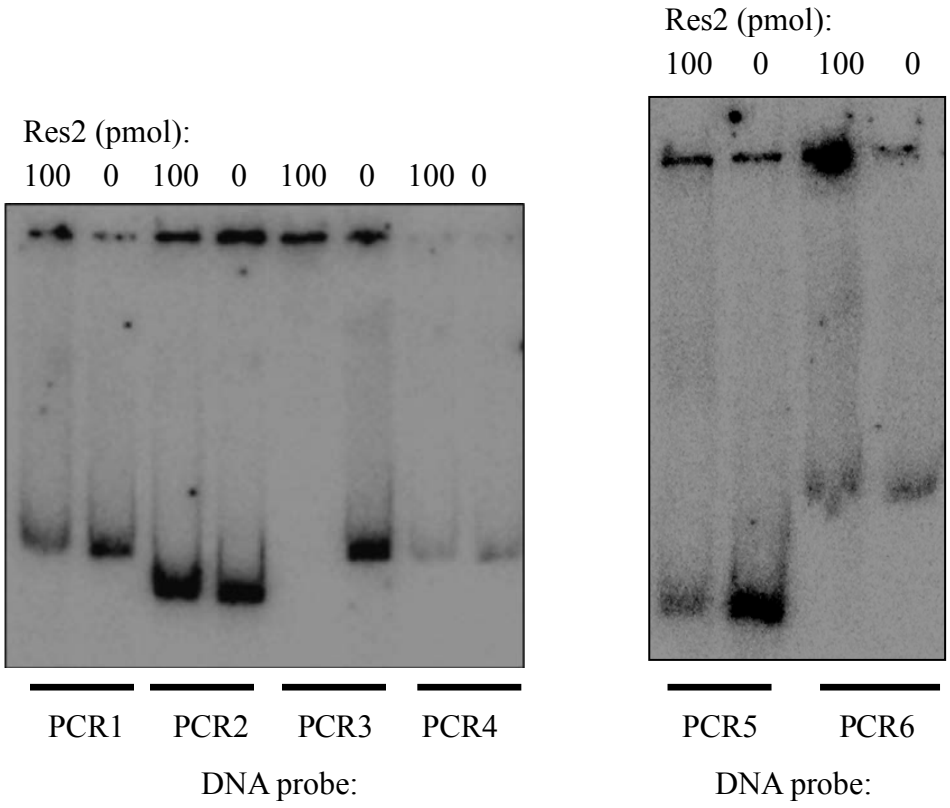
Res2 (pmol):
100 0 100 0 100 0 100 0
PCR1 PCR2 PCR3 PCR4
DNA probe:
Res2 (pmol):
100 0 100 0
PCR5 PCR6
DNA probe:

Figure 3.2.12. Analysis of binding of His_{10}-C7P to promoter regions of genes in the clavam and paralogue gene clusters. DNA probe used corresponds to intergenic regions between *snk* and *c7p* (PCR2, 3), *cvm5* and *cvm6* (PCR4), and *cvm1* and *cas1* (PCR5 and 6). Reactions were prepared in a total volume of 20 µl by mixing 20 fmol of each ^{32}P end- labeled fragment with 100 pmol of enriched His_{10}-C7P protein preparation in binding buffer containing 10 mM Tris-HCl (pH 8.0), 1 mM DTT, 10% glycerol, 150 mM NaCl and 1 µg of poly d(I-C). Binding reactions were carried out at 21^{o}C for 25 minutes. Samples were separated on 1.5% glycerol containing 6% non-denaturing polyacrylamide gels in 1X Tris-glycine buffer. Gels were dried for 45 minutes, placed on a phosphor screen and exposed for 16 hours. *Data in these figures were obtained by Annie Wong.*

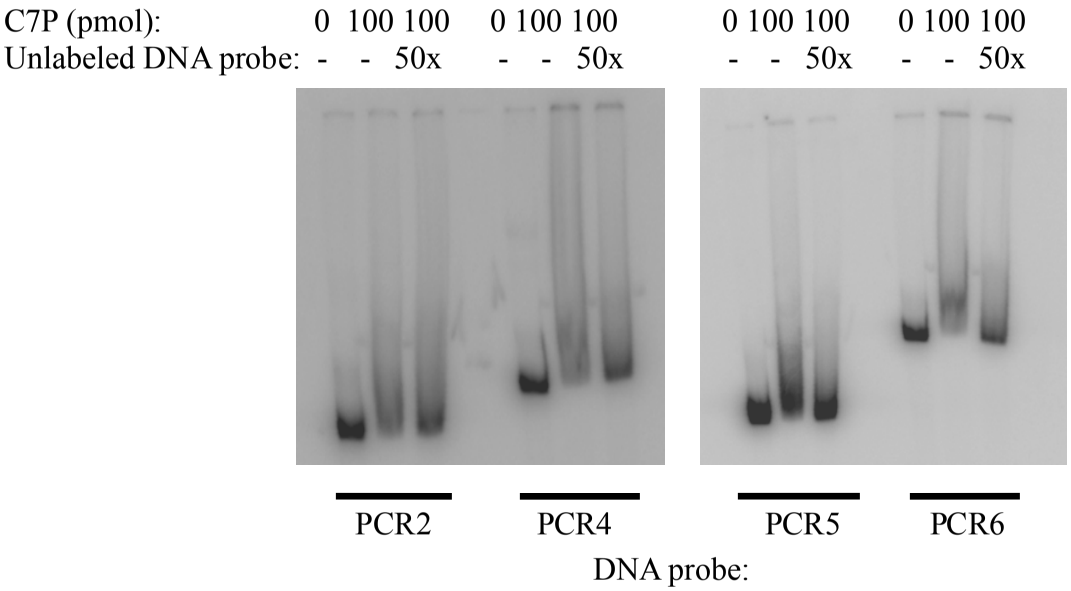
C7P (pmol): 0 100 100 0 100 100 0 100 100 0 100 100
Unlabeled DNA probe: - - 50x - - 50x - - 50x - - 50x
PCR2
PCR4
PCR5
PCR6
DNA probe:

excess unlabeled probe (PCR6) to the binding reactions reduced protein binding to the labeled fragment (Figure 3.2.12). With the same conditions used, C7P also showed at least some ability to bind PCR 2, 4 and 5 (Fig 3.2.12), which are the regions upstream of *c7p*, *cvm5* and *cvm6*, and *cvm1*, respectively (Figure 3.2.12). This suggested that C7P regulates 5*S* clavam production by binding to these biosynthetic genes, and also that transcription of *c7p* may be under auto regulation by C7P binding to its own promoter. However, instead of distinct bands, the shifted DNA appeared as smears, suggesting that the conditions used were not optimal for C7P binding. Therefore, attempts were made to improve the shifting quality including the changes as described in section 3.2.4.1. However, none of the changes helped significantly to resolve the problem and so the evidence for interaction between C7P and *c7p*, *cvm5*, *cvm6* and *cvm1* remains inconclusive.

Among the targets that appeared to be bound by C7P, the region between the divergently oriented *cvm1* and *cas1* genes (PCR 6) was chosen for a more detailed study as it showed the most promising result (Figure 3.2.12). PCR 6 was mixed with His_{10}-C7P (0-100 pmol) in the presence of excess poly d(I-C) as non-specific DNA competitor. As expected, as the amount of protein added to the binding reaction increased, more DNA probe was shifted (Figure 3.2.13).

Competition mobility shift assays were then carried out to demonstrate the specificity of C7P binding. C7P binding to labeled probe was reduced when 50-fold excess of unlabeled probe (PCR 6) was added to the EMSA reaction (Figure 3.2.14). In contrast, excess unlabeled nonspecific DNA (internal region of *hrdB*, amplified by hrdB RT-forward and hrdB RT-reverse primers) did not affect C7P

Figure 3.2.13. Electrophoretic mobility shift of a 454 bp DNA fragment spanning the intergenic region between *cvm1* and *cas1* (PCR6) when bound by His_{10}-C7P. Reactions were prepared in a total volume of 20 µl by mixing 20 fmol of ^{32}P end-labeled fragment with 0-100 pmol of purified His_{10}-C7P protein in binding buffer. Reactions were incubated at 21^{o}C for 25 minutes. Samples were separated on 1.5% glycerol-containing 8% non-denaturing PAG 1X Tris-glycine buffer. Gels were dried, placed in contact with a phosphor screen and exposed for 16 hours. *Data in these figures were obtained by Annie Wong.*

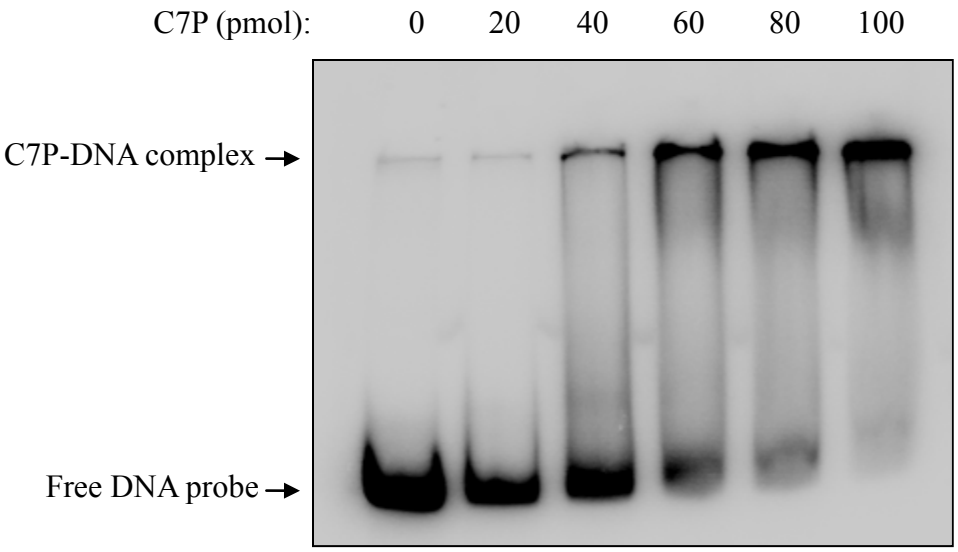
C7P (pmol):
0
20
40
60
80
100
C7P-DNA complex
Free DNA probe

Figure 3.2.14. Specificity of His_{10}-C7P binding to a 454 bp DNA fragment spanning the intergenic region between *cvm1* and *cas1* (PCR6). For each reaction, 20 fmol of ^{32}P end- labeled fragment was mixed with 100 pmol of purified His_{10}-C7P protein in binding buffer in a total volume of 20 µl and incubated at 21°C for 25 minutes. Specificity of C7P binding was demonstrated by addition of 5 or 50-fold excess of unlabeled competitor DNA (PCR6) to the reaction and by addition of 5 or 50-fold excess of unlabeled nonspecific competitor DNA (350bp fragment of *hrdB*). Samples were separated on 1.5% glycerol-containing 8% non-denaturing PAG in 1X Tris-glycine buffer. Gels were dried, placed in contact with a phosphor screen and exposed for 16 hours. *Data in these figures were obtained by Annie Wong.*

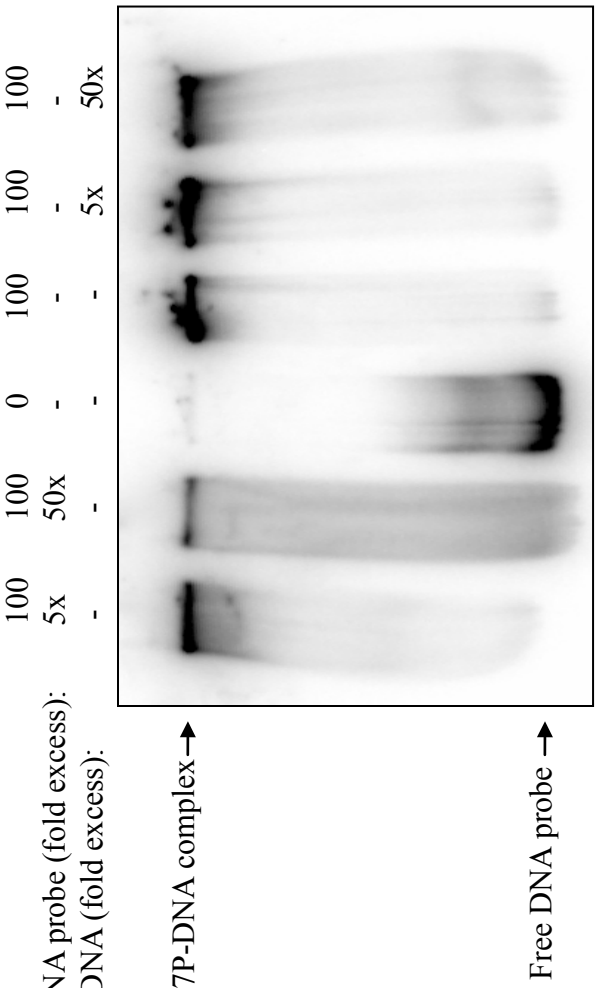
C7P (pmol): 100 100 0 100 100 100
Unlabeled DNA probe (fold excess): 5x 50x - - 5x 50x
Nonspecific DNA (fold excess): - - - - - -
C7P-DNA complex
Free DNA probe

binding when added to the EMSA reaction (Figure 3.2.14). Taken together these results suggested that C7P was able to bind and shift the mobility of the labeled PCR 6 fragment.

3.3 Analysis of proteins involved in the two-component system

Typical two-component regulatory systems involve one sensor kinase protein and one response regulator protein. However, atypical two-component systems with more than two components have also been described. In particular, systems with components similar to RocS1 (a sensor kinase), RocA1 (a typical response regulator), and RocR (a response regulator without a DNA-binding domain) from *Pseudomonas aeruginosa* (this system is further described in Section 4.3), have also been identified in several different organisms. Even though *S. clavuligerus* has been shown to carry such an atypical two-component system, experimental characterization of the system has not yet been done. Furthermore, the reason for carrying two response regulators is not clear. It is also not apparent if these response regulators interact only with the sensor kinase or also with each other once they are phosphorylated by the sensor kinase. Therefore, studies were initiated to investigate the phosphorylation dynamics between these proteins.

3.3.1 Overproduction and purification of wild type proteins of the two-component regulatory system

Expression vectors for overproducing Snk and Res1 were available from a previous study (prepared by N. Zelyas). Res2 was obtained previously as

described in Section 3.2.3.1 (Figure 3.2.5). Proteins were overproduced as described in Section 2.9.4, and 2.9.5. Since overproduced proteins carried a His-tag either at the N or C-terminus, they were purified by combining the cell lysates with Ni-NTA resin under conditions where His-tagged protein binds to the resin and can thus be separated from the bulk proteins in the lysate. The entire mixture was incubated for one hour at 4ºC and after washing away unbound proteins, bound protein was eluted by using a gradient of imidazole. For Snk-His_7, each collected fraction was electrophoresed on 8% SDS-PAG to identify fractions that contained the desired protein, which has an expected molecular weight of about 59 kDa (Figure 3.3.1.). Similarly, samples collected during the His_{10}-Res1 purification process were visualized by electrophoresing on 12% SDS-PAG and appeared to run at the expected molecular weight of about 16 kDa (Figure 3.3.2). Fractions identified as containing the desired proteins were then concentrated using centrifugal concentrators with a molecular weight cutoff of 10 kDA, resuspended in protein storage buffer and stored at -80^{o}C.

In vitro phosphorylation assays were carried out with wild type proteins to optimize conditions used for subsequent assays and to determine if the expression and purification processes used had yielded active proteins. Different combinations of Snk-His_7, His_{10}-Res1 and Res2-His_7 were incubated together for 30 minutes at 30ºC with excess [γ-^{32}P] ATP as the phosphate donor. Each reaction was done in duplicate. After incubation, reaction mixtures were electrophoresed on SDS-PAG to separate the proteins and the dried gels were exposed to a phosphor screen to detect signals from the radioactive γ-phosphate. In all reaction

Figure 3.3.1. Purification of Snk-His_7 from *E. coli* BL21(DE3) carrying pT7-7His-*snk*. Protein samples were taken at different stages of the overexpression and purification processes and analyzed by SDS-PAGE. Proteins were visualized by staining with Coomassie blue. Lane M, PageRuler™ prestained Protein Ladder Plus molecular weight marker. Lane I, induced total protein sample. Lane CL, cleared lysate. Lane WT, wash-through. Numbers above lanes indicate the concentration of imidazole (in mM) used to elute the protein samples.

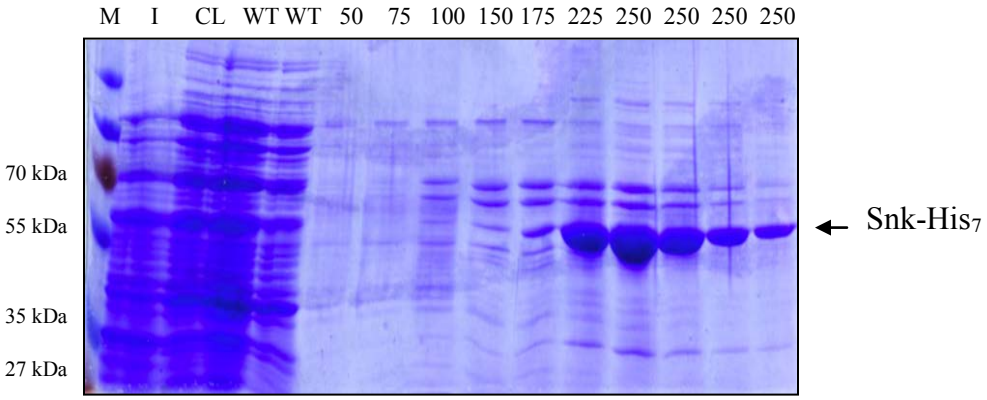
M I CL WT WT 50 75 100 150 175 225 250 250 250 250
70 kDa
55 kDa
35 kDa
27 kDa
Snk-His7

Figure 3.3.2. Purification of His_{10}-Res1 from *E. coli* BL21(DE3) carrying pET-19b-*res1*. Protein samples were taken during different stages of the overexpression and purification processes and analyzed by SDS-PAGE. Proteins were visualized by staining with Coomassie blue. Lane M, PageRuler™ Protein Ladder Plus molecular weight marker. Lane I, induced total protein sample. Lane CL, cleared lysate. Lane WT, wash-through. Numbers above lanes indicate the concentration of imidazole (in mM) used to elute the protein samples.

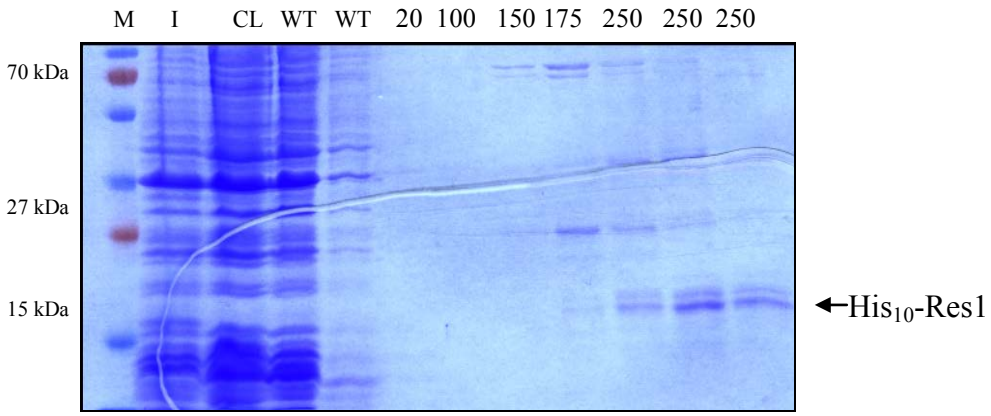
M I CL WT WT 20 100 150 175 250 250 250
70 kDa
27 kDa
15 kDa
←His10-Res1

mixtures that contained Snk-His_7, signals corresponding to Snk were detected as shown on the image obtained from the phosphorimager (Figure 3.3.3). Radioactive signals were not observed from Res1 or Res2 when Snk was not present in the reaction mixtures but phosphorylated Res1 and Res2 were detected when either protein, or both proteins, was incubated with Snk in the reaction mixture (Figure 3.3.3). This indicated Snk-His_7 is capable of autophosphorylation and is also able to transfer phosphate to His_{10}-Res1 and Res2-His_7.

3.3.2 Sequence comparison

To further understand the role of Snk, Res1 and Res2 in the two-component system, the protein sequence of each member was first compared to other known sequences in GenBank. Through BLAST analysis, the conserved histidine residue, which is involved in auto-phosphorylation of the sensor kinase in two-component systems from other bacteria, was identified in Snk (H-365) (Figure 3.3.4). Similarly, the conserved asparatic acid residue, which acts as the phosphate acceptor site in response regulators from other bacteria, was also identified in Res1 (D-65) and Res2 (D-52) (Figure 3.3.4).

3.3.3 Site-directed mutagenesis of phosphorylation site of Snk, Res1 and Res2

To investigate if the residues identified from Section 3.3.2 are involved in phosphorylation, site-directed mutagenesis was employed to change the histidine or aspartic acid residue from the sensor kinase or response regulators, respectively, to an alanine residue. Initially, QuickChange® II-E Site-Directed Mutagenesis kit (Stratagene) was used to generate such mutations. However, for

Figure 3.3.3. *In vitro* phosphorylation of Snk-His_7, His_{10}-Res1 and Res2-His_7. Reaction mixtures were incubated at 30^{o}C for 30 minutes with excess [γ-^{32}P] ATP. Reactions were stopped by cooling on ice and addition of 5x SDS-PAGE loading buffer. Samples were electrophoresed on a 15% SDS-PAG, dried and then exposed for 16 hours to a phosphor screen. Labels above each lane indicate the protein or proteins included in the reaction mixture.

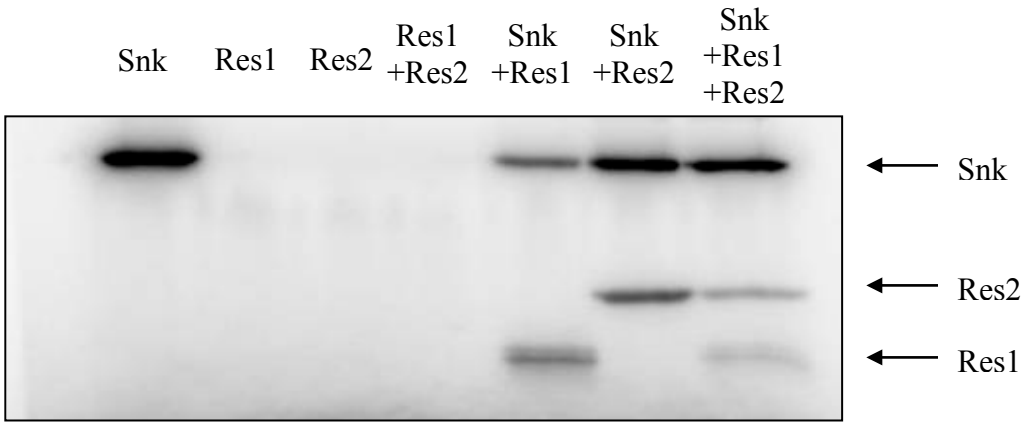
Snk
Res1
Res2
Res1 +Res2
Snk +Res1
Snk +Res2
Snk +Res1 +Res2
Snk
Res2
Res1

Figure 3.3.4. Sequence comparison through BLAST analyses of the proteins of the two-component regulatory system. (A) Alignment of the amino acid sequence of Snk with sensor kinases from various bacteria. Conserved histidine residues involved in auto-phosphorylation are shown in bold. (B) Alignment of the amino acid sequences of Res1 and Res2 with response regulators from various bacteria. Conserved asparatic acid residues involved in phosphorylation are shown in bold. Numbers refer to the amino acid positions within the protein.

A.

Streptomyces clavuligerus Snk	357.RRRIERDL**H**DGPQQRLVSLALRVRTV
Streptomyces avermitilis putative sensor kinase	237.RRRIERDL**H**DGAQQRLVALTMTLGLA
Streptomyces coelicolor putative sensor kinase	227.LRRIERSL**H**DGAQNRLVSVTVLLGAA
Mycobacterium tuberculosis DosT	384.RDRIARDL**H**DHVIQRLFAVGLTLQGA
Rhodococcus sp. CprS	359.RDRIARDL**H**DNVIQRLFASGMSLQST

B.

Streptomyces clavuligerus Res1	59.PDVALV**D**LDLGESGLDLAERLY
Streptomyces clavuligerus Res2	46.PDLVIV**D**IRMPTHTTEGLAAAR
Escherichia coli PhoB	47.PDLILL**D**WMLPGSGIQFIKHLK
Sinorhizobium meliloti FixJ	48.NGVLVT**D**LRMPMSGVELLRNLG
Pseudomonas aeruginosa AlgB	53.FDLCFL**D**LRLGDNGLDVLAQMR

unknown reasons, it was not possible to transform competent cells with the plasmids that carry the mutated versions of *snk*, *res1* or *res2*. As a result, two-step site-directed mutagenesis, which required two separate PCR reactions to generate the mutations, was used (Thai *et al*., 2001). The procedure is illustrated in Figure 3.3.5. Although this method was relatively more laborious, the mutations were successfully introduced into the genes of interest as confirmed by sequencing (data not shown). Similar to the *res2* overexpression construct described previously, each of the forward primers used for amplification had an engineered 5' *Nde*I site and the reverse primers contained a 5' *Bam*HI site (Figure 3.3.5). This allowed the amplified genes to be cloned into expression vectors easily as *Nde*I/*Bam*HI fragments and in this way pET-19b-*res1*-SD, pT7-7His-*res2*-SD and pT7-7His-*snk*-SD were constructed (Table 2.3).

3.3.4 Two-component regulatory system protein overproduction and purification

pET-19b-*res1*-SD, pT7-7His-*res2*-SD and pT7-7His-*snk*-SD were transformed into *E. coli* BL21(DE3) to overproduce the two-component regulatory proteins with altered putative phosphorylation sites, hereafter referred as His_{10}-Res1-SD, Res2-SD-His_7 and Snk-SD-His_7, respectively. Snk-SD-His_7, and Res2-SD-His_7 were overproduced with the same conditions as described earlier for Res2-His_7 (Section 2.9.4). Conditions similar to those used to obtain His_{10}-C7P were used for His_{10}-Res1-SD overproduction (Section 2.9.5).

Figure 3.3.5. Schematic representation of the first PCR reaction of the two step site-directed mutagenesis used to change the phosphorylation site of Snk, Res1 and Res2 to an alanine residue.

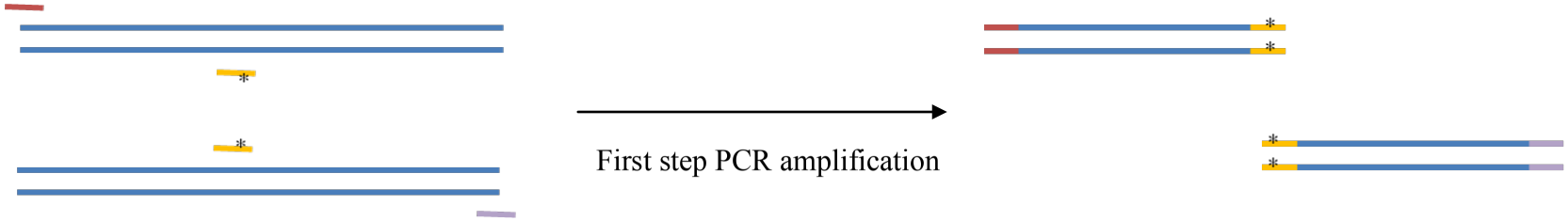

- Forward primer with engineered *Nde*I restriction sites
  - res1-pfwd
  - res2-pfwd
  - snk-pfwd

- Reverse primer with engineered *BamH*I restriction site
  - res1-prev
  - res2-prev
  - snk-prev2

- Forward or Reverse primer with site directed mutation to alanine codon
  - res1 site-directed-For
  - res1 site-directed-Rev
  - res2 site-directed-For
  - res2 site-directed-Rev
  - snk site-directed-For
  - snk site-directed-Rev

Figure 3.3.5. (Continued). Schematic representation of the second PCR reaction of the two step site-directed mutagenesis used to obtain complete gene products with engineered terminal restriction sites and site specific mutation.

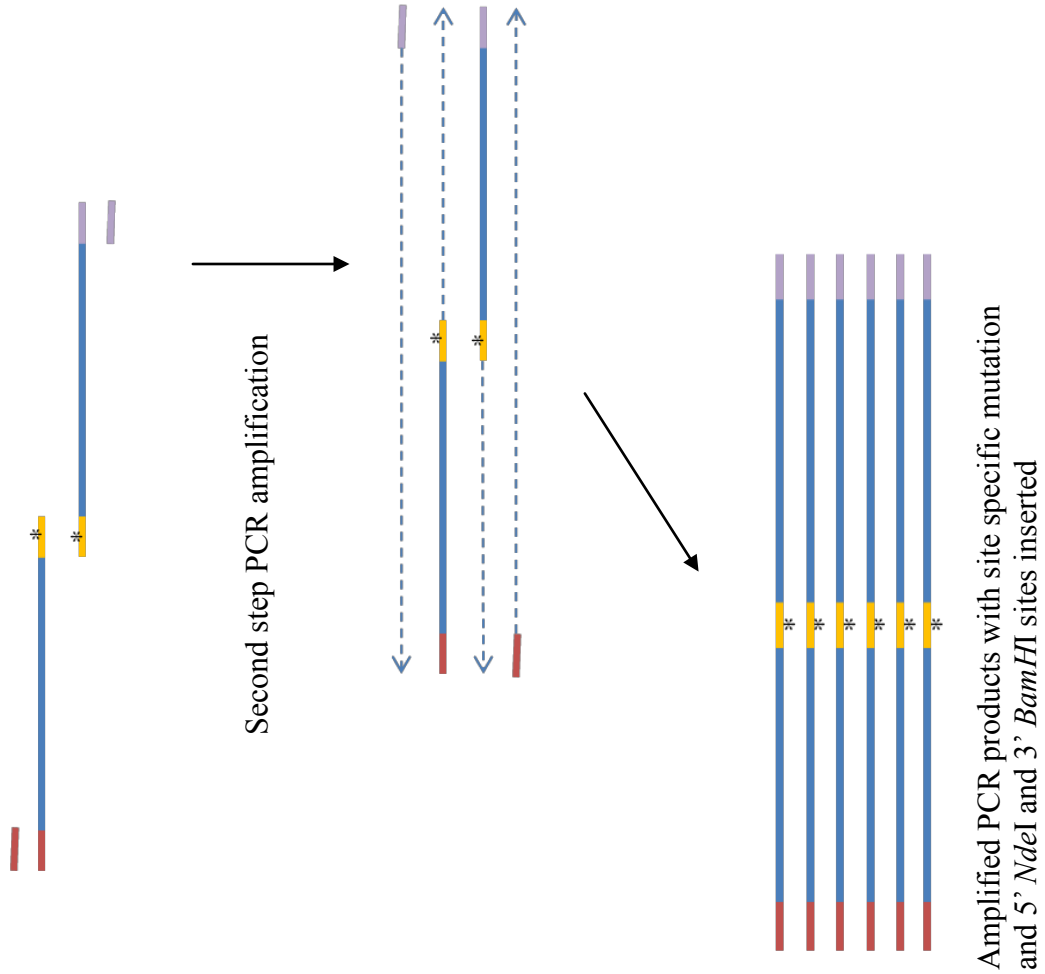
Second step PCR amplification
Amplified PCR products with site specific mutation and 5' NdeI and 3' BamHI sites inserted

Since these proteins contained the same His-tag as their wild type version, they were purified from crude lysates and eluted with a gradient of imidazole as described for their counterparts in previous sections. This purification procedure allows soluble native proteins to be isolated. Samples collected at different stages of the purification process for Snk-SD-His_7 were visualized by electrophoresis on an 8% SDS-PAG (Figure 3.3.6). Similarly, samples collected during the His_{10}-Res1-SD and Res2-SD-His_7 purification process were visualized by electrophoresis on 12% SDS-PAG (Figure 3.3.7). All of these proteins appeared to run at their expected molecular weights and fractions that contained the desired proteins were pooled and concentrated by using centrifugal concentrators with molecular weight cutoff of 10kDA and then resuspended in protein storage buffer and stored at -80ºC in small aliquots.

3.3.5 *In vitro* phosphorylation assays

When proteins (both wild type and with altered putative phosphorylation sites) of each component of the two-component system were obtained in sufficient amounts, phosphorylation assays were carried out with different combinations of wild type proteins and proteins with altered phosphorylation sites. Each combination was done in duplicate. Unlike wild type Snk-His_7 protein, radioactive phosphate signal from Snk-SD-His_7 was not observed (Figure 3.3.8). When His_{10}-Res1-SD and Res2-SD-His_7 were incubated separately or together with Snk-His_7, only the band corresponding to Snk-His_7 was observed and phosphorylated response regulators could not be detected. This strongly indicated that H-365 of Snk and the conserved asparatic acid residues, D-65 of Res1 and D-

Figure 3.3.6. Purification of Snk-SD-His_7 from *E. coli* BL21(DE3) carrying pT7-7His-*snk*-SD. Protein samples were taken at different stages of the overexpression and purification processes and analyzed by SDS-PAGE. Proteins were visualized by staining with Coomassie blue. Lane M, PageRuler™ prestained Protein Ladder Plus molecular weight marker. Lane I, induced total protein sample. Lane CL, cleared lysate. Lane WT, wash-through. Numbers above lanes indicate the concentration of imidazole (in mM) used to elute the protein samples.

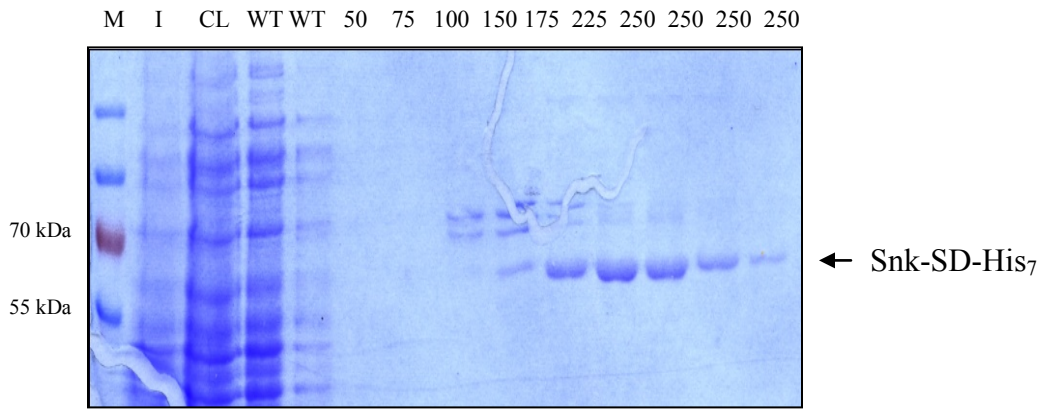
M I CL WT WT 50 75 100 150 175 225 250 250 250 250
70 kDa
55 kDa
Snk-SD-His7

Figure 3.3.7. Purification of (A) His_{10}-Res1-SD and Res2-SD- His_7 from *E. coli* BL21(DE3) carrying pET-19b-*res1*-SD and pT7-7His-*res2*-SD, respectively. Protein samples were taken during different stages of the overexpression and purification processes and analyzed by SDS-PAGE. Proteins were visualized by staining with Coomassie blue. Lane M, PageRuler™ Protein Ladder Plus molecular weight marker. Lane I, induced total protein sample. Lane CL, cleared lysate. Lane WT, wash-through. Numbers above lanes indicate the concentration of imidazole (in mM) used to elute the protein samples.

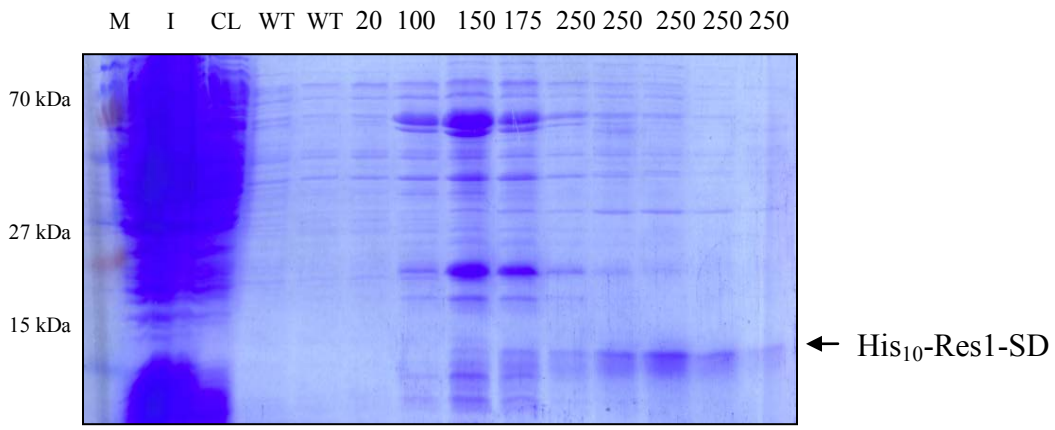
M I CL WT WT 20 100 150 175 250 250 250 250 250
70 kDa
27 kDa
15 kDa
← His10-Res1-SD

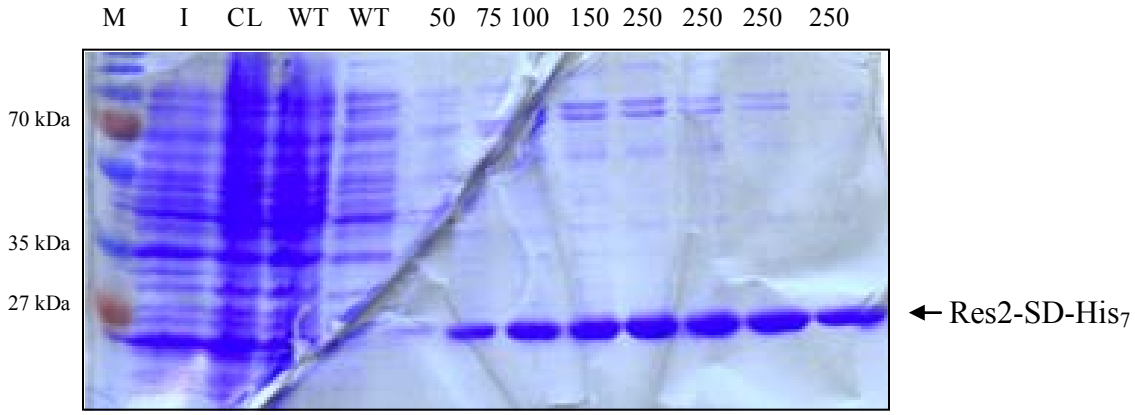
M I CL WT WT 50 75 100 150 250 250 250 250
70 kDa
35 kDa
27 kDa
← Res2-SD-His7

Figure 3.3.8. *In vitro* phosphorylation of Snk-His_7, His_{10}-Res1 and Res2-His_7 and Snk-SD-His_7, His_{10}-Res1-SD and Res2-SD-His_7. Reactions were incubated at 30^oC for 30 minutes with excess [γ-^{32}P] ATP. Reactions were stopped by cooling on ice and addition of 5x SDS-PAGE loading buffer. Samples were electrophoresed on a 15% SDS-PAG, dried and then exposed for 16 hours to a phosphor screen. Labels above each lane indicate the protein or proteins included in the reaction mixture.

SD = site-directed mutant versions of the corresponding proteins.

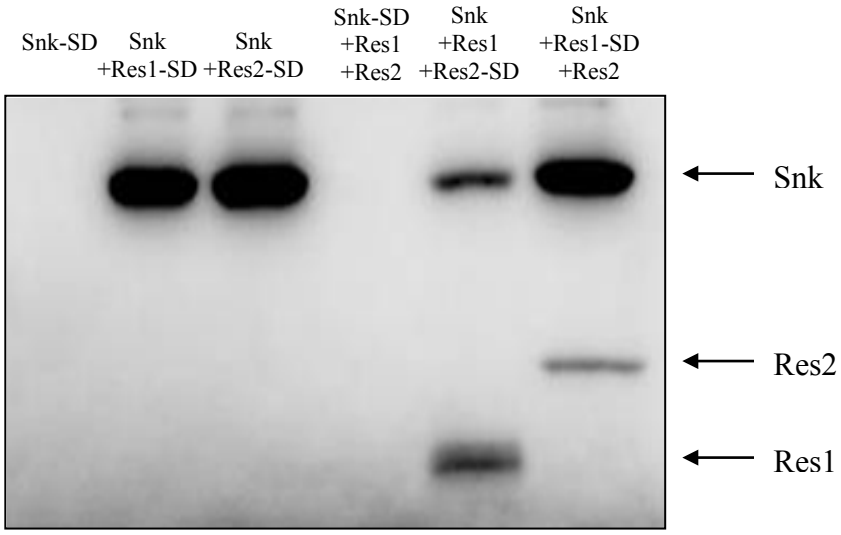
Snk-SD
Snk +Res1-SD
Snk +Res2-SD
Snk-SD +Res1 +Res2
Snk +Res1 +Res2-SD
Snk +Res1-SD +Res2
Snk
Res2
Res1

52 of Res2 identified previously were the actual phosphorylation sites, since changing these residues to alanines prevented Snk autophosphorylation and abolished the ability of Res1 and Res2 to undergo phosphorylation by receiving phosphate molecules.

3.3.6 Phosphorylation dynamics between Res1 and Res2

One interesting finding when carrying out phosphorylation assays as described above, was that whenever His_{10}-Res1 was present in the reaction mixtures, the signal intensity of either labelled Snk-His_7 or Res2-His_7 dropped significantly (Figure 3.3.3 and 3.3.8). Since γ-P^{32}-ATP was always used in excess, one possible explanation was that Res1 might possess phosphatase activity that constantly removes phosphate from these two proteins; another possible explanation is that Res1 can interact with and induce conformational change on Snk, thus revealing its phosphatase domain, which could in turn cause phosphate to be removed from these proteins. Studies were carried out to investigate this observation.

3.3.6.1 Construction of MBP fusion protein overproduction vector

The presence of Snk in reaction mixtures is necessary to initiate the phospho-relay, but its continued presence would then interfere with studies to examine possible reactions between Res1 and Res2. Since all three of *snk*, *res1* or *res2* expression systems use His-tags for protein purification, removal of Snk specifically from reaction mixtures was not possible. Therefore, to carry out *in vitro* dephosphorylation and phospho transfer assays, a new Snk protein

producing strain first had to be constructed. pMAL-*snk*, which upon induction will produce a maltose binding protein (MBP) fusion protein, was prepared. This would allow phosphorylated His_{10}-Res1 or Res2-His_7 to be separated from MBP-Snk after *in vitro* phosphorylation. *snk* from pT7-7-*snk* was cloned downstream of *malE*, which encodes MBP, in the pMAL-C5X expression vector as an *Nde*I/*BamH*I fragment. pMAL-*snk* was then transformed into BL21(DE3) for high level protein production. MBP-Snk was produced and purified successfully by following the protocol provided by the manufacturer (NEB) (data not shown). However, *in vitro* phosphorylation assays indicated that MBP-Snk was unable to phosphorylate His_{10}-Res1 and Res2-His_7 (data not shown). This may be due to the presence of the large MBP tag (~42 kDa), which physically blocked the interaction between Snk and the response regulators, thus inhibiting the transfer of the phosphate molecules. As a result, the coding sequences of *res1* and *res2* from pET-19b-*res1* and pT7-7-*res2*, respectively, were cloned into the pMAL-C5X expression vector with the same strategy as described above to obtain pMAL-*res1* and pMal-*res2* and transformed into BL21(DE3). MBP-Res1 and MBP-Res2 were produced and purified successfully by using the protocol as described in 2.9.6. Samples collected during the purification process were visualized by electrophoresing on 8% SDS-PAG. MBP-Res1 and MBP-Res2 appeared to run at their expected molecular weights of about 58 kDa and 67 kDa, respectively (Figure 3.3.9).

After purification, phosphorylation assays were first carried out to determine if the proteins were still intact and could undergo phosphorylation by

Figure 3.3.9. Purification of (A) MBP-Res1 and (B) MBP-Res2 from *E. coli* BL21(DE3) carrying pMal-*res1* and pMal-*res2*, respectively. Protein samples were taken during different stages of the overexpression and purification processes and analyzed by SDS-PAGE. Proteins were visualized by staining with Coomassie blue. Lane M, PageRuler™ Protein Ladder Plus molecular weight marker. Lane I, induced total protein sample. Lane CL, cleared lysate. Lane WT, wash-through. Numbers above lanes represent fractions eluted from the amylose affinity column with column buffer supplemented with 10 mM maltose.

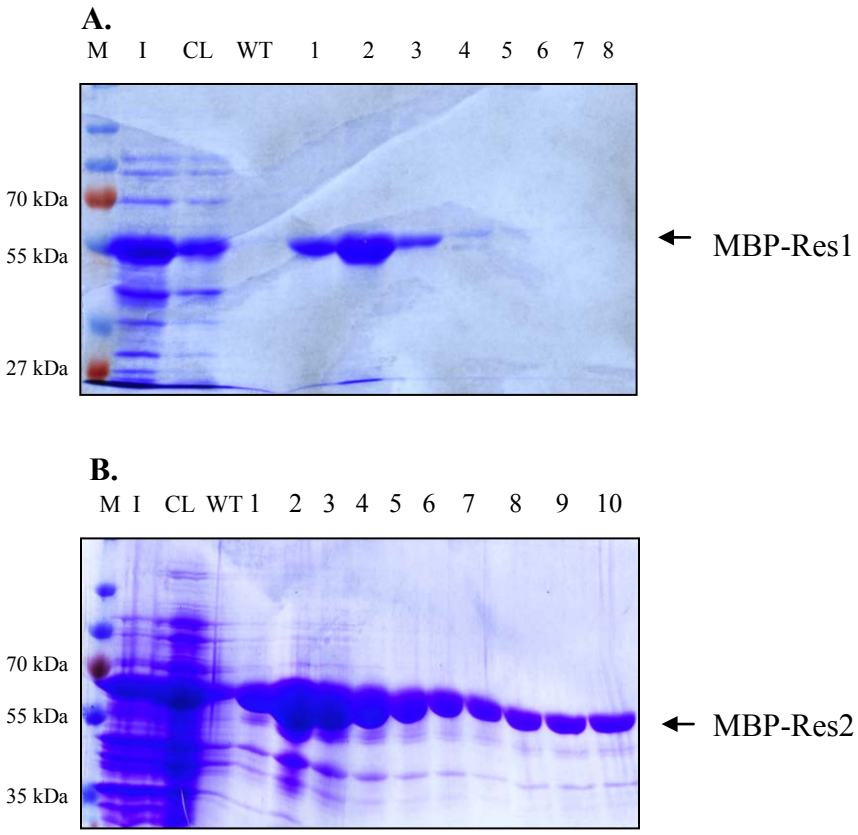
A.
M I CL WT 1 2 3 4 5 6 7 8
70 kDa
55 kDa
27 kDa
MBP-Res1
B.
M I CL WT 1 2 3 4 5 6 7 8 9 10
70 kDa
55 kDa
35 kDa
MBP-Res2

WT Snk-His_7. Despite the presence of the large MBP tag, both MBP-Res1 and MBP-Res2 were confirmed to undergo phosphorylation in the presence of Snk-His_7 (Figure 3.3.10). After confirmation that both MBP fusion proteins could be phosphorylated by Snk, MBP-Res1 and MBP-Res2 were further purified by running through a HiLoad 26/10 Q Sepharose High Performance anion exchange column to remove maltose that was present in the elution buffer. The presence of maltose would otherwise inhibit MBP fusion proteins from re-binding to amylose resin, which is a crucial step as described in the next section. Proteins were eluted from the anion exchange column with a gradient of NaCl and fractions were monitored by measuring absorbance at 280 nm. Identity of the protein was confirmed by SDS-PAGE. Fractions that contained the desired proteins were pooled, concentrated and stored as described previously (Section 2.9.8; Figure 3.3.11).

3.3.6.2 Purification of phosphorylated MBP-Res1 and MBP-Res2

Pure phosphorylated MBP-Res1 and MBP-Res2 were obtained by using the procedures illustrated in Figure 3.3.12. *In vitro* phosphorylation assays were first carried out between purified MBP-Res1 or MBP-Res2 and Snk-His_7 protein in the presence of excess [γ-^{32}P] ATP. Once the reactions were complete, phosphorylated MBP-Res1 and MBP-Res2 were separated from Snk-His_7 by combining the reaction mixtures with amylose resin and incubating on ice for 15 minutes. After incubation, the resins were washed extensively with kinase buffer at 4^{o}C to remove unbound proteins and small molecular weight components including ATP. Phosphorylated MBP-Res1 and MBP-Res2 were isolated

Figure 3.3.10. Phosphorylation of MBP-tagged response regulators. (A) *In vitro* phosphorylation of wild type Snk-His_7 and MBP-Res2. Lane C, control reaction mixture, contained Snk-His_7 only. Lane 1, both wild type Snk-His_7 and MBP-Res2 were added to the reaction mixture. (B) *In vitro* phosphorylation of wild type Snk-His_7 and MBP-Res1. Reactions were incubated at 30^oC for 30 minutes with excess [γ-^{32}P] ATP. Reactions were stopped by cooling on ice and addition of 5x SDS-PAGE loading buffer. Samples were electrophoresed on a 12% SDS-PAG, dried and then exposed for 16 hours to a phosphor screen.

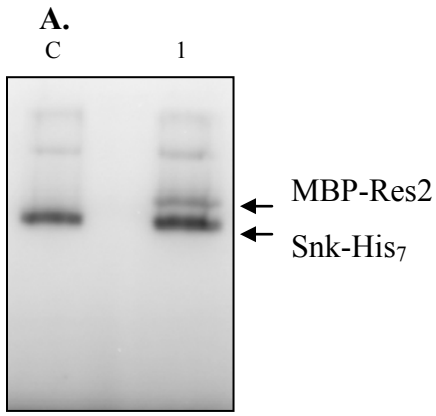
A.
C
1
MBP-Res2
Snk-His7

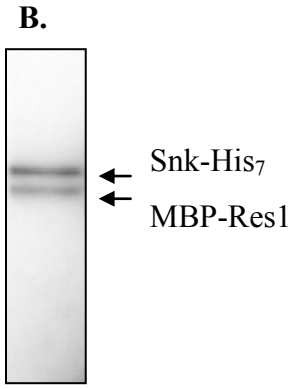
B.
Snk-His7
MBP-Res1

Figure 3.3.11. Anion exchange chromatography of MBP fusion proteins. Recovery of (A) MBP-Res1 and (B) MBP-Res2 after purification with the HiLoad 26/10 Q Sepharose High Performance anion exchange column. Proteins were eluted from the column by increasing concentration of NaCl. Protein-containing fractions, identified by measuring A_{280}, were analyzed by SDS-PAGE and visualized by staining with Coomassive blue. Lane M, PageRuler™ Protein Ladder Plus molecular weight marker.

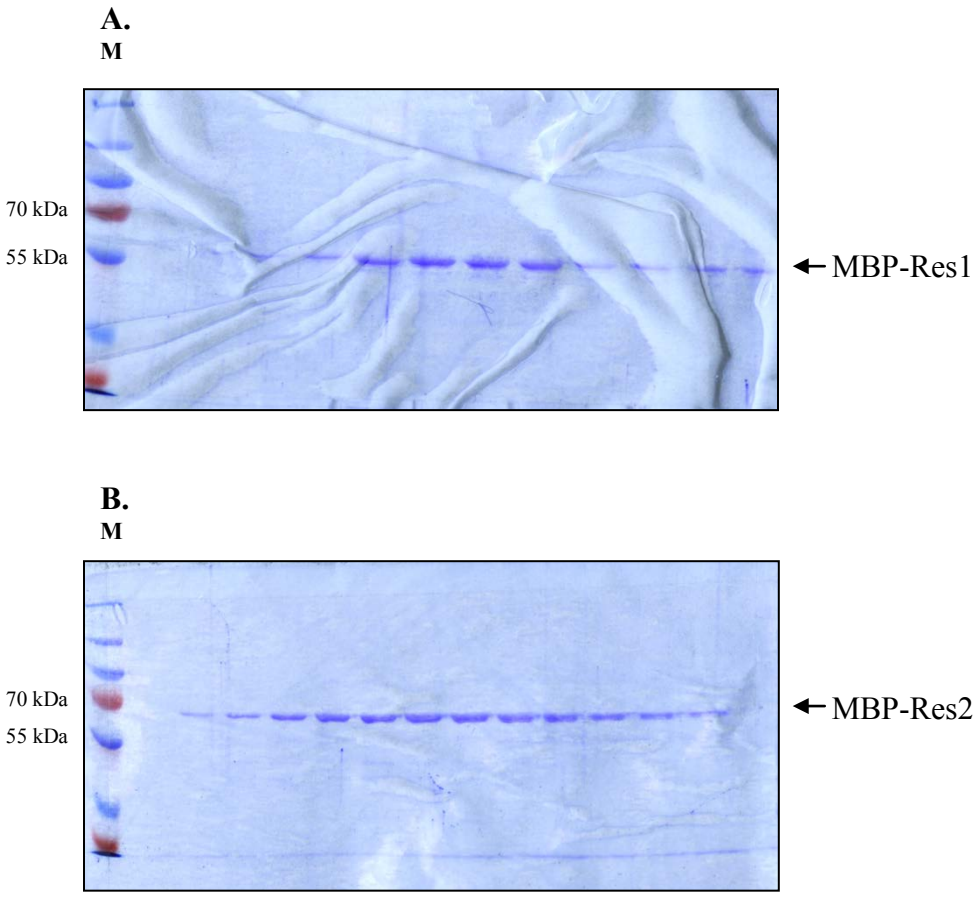
A.
M
70 kDa
55 kDa
MBP-Res1
B.
M
70 kDa
55 kDa
MBP-Res2

Figure 3.3.12. Schematic diagram of the process leading to the purification of phosphorylated MBP-Res1 and MBP-Res2.

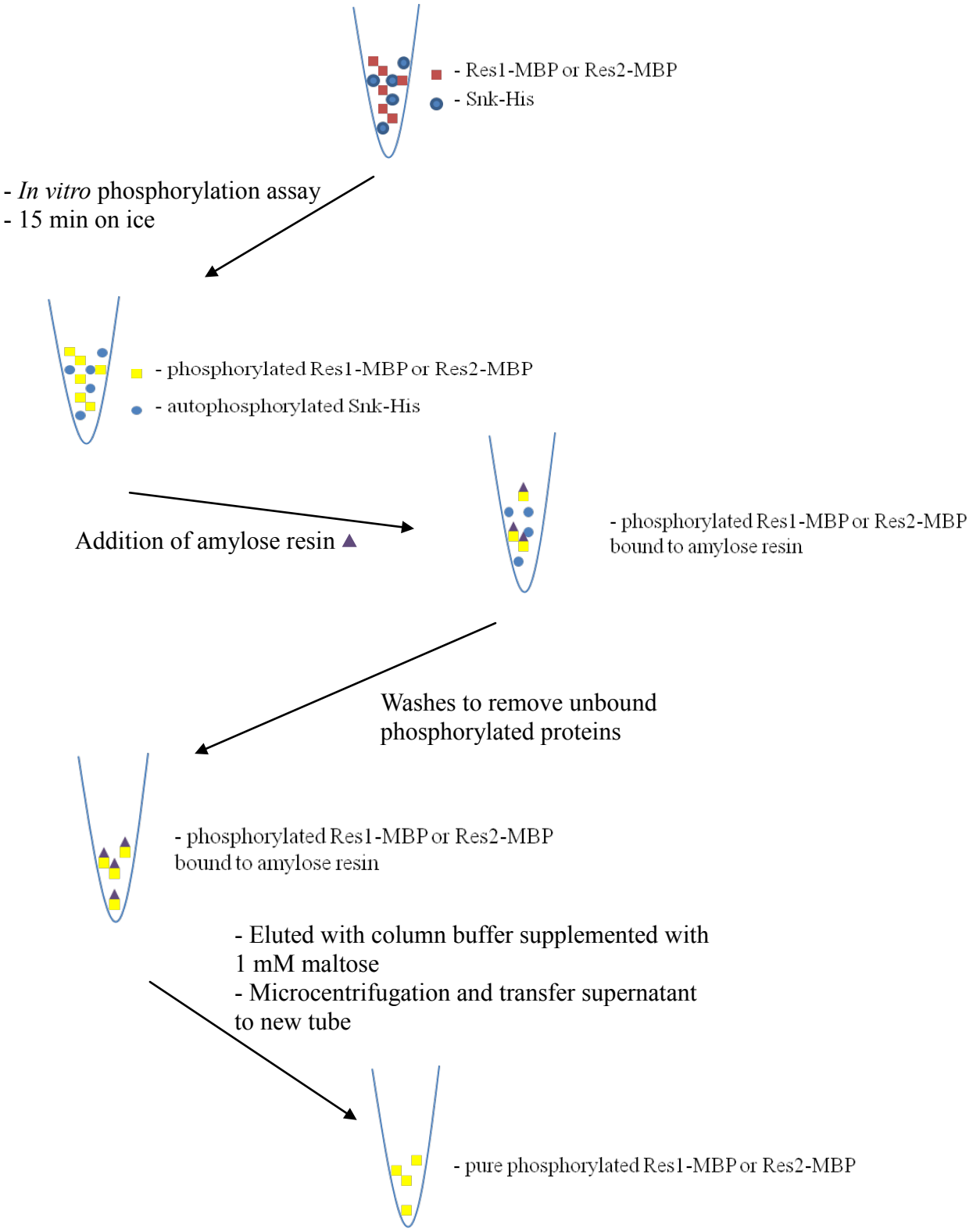
- Res1-MBP or Res2-MBP
- Snk-His
- *In vitro* phosphorylation assay
- 15 min on ice
- phosphorylated Res1-MBP or Res2-MBP
- autophosphorylated Snk-His
Addition of amylose resin
- phosphorylated Res1-MBP or Res2-MBP bound to amylose resin
Washes to remove unbound phosphorylated proteins
- phosphorylated Res1-MBP or Res2-MBP bound to amylose resin
- Eluted with column buffer supplemented with 1 mM maltose
- Microcentrifugation and transfer supernatant to new tube
- pure phosphorylated Res1-MBP or Res2-MBP

successfully, for use in the following *in vitro* protein assays, by eluting bound proteins from the resin with kinase buffer supplemented with 1 mM maltose (data not shown). Nonradioactive trial experiments were also carried out to confirm that Snk-His_7 was efficiently removed and no detectable amount was present in the eluate, as determined by running samples collected at different stages by SDS-PAGE and visualizing proteins by staining with Coomassie brilliant blue (data not shown).

3.3.6.3 *In vitro* dephosphorylation assays

Once phosphorylated MBP-Res2 was isolated (Section 3.3.5.2), *in vitro* dephosphorylation assays were carried out. Phosphorylated MPB-Res2 was mixed with His_{10}-Res1 and incubated at 30^{o}C. Samples were then taken at different time points to a maximum of 5 hours. Reactions were stopped by addition of SDS-PAGE sample buffer and placed at 4^{o}C. All collected samples were then electrophoresed on 10% SDS-PAG to separate the proteins and the dried gel was exposed to a phosphor screen. This experiment was carried out multiple times with minor condition changes and the best data are shown in Figure 3.3.13. In the control reactions that contained phosphorylated Res2-MPB alone, some spontaneous dephosphorylation was observed (Figure 3.3.13). When phosphorylated MBP-Res2 was incubated with His_{10}-Res1, a much more rapid rate of dephosphorylation of Res2 was observed (Figure 3.3.13). This suggested that Res1 may possess phosphatase activity or enhance autophosphatase activity of Res2.

Figure 3.3.13. *In vitro* dephosphorylation assays. (A) Phosphorylated MBP-Res2 was incubated at 30^{o}C alone for the times indicated. (B) Phosphorylated MBP-Res2 was incubated with His_{10}-Res1 at 30^{o}C for the times indicated. Reactions were stopped by cooling on ice and addition of 5x SDS-PAGE sample buffer. Samples were electrophoresed on 12% SDS-PAG. Gels were dried and then exposed overnight to a phosphor screen.

A.

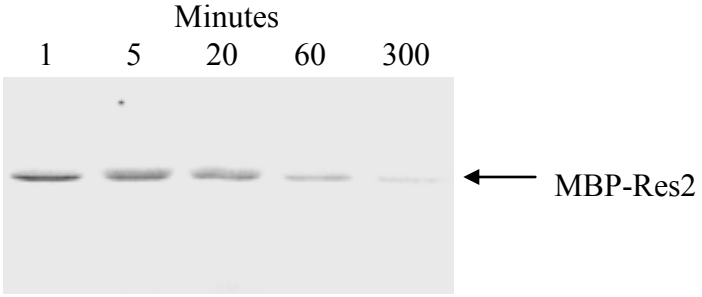

B.

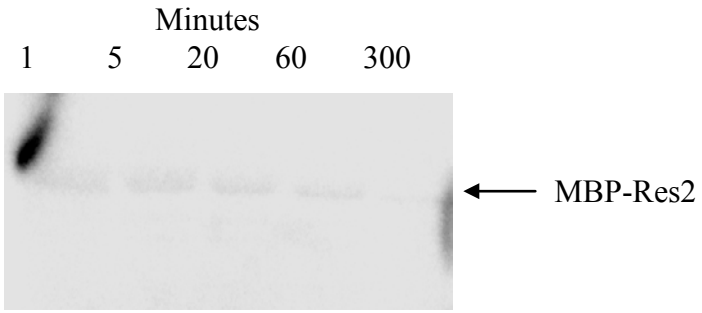

3.3.6.4 Phospho-transfer assays

To determine the phosphorylation dynamics between Res1 and Res2, phospho-transfer assays were carried out. After phosphorylated MBP-Res1 was isolated (Section 3.3.5.2), it was mixed with unlabeled Res2-His_7 protein and incubated at 30^{o}C for 10 minutes. A normal kinase reaction was also set up with Snk-His_7, MBP-Res1 and Res2-His_7 as a control. Reactions mixtures were then electrophoresed on 10% SDS-PAG. Dried gels were exposed to a phosphor screen to detect radioactive signals. The experiment was carried out multiple times with minor condition changes and the best data are shown in Figure 3.3.14. As expected, radioactive phosphate signals were detected from all three proteins of the two-component system in the control reactions. In the test reaction, radioactive signals were detected from phosphorylated MBP-Res1. Surprisingly, a band corresponding to Res2-His_7 was also observed from this test reaction, in which Snk-His_7 was not present (Figure 3.3.14). This indicated that Res1 was able to transfer its phosphate molecules to Res2.

Figure 3.3.14. Phosphotransfer activity between phosphorylated Res1 and Res2. Lane C, standard phosphorylation assay with Snk-His_7, MBP-Res1 and Res2-His_7 present in the reaction mixture; lane 1, phosphotransfer between phosphorylated MBP-Res1 and Res2-His_7, where Snk-His_7 was not added to the reaction mixture. Phosphorylated MBP-Res1 was mixed with Res2-His_7 and incubated at 30^{o}C for 15 minutes. Reaction mixtures were cooled on ice and combined with 5x SDS-PAGE loading buffer. Both samples were electrophoresed on a 12% SDS-PAG, dried and exposed 16 hours to a phosphor screen.

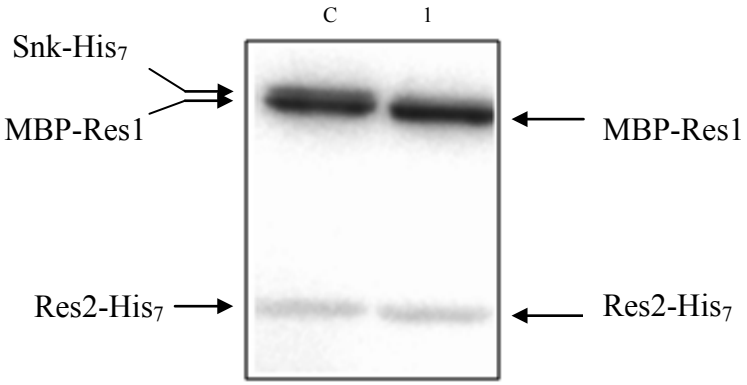
C
1
Snk-His7
MBP-Res1
MBP-Res1
Res2-His7
Res2-His7

Chapter 4

Discussion

4. Discussion

The main objective of this thesis was to investigate the regulation of clavam biosynthesis in *S. clavuligerus*. The first approach taken was to characterize the unexpected severity of the defect in clavam biosynthesis in *ceaS2* mutants and explore the relationship between *ceaS1* and *ceaS2*. In subsequent studies, the regulation of 5*S* clavam biosynthesis by the *snk*/*res1*/*res2* atypical two-component system, and the pathway specific transcriptional regulator, C7P, was also investigated. Each component, and the phosphorelay mechanism of the two-component system were further characterized. Compiling the results from this thesis and other studies, the major findings will be discussed in the following sections.

4.1 Polar effect exerted on transcription of downstream genes

When the Δ*ceaS2*-IF mutant prepared by Tahlan (2005) was first analyzed, it was found that this mutant was still severely compromised in clavam biosynthesis, a phenotype similar to that seen in *ceaS2*::apra, *ceaS2*-Fs and Δ*ceaS2*::apra mutants constructed previously. A complementation test with a copy of *ceaS2* did not restore clavam production (Tahlan, 2005). In contrast, by complementing these mutants with a large fragment of DNA, which included the *ceaS2* to the *cad* genes from the clavulanic acid gene cluster (Figure 1.3), clavulanic acid production was restored (Table 3.1). Since *ceaS2*, *bls2* and *pah2* are transcribed together as a polycistronic transcript, this suggested that a polar effect still affected transcription of the downstream genes in Δ*ceaS2*-IF. To

examine this hypothesis, RT-PCR and Western analyses were carried out to assess *bls* transcription and Bls production, respectively. On analysis, it was found that all *ceaS2* mutants were incapable of producing Bls protein (Section 3.1.4) and *bls* transcripts were not detected in Δ*ceaS2*-IF (Section 3.1.6). This indicated that although Δ*ceaS2*-IF was expected to have little or no effect on transcription of downstream genes, polarity still prevented transcription of the downstream genes that encode proteins involved in catalyzing the early steps of the clavam biosynthetic pathway.

The Δ*ceaS2*-IF mutant was prepared by using the REDIRECT method™ (Gust *et al*. 2003). A gene cassette, which contains an origin of transfer (*oriT*) and an antibiotic resistance gene, flanked by two FRT (FLP recombinase target) sites in the same orientation was amplified by PCR with specially designed primers. These primers were designed so that one end of each primer is homologous to the gene cassette and the other end is homologous to the appropriate region on a cosmid that carries the target gene to be disrupted. The amplified cassette was then introduced into an *E. coli* strain already carrying the λ RED recombination genes as well as the target cosmid. Homologous recombination allowed the amplified cassette to replace the target gene, therefore disrupting the target gene on the cosmid. Finally, the mutated cosmid was conjugated into *Streptomyces* cells, and through a double cross-over recombination, the desired gene(s) in the *Streptomyces*' chromosome was replaced by the disruption cassette. To generate an unmarked and in-frame mutant, presumed to be non-polar, another plasmid carrying the *flp* gene, which encodes FLP recombinase and catalyzes

recombination between the two FRT sites, was transiently introduced into *S. clavuligerus*. Expression of Flp would excise the intervening DNA between the FRT sites of the gene cassette on the chromosome and leave just the start and stop codons of the original target gene and an 81-bp scar sequence.

A close inspection of the scar sequence revealed the presence of a rare CTA codon. Codon usage has been shown to be highly biased in *Streptomyces* spp. because of the high G+C content of *Streptomyces* DNA. TTA codons and the *bldA* gene, which encodes the tRNA for this rare leucine codon have been shown to be involved in regulating secondary metabolism in *S. coelicolor* and various *Streptomyces* spp. (Chater and Chandra, 2008). A *S. coelicolor bldA* mutant is unable to produce actinorhodin, undecylprodigiosin and methylenomycin and TTA codons have been identified in *actII-ORF4*, *redZ*, *mmfL* and *mmyB* that encode pathway-specific transcriptional regulators, which control the biosynthesis of previously mentioned secondary metabolites, respectively (Chater and Chandra, 2008). A *bldA* mutant of *S. avermitilis* was found to be incapable of producing avermectin, which is an important macrocyclic polyketide widely used as an anthelmintic agent and has a high value in the medical, veterinary, and agricultural fields (Tao *et al*. 2007). The pathway-specific regulator AveR, which positively controls avermectin production by direct binding to promoter region of regulated genes, also contains a TTA codon (Guo *et al*., 2010).

Both studies indicated that ribosome stalling at the TTA codon could lead to transcriptional polarity. Based on these results, although the scar sequence mentioned above is small, in-frame and a TTA codon is not present, the presence

of a rare CTA codon in this sequence in the Δ*ceaS2*-IF mutant, might still exert a polar effect on transcription of genes downstream from *ceaS2*. In such a situation, the CTA codon could lead to pre-mature termination of transcription by stalling the ribosome at that point, therefore *bls2* would not be transcribed and Bls2 would not be produced. It may also be possible that the CTA codon context can influence the severity of the phenotype in a way similar to that proposed for TTA codons (Trepanier *et al*., 2002).

Although the REDIRECT method™ provides a relatively simple and effective way to generate in-frame deletion mutants and has been widely used in different laboratories, as co-transcription is a common phenomenon to save resources by co-regulating genes that belong to the same gene cluster, caution should be taken to ensure that the phenotype observed is not still due to a polarity effect on downstream genes. Similar to the *egfp* gene, in which the codon usage of the original version has been modified to facilitate expression in high G+C *Streptomyces* DNA, the CTA codon could be substituted with alternative leucine codon such as CTC or CTG, which is commonly used in *Streptomyces*, to alleviate possible polarity. However, as the CTA codon is located within the FRT site, it is not certain that such changes would not interfere with FLP recognization and excision of the intervening DNA.

4.2 *ceaS1* and *ceaS2* regulation

Even though polarity still persists in these mutants, this alone still does not explain why clavam production was so severely affected in the various *ceaS2*

mutants, as *ceaS1* and *ceaS2* encode proteins that both catalyze the same reaction. Even if disrupting *ceaS2* led to polarity, a reduced level of clavam biosynthesis instead of a total loss of production should be observed because *ceaS1* was still intact. Since the crystal structure of CeaS2 was shown to be a tetramer (dimer of dimers) (Caines *et al*. 2004), it was initially considered that for CeaS1 to function, it may need to form heterodimers with CeaS2, or that CeaS1 does not have the same activity as CeaS2. However, since production of clavam metabolites was restored when Δ*ceaS2*-IF was grown on solid medium, this indicated that *ceaS1* was transcribed and the encoded protein was functional in the absence of any CeaS2 protein (Section 3.1.8). Therefore, this leads to an altenative hypothesis that cross regulation must be taking place between *ceaS1* and *ceaS2*. This regulation is possibly at the transcription level because the bacterium could be at a disadvantage due to the high energy cost to regulate at the post-transcription level (transcribe or translate a gene that will not function). This was addressed by determining *ceaS1* transcription and CeaS1 production in various *ceaS2* mutants. On analysis, all *ceaS2* mutants were shown to be incapable of producing CeaS1protein (Section 3.1.3) and *ceaS1* transcripts were at much lower abundance, or absent, in Δ*ceaS2*-IF compared to wild type *S. clavuligerus* (Section 3.1.6). These results provided evidence that *ceaS1* and *ceaS2* are cross regulated through an unknown mechanism. Previous studies have shown that the two different copies of *ceaS* gene are under different regulation, where *ceaS1* and *ceaS2* are both expressed in complex Soy medium but only *ceaS2* is expressed in defined starch asparagine medium (Tahlan *et al*. 2004). This study, however,

clearly indicated that an additional regulatory mechanism governing transcription of *ceaS1* and *ceaS2* must exist such that transcription of the two genes is interconnected, at least in liquid medium. Interestingly, complementation studies as described in Section 3.1.3 showed that CeaS1production was not restored, even though clavulanic acid production was restored in the complemented strains. This suggested that the integrity of the *ceaS2* in its native chromosomal position is required for efficient transcription of *ceaS1* and downstream genes. The mechanism employed by *Myxococcus xanthus* to control the formation of multicellular fruiting bodies might be able to explain this observation.

Under nutrient limitation conditions, *M. xanthus* undergoes morphological differentiation and develops into fruiting bodies, which contains spores. Many of these developmental genes were shown to be expressed from σ^{54}-dependent promoters. To activate transcription from these promoters, additional activator proteins are also required to bind to DNA sequences, which are similar to enhancer sequences from eukaryotes, thus, these regulatory proteins are referred to as enhancer-binding proteins (EBPs) (Ghosh *et al*., 2010; Jelsbak *et al*., 2005). DNA looping allows bound EBPs to interact with RNA polymerase, forming an open complex and activating transcription (Ghosh *et al*., 2010). Although these enhancer elements are typically located 70-150 bp upstream of transcription start site (Buck *et al*., 2000), regulatory elements located >400 bp have been identified in *M. xanthus* (Viswanathan *et al*., 2007).

Although *S.coelicolor* (and presumably also *S. clavuligerus*) does not encode recognizable EBPs or σ^{54}, that does not rule out the possibility that an

analogous system may exist in *Streptomyces* spp. Based on the data obtained, it might be possible that an enhancer-type element is located in close proximity or within *ceaS2*. Therefore, disrupting *ceaS2* by inserting an antibiotic resistance gene or introducing a frame shift mutation, or deleting *ceaS2* would either alter the relative location of the enhancer element or prevented binding of EBP. This would then interrupt the interaction between EBP bound at the enhancer element and the RNA polymerase. As a result, transcription would not be initiated. Since the paralogue gene cluster is located on the pSCL4 plasmid (Medema *et al*., 2010), this also suggested a possible interaction between the chromosome and plasmid.

EBPs have N-terminal domains that can respond to environmental stimuli and some of these resemble the two-component response regulator receiver domain (Studholme and Dixon, 2003). A few EBPs identified from *M*. *xanthus* contained a forkhead-associated (FHA) sensory domain. Since the FHA domain specifically recognizes phosphothreonine residues and Ser/Thr protein kinases (STPK) are highly abundant in this organism (Kroos, 2005), it was proposed that Thr of the STPK undergoes autophosphorylation in response to environmental signals and the FHA domain of EBPs recognizes and interacts with the phosphorylated STPK. Transfer of phosphate from the STPK to the EBP activates and promotes interaction with RNA polymerase, and activates transcription (Jelsbak *et al*., 2005).

As complete genome sequencing revealed that two-component systems are highly abundant in *Streptomyces* spp., and cognate response regulators have not

been identified for some of these sensor kinases, it is possible that sensor kinases autophosphorylate in response to an environmental signal and then phosphorylate EBP-type-regulatory proteins, which in turn control transcription of *ceaS1* (Figure 4.1). Such a system, if it exists, would have to be active only when *S. clavuligerus* was grown in liquid medium to explain the discrepancy between liquid and solid medium. Since *S. clavuligerus* cannot sporulate in liquid medium, the sensor kinases involved could be sensing osmolarity difference or recognizing some other signals that regulate sporulation. However, at this point, the mechanism controlling *ceaS1* transcription remains elusive.

4.3 Effect of the atypical two-component system and C7P on 5*S* clavam metabolite biosynthesis

Previous studies have shown that the Snk/Res1/Res2 two-component system and the pathway-specific transcriptional regulator, C7P, are important for 5*S* clavam biosynthesis (Tahlan, 2005; Zelyas, 2007; Figure 3.2.1). Therefore, studies were initiated to further characterize how this system and C7P regulate production of 5*S* clavams. RT-PCR was carried out to determine genes that might be controlled by these proteins. Besides biosynthetic genes that are specifically involved in late steps for 5S clavam production, *c7p* transcription was also shown to be affected in a *snk* and *res2* mutants, but not the opposite (Table 3.2). This indicated that this two-component system operates at a higher level in the regulatory hierarchy controlling 5*S* clavam production in *S. clavuligerus*. EMSA further indicated that Res2 binds to the putative promoter region of *c7p*, and the encoded C7P protein binds to promoter regions of some tested late biosynthetic

Figure 4.1. A proposed mechanism for regulation of *ceaS1* transcription by *ceaS2* of *S. clavuligerus*.

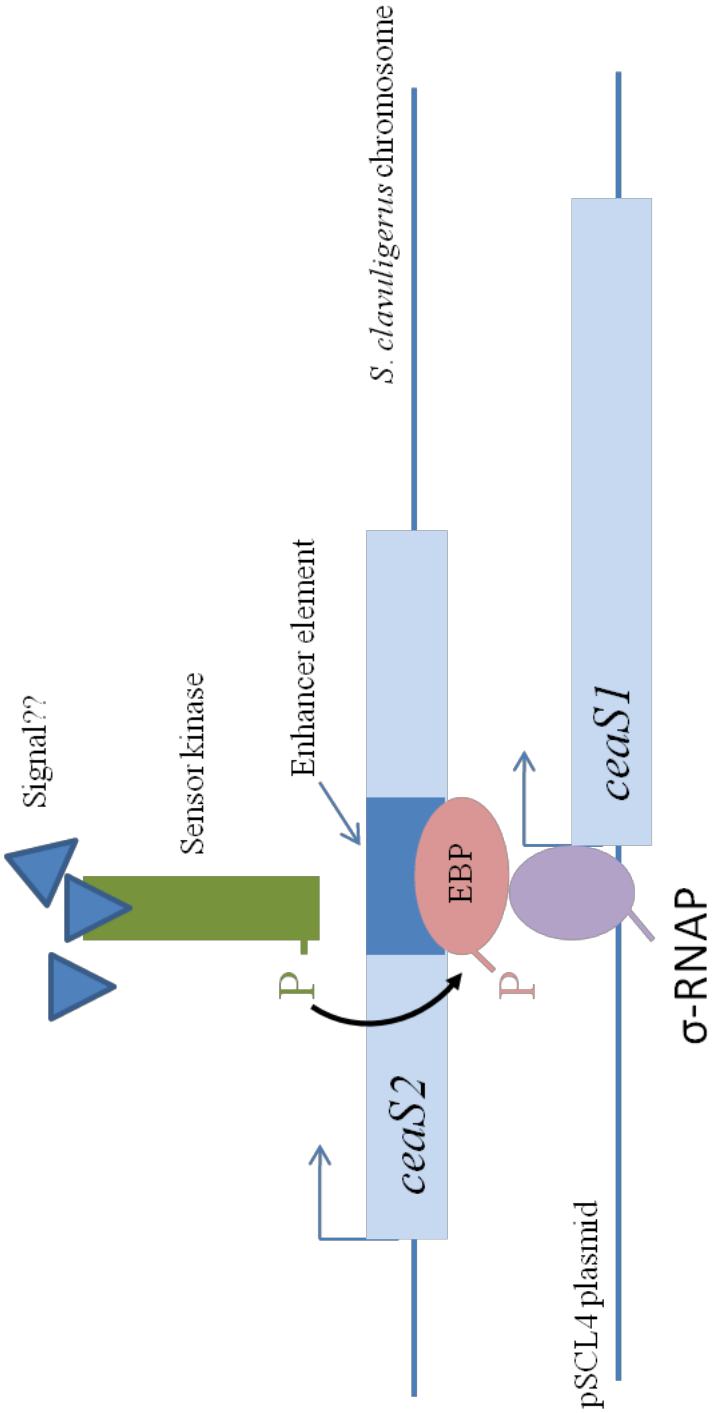
Signal??
Sensor kinase
Enhancer element
S. clavuligerus chromosome
P
EBP
P
ceaS1
ceaS2
σ-RNAP
pSCL4 plasmid

genes (Section 3.2.4.1 and 3.2.4.2). This suggested Res2 controls transcription of *c7p*, which in turns controls transcription of biosynthetic genes.

Snk is a soluble sensor kinase and contains two tandem GAF domains at the N-terminus (Tahlan, 2005). Although the exact stimulus detected by Snk is not known, GAF domains have been shown to be involved in binding small molecules such as cyclic nucleotides (cGMP and cAMP), heme, 2-ketoglutarate, formate, and Na^+ (Cann 2007; Ho *et al*. 2000; Hopper and Bock 1995; Little and Dixon 2003; Sardiwal *et al.,* 2005). Therefore, it was proposed that binding of some type of these small molecules would stimulate Snk autophosphorylation.

Both Res1 and Res2 showed similarity to response regulators. Although Res2 contains both an N-terminal phosphorylation receiver domain and a C-terminal DNA binding domain, typical of a response regulator, Res1 only contains the N-terminal phosphorylation domain (Zelyas, 2007). In order to characterize the phosphorylation dynamics between these three proteins, they were overproduced and purified as His-tagged proteins (Section 3.2.3). *In vitro* phosphorylation assays demonstrated that, with the conditions used, Snk is capable of autophosphorylation and both Res1 and Res2 can be phosphorylated by Snk (Section 3.3.1). The conserved histidine residue, H-365 of Snk and the conserved asparatic acid residues, D-65 of Res1 and D-52 of Res2, are the actual phosphorylation sites, as changing these residues to alanines prevented Snk autophosphorylation and blocked the ability of Res1 and Res2 to receive the phosphate molecules from Snk (Section 3.3.2 and 3.3.4). To further characterize the phosphorelay mechanism between Res1 and Res2, *in vitro* protein assays were

carried out. The results not only indicated that Res1 possesses phosphatase activity (Section 3.3.5.3), but also strongly suggested that it is capable of transferring phosphate molecules to Res2 (Section 3.3.5.4).

Although three-component systems have been identified in different bacteria, the mechanism governing their regulation remains largely unknown (Buelow and Raivio, 2010). These systems have been shown to play a key role in regulating a wide variety of activities. One of these is the RocSAR system from *Pseudomonas aeruginosa* that is involved in biofilm formation and maturation (Kuchma *et al*., 2005; Kulasekara *et al*., 2005). This system contains a sensor kinase, RocS1, and two response regulators, RocA1 and RocR. Similar to Res2, RocA1contains a response regulator domain and a DNA-binding domain. Although RocR also contains a response regulator domain, it is linked to an glutamate-alanine-leucine (EAL) domain instead of a DNA-binding domain (Kulasekara *et al*. 2005). Disrupting *rocS1*, *rocA1*, or *rocR* resulted in immature biofilm formation (Kuchma *et al*. 2005). Since bacterial two-hybrid systems showed that RocS1 can interact with both RocA1 and RocR, it was proposed that an environmental signal will induce RocS1 autophosphorylation, which can then phosphorylate RocA1 and RocR (Kulasekara *et al*. 2005). Phosphorylated RocA1 can then control transcription of target genes by direct binding to promoter region through its DNA-binding domain. In contrast, RocR is believed to regulate gene expression indirectly by controlling the intracellular concentration of cyclic di-GMP, as its EAL domain is associated with degradation of cyclic di-GMP to GMP, which serves as a signalling molecule to control biofilm formation, surface

motility and morphological development (Schmidt *et al*., 2005). However, these roles remain speculative, and it is still not clear how, or if, these two response regulators interact with each other.

Another three-component system is the CbbRRS system from *Rhodopseudomonas palustris*. This system was shown to regulate expression of the *cbbLS* genes, which encode the form I ribulose 1,5-bisphosphate carboxylase/oxygenase (RubisCO) involved in CO_2 fixation (Romagnoli and Tabita 2006). It is composed of the CbbSR sensor kinase and two response regulators, CbbRR1 and CbbRR2. Both of these response regulator proteins lacked the DNA-binding domain that is typical for a response regulator (Romagnoli and Tabita, 2006). Therefore, it is still unclear how this system regulates the expression of RubisCO. Interestingly, a complex phosphorelay mechanism that involves multiple domains on both the sensor kinase and the response regulators has been described (Romagnoli and Tabita, 2007).

Although the reason for *S. clavuligerus* to maintain this atypical two-component system to regulate 5S clavam biosynthesis is not clear, it is likely that Res1serves as an additional checkpoint for fine-tuning 5*S* clavam production. Based on the work from this thesis and data from previous studies, a mechanism for how this system may work can be proposed (Figure 4.2). Upon binding to small molecules through the GAF domains, Snk undergoes autophosphorylation. Res1 and Res2 then compete with each other for the phosphate molecules from Snk. At this point, if the signal persists, more of the response regulators can be phosphorylated. Phosphorylated Res1 may interact and then transfer its phosphate

Figure 4.2. A proposed mechanism for interaction between the Snk/Res1/Res2 atypical two-component system and the transcriptional regulator C7P of *S. clavuligerus*. Speculative steps that have not been verified experimentally are shown in broken arrows.

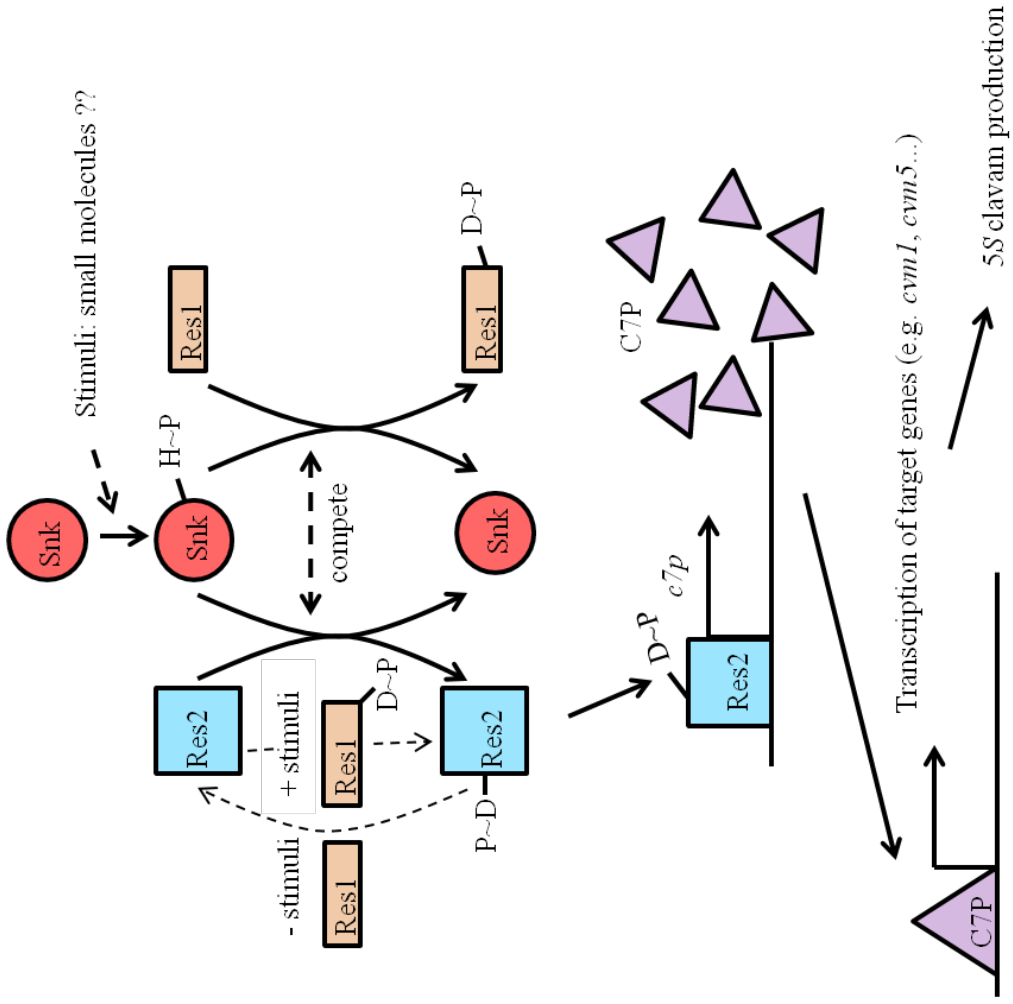
Stimuli: small molecules ??
Snk
Snk
H~P
Res1
compete
Snk
Res1
D~P
Res2
+ stimuli
Res1
D~P
Res2
- stimuli
Res1
P~D
C7P
D~P
c7p
Res2
Transcription of target genes (e.g. cvm1, cvm5...)
5S clavam production
C7P

molecules to Res2, which further enhances the amount of phosphorylated Res2. As a result, 5*S* clavam biosynthesis is up-regulated as Res2~P activates *c7p* transcription by binding to its own promoter and the encoded C7P protein activates transcription of 5*S* clavam biosynthetic genes. On the other hand, if the signal diminishes, phosphatase activity of Res1 will desphosphorylate Res2~P, therefore, resetting the system and reducing the amount of 5*S* clavams being produced. Obviously, additional work is required to confirm this mechanism. Another possibility is that Res1 may actually form a heterodimer with Res2 and modulate Res2 activity. To investigate this hypothesis, a bacterial two-hybrid system can be employed to test whether or not Res1 and Res2 interact.

4.4 Conclusions

Despite the work discussed here, the exact mechanism of regulation of 5*S* clavam biosynthesis in *S. clavuligerus* remains elusive. Since sequencing of the *S. clavuligerus* genome sequence, at least in draft form, has just been completed (Medema *et al*., 2010), future studies could include microarray analyses comparing a Δ*ceaS2*-IF mutant grown in liquid and solid medium to provide some insight of how *ceaS1* is being affected by *ceaS2*. In addition, because RT-PCR pointed out that, besides the late genes, some of the early genes of clavam biosynthesis are also affected in a *res2* mutant (Table 3.2), it is likely that this complex regulatory network would control a much larger number of genes. Therefore, *S. clavuligerus* genomic DNA microarrays can also help to provide a more comprehensive list of genes being regulated by this two-component system. Continued examination of the Snk/Res1/Res2 system will provide a better

understanding of the regulatory circuits of clavam biosynthesis. This may lead to higher clavulanic acid production at the industrial level through strain improvement by directing more resources from 5*S* clavam to the clavulanic acid biosynthetic pathway.

Chapter 5

References

5. References

Aceti, D.J., and Champness, W.C. 1998. Transcriptional regulation of *Streptomyces coelicolor* pathway-specific antibiotic regulators by the *absA* and *absB* loci. J. Bacteriol. **180**:3100-3106.

Adamidis, T., Riggle, P., and Champness, W. 1990. Mutations in a new *Streptomyces coelicolor* locus which globally block antibiotic biosynthesis but not sporulation. J. Bacteriol. **172**:2962-2969.

Alexander, D.C., and Jensen, S.E. 1998. Investigation of the *Streptomyces clavuligerus* cephamycin C gene cluster and its regulation by the CcaR protein. J. Bacteriol. **180:**4068-4079.

Ambler, R.P. 1980. The structure of β-lactamases. Phil. Trans. R. Sec. Lond. B **289**:321-331.

Arias, P., Fernandez-Moreno, M.A., and Malpartida, F. 1999. Characterization of the pathway-specific positive transcriptional regulator for actinorhodin biosynthesis in *Streptomyces coelicolor* A3(2) as a DNA-binding protein. J. Bacteriol. **181**:6958-6968.

Arulanantham, H., Kershaw, N.J., Hewitson, K.S., Hughes, C.E., Thirkettele, J.E., and Schofield, C.J. 2006. *Orf17* from the clavulanic acid biosynthesis gene cluster catalyzes the ATP-dependent formation of *N*-glycyl-clavaminic acid. J. Biol. Chem. **281**:279-287.

Bachmann, B.O., Li, R., and Townsend, C.A. 1998. β-lactam synthetase: a new biosynthetic enzyme. Proc. Natl. Acad. Sci. USA. **95**:9082-9086.

Baggaley, K.H., Brown, A.G., and Schofield, C.J. 1997. Chemistry and biosynthesis of clavulanic acid and other clavams. Nat. Prod. Rep. **14:**309-333.

Baldwin, J.E., Lloyd, M.D., Wha-Shon, B., Schofield, C.J., Elson, S.W., Baggaley, K.H., Nicholson, N.H. 1993. A substrate analogue study on clavaminic acid synthase: possible clues to the biosynthetic origin of proclavaminic acid. J. Chem. Soc. Chem. Commun. 500-502.

Baltz, R.H. 1980. Genetic recombination by protoplast fusion in *Streptomyces*. Dev. Ind. Microbiol. **21**:43-54.

Bentley, S.D., Brown, S., Murphy, L.D., Harris, D.E., Quail, M.A., Parkhill, J., Barrell, B.G., McCormick, J.R., Santamaria, R.I., Losick, R., Yamasaki, M., Kinashi, H., Chen, C.W., Chandra, G., Jakimowicz, D., Kieser, H.M., Kieser, T., and Chater, K.F. 2004. SCP1, a 356 023 bp linear plasmid adapted to the

ecology and developmental biology of its host, *Streptomyces coelicolor* A3(2). Mol. Microbiol. **51**(6): 1615-1628.

Bentley, S.D., Chater, K.F., Cerdeño-Tárraga, A.-., Challis, G.L., Thomson, N.R., James, K.D., Harris, D.E., Quail, M.A., Kieser, H., Harper, D., Bateman, A., Brown, S., Chandra, G., Chen, C.W., Collins, M., Cronin, A., Fraser, A., Goble, A., Hidalgo, J., Hornsby, T., Howarth, S., Huang, C.-., Kieser, T., Larke, L., Murphy, L., Oliver, K., O'Neil, S., Rabbinowitsch, E., Rajandream, M.-., Rutherford, K., Rutter, S., Seeger, K., Saunders, D., Sharp, S., Squares, R., Squares, S., Taylor, K., Warren, T., Wietzorrek, A., Woodward, J., Barrell, B.G., Parkhill, J., and Hopwood, D.A. 2002. Complete genome sequence of the model actinomycete *Streptomyces coelicolor* A3 (2). Nature **417:1**41-147.

Bignell, A.G., Lau, L.H., Colvin, K.R., and Leskiw, B.K. 2003. The putative anti-anti-sigma factor BldG is post-translationally modified by phosphorylation in *Streptomyces coelicolor*. FEMS Microbiol. Lett. **25**:93-99.

Bignell, D.R.D., Tahlan, K., Colvin, K.R., Jensen, S.E., and Leskiw, B.K. 2005. Expression of *ccaR*, encoding the positive activator of cephamycin C and clavulanic acid production in *Streptomyces clavuligerus*, is dependent on *bldG*. Antimicrob. Agents Chemother. **49:**1529-1541.

Brian, P., Riggle, P.J., Santos, R.A., and Champness, W.C. 1996. Global negative regulation of *Streptomyces coelicolor* antibiotic synthesis mediated by an *absA*-encoded putative signal transduction system. J. Bacteriol. **178**:3221-3231.

Brown, A.G., Butterworth, G., Cole, M., Hanscombe, G., Hood, J.D., Reading, C., and Robinson, G.N. 1976. Naturally occurring β-lactamase inhibitors with antibacterial activity. J. Antibiot. **29**:668-669.

Brown, K.L., Evans, J.R., and Fletton, R.A. 1979. Structures of three novel β-lactams isolated from three *Streptomyces clavuligerus*. J. Chem. Soc. Chem. Commun. **1979**:282-283.

Buck, M., Gallegos, M.T., Studholme, D.J., Guo, Y.L., and Gralla, J.D. 2000. The bacterial enhancer-dependent sigma(54) (sigma(N)) transcription factor. J. Bacteriol. **182**(15): 4129-4136.

Buelow, D.R., and Raivio, T.L. 2010. Three (and more) component regulatory systems - auxiliary regulators of bacterial histidine kinases. Mol. Microbiol. **75**(3):547-566.

Cai, H. 2003. Transposon mutagenesis and characterization of clavam biosynthetic genes in *Streptomyces clavuligerus*. M.Sc. Thesis, University of Alberta, Edmonton, Alta.

Caines, M.E.C., Elkins, J.M., Hewitson, K.S., and Schofield, C.J. 2004. Crystal structure and mechanistic implications of N 2-(2-Carboxyethyl) arginine synthase, the first enzyme in the clavulanic acid biosynthesis pathway. J. Biol. Chem. **279:**5685-5692.

Cann, M. 2007. A subset of GAF domains are evolutionarily conserved sodium sensors. Mol. Microbiol. **64**:461-472.

Chakraburtty, R., and Bibb, M.J. 1997. The ppGpp synthase gene (*relA*) of *Streptomyces coelicolor* A3(2) plays a conditional role in antibiotic production and morphological differentiation. J. Bacteriol. **179**:5854-5861.

Chater, K.F. 1993. Genetics of differentiation in *Streptomyces*. Annu. Rev. Microbiol. **47:**685-713.

Chater, K.F., and Bibb, M.J. 1997. Regulation of bacterial antibiotic production. *In* Biotechnology. *Edited by* H. Kleinkauf and H. von Döhren. VCH, Weinheim, Germany. pp. 57-105.

Chater, K.F., and Chandra, G. 2008. The use of the rare UUA codon to define "expression space" for genes involved in secondary metabolism, development and environmental adaptation in *Streptomyces*. J. Microbiol. **46**(1): 1-11.

Demain, A.L. 2000. Small bugs, big business: the economic power of the microbe. Biotechnol. Adv. **18**:499-514.

Demain, A.L., and Elander, R.P. 1999. The β-lactam antibiotics: Past, present, and future. Antonie van Leeuwenhoek **75:**5-19.

Egan, L.A., Busby, R.W., Iwata-Reuyl, D., and Townsend, C.A. 1997. Probable role of clavaminic acid as the terminal intermediate in the common pathway to clavulanic acid and the antipodal clavam metabolites. J. Am. Chem. Soc. **119:**2348-2355.

Elander, R.P. 2003. Industrial production of β-lactam antibiotics. Appl. Microbiol. Biotechnol. **61:**385-392.

Elkins, J.M., Clifton, I.J., Hernandez, H., Doan, L.X., Robinson, C.V., Schofield, C.J., and Hewitson, K.S. 2002. Oligomeric structure of proclavaminic acid amidino hydrolase: evolution of a hydrolytic enzyme in clavulanic acid biosynthesis. Biochem. J. **366**:423-434.

Elson, S.W., Baggaley, K.H., Davison, M., Fulston, M., Nicholson, N.H., Risbridger, G.D., and Tyler, J.W. 1993a. The identification of three new biosynthetic intermediates and one further biosynthetic enzyme in the clavulanic acid pathway. J. Chem. Soc. Chem. Commun. **1993**:1212-1214.

Fernandez-Moreno, M.A., Caballero, J.L., Hopwood, D.A., and Malpartida, F. 1991. The act cluster contains regulatory and antibiotic export genes, direct targets for translational control by the *bldA* tRNA gene of *Streptomyces*. Cell **66**:769-780.

Floriano, B., and Bibb, M. 1996. *afsR* is a pleiotropic but conditionally required regulatory gene for antibiotic production in *Streptomyces coelicolor* A3(2). Mol. Microbiol. **21**(2): 385-396.

Foulstone, M. and Reading, C. 1982. Assay of amoxicillin and clavulanic acid, the components of Augmentin, in biological fluids with high-performance liquid chromatography. Antimicrob. Agents Chemother. **22**:753-762.

Ghosh, T., Bose, D., and Zhang, X. 2010. Mechanisms for activating bacterial RNA polymerase. FEMS Microbiol. Rev. **34**(5): 611-627.

Gomez-Escribano, J.P., Martin, J.F., Hesketh, A., Bibb, M.J., and Liras, P. 2008. *Streptomyces clavuligerus reIA*-null mutants overproduce clavulanic acid and cephamycin C: negative regulation of secondary metabolism by (p)ppGpp. Microbiol. Sgm **154**: 744-755.

Guo, J., Zhao, J., Li, L., Chen, Z., Wen, Y., and Li, J. 2010. The pathway-specific regulator AveR from *Streptomyces avermitilis* positively regulates avermectin production while it negatively affects oligomycin biosynthesis. Mol. Genet. Genomics **283**(2): 123-133.

Gust, B., Challis, G.L., Fowler, K., Kieser, T. and Chater, K.F. 2003. PCR-targeted *Streptomyces* gene replacement identifies a protein domain needed for biosynthesis of the sesquiterpene soil odor geosmin. Proc. Natl. Acad. Sci USA. **100**:1541-1546.

Hardisson, C., and Manzanal, M.B. 1976. Ultrastructural studies of sporulation in *Streptomyces*. J. Bacteriol. **127:**1443-1454.

Hesketh, A., Chen, W.J., Ryding, J., Chang, S., and Bibb, M. 2007. The global role of ppGpp synthesis in morphological differentiation and antibiotic production in *Streptomyces coelicolor* A3(2). Genome Biol. **8**(8): R161.

Higgens, C.F., and Kastnar, R.E. 1971. *Streptomyces clavuligerus* sp. nov. a β-lactam antibiotic producer. Int. J. Syst. Bacteriol. **21**:326-331.

Ho, Y.S.J., Burden, L.M., and Hurley, J.H. 2000. Structure of the GAF domain, a ubiquitous signaling motif and a new class of cyclic GMP receptor. EMBO J. **19**:5288-5299.

Hodgson, J.E., Fosberry, A.P., Rawlinson, N.S., Ross, H.N.M., Neal, R.J., Arnell, J.C., Earl, A.J., and Lawlor, E.J. 1995. Clavulanic acid biosynthesis in *Streptomyces clavuligerus*: gene cloning and characterization. Gene **166**:49-55.

Hopper, S., and Bock, A. 1995. Effector-mediated stimulation of ATPase activity by the sigma 54-dependent transcriptional activator FHLA from *Escherichia coli*. J. Bacteriol. **177**:2798-27803.

Horinouchi, S., and Beppu, T. 1992. Autoregulatory factors and communication in Actinomycetes. Annu. Rev. Microbiol. **46:**377-398.

Howarth, T.T., Brown, A.G., and King, T. 1976. Clavulanic acid, a novel β-lactam from *Streptomyces clavuligerus*; X-ray crystal structure and analysis. J. Chem. Soc. Commun.: 266-267.

Hutchings, M.I., Hoskisson, P.A., Chandra, G., and Buttner, M.J. 2004. Sensing and responding to diverse extracellular signals? Analysis of the sensor kinases and response regulators of *Streptomyces coelicolor* A3(2). Microbiology **150**:2795-2806.

Ikeda, H., Ishikawa, J., Hanamoto, A., Shinose, M., Kikuchi, H., Shiba, T., Sakaki, Y., Hattori, M., and Omura, S. 2003. Complete genome sequence and comparative analysis of the industrial microorganism *Streptomyces avermitilis*. Nat. Biotechnol. **21:**526-531.

Jelsbak, L., Givskov, M., and Kaiser, D. 2005. Enhancer-binding proteins with a forkhead-associated domain and the sigma(54) regulon in *Myxococcus xanthus* fruiting body development. Proc. Natl. Acad. Sci. USA. **102**(8): 3010-3015.

Jensen, S.E., and Paradkar, A.S. 1999. Biosynthesis and molecular genetics of clavulanic acid. Antonie van Leeuwenhoek **75:**125-133.

Jensen, S.E., Elder, K.J., Aidoo, K.A., and Paradkar, A.S. 2000. Enzymes catalyzing the early steps of clavulanic acid biosynthesis are encoded by two sets of paralogous genes in *Streptomyces clavuligerus*. Antimicrob. Agents Chemother. **44**:720-726.

Jensen, S.E., Paradkar, A.S., Mosher, R.H., Anders, C., Beatty, P.H., Brumlik, M.J., Griffin, A., and Barton, B. 2004a. Five additional genes are involved in clavulanic acid biosynthesis in *Streptomyces clavuligerus*. Antimicrob. Agents Chemother. **48**:192-202.

Jensen, S.E., Wong, A., Griffin, A., and Barton, B. 2004b. *Streptomyces clavuligerus* has a second copy of the proclavaminate amidinohydrolase gene. Antimicrob. Agents Chemother. **48**:514-520.

Jin, W., Ryu, Y., Kang, S.G., Kim, S.K., Saito, N., Ochi, K., Lee, S.H., and Lee, K.J. 2004. Two *relA*/*spoT* homologous genes are involved in the morphological and physiological differentiation of *Streptomyces clavuligerus*. Microbiology **150**:1485-1493.

Kenig, M., and Reading, C. 1979. Holomycin and an antibiotic (MM 19290) related to tunicamycin, metabolites of *Streptomyces clavuligerus*. J. Antibiot. **32**:549-554

Kershaw, N.J., McNaughton, H.J., Hewitson, K.S., Hernandez, H., Griffin, J., Hughes, C, Greaves, P., Barton, B., Robinson, C.V., and Schofield, C.J. 2002. ORF6 from the clavulanic acid gene cluster of *Streptomyces clavuligerus* has ornithine acetyltransferase activity. Eur. J. Biochem. **269**:2052-2059.

Khaleeli, N., Li, R., and Townsend, C.A. 1999. Origin of the β-lactam carbons in clavulanic acid from an unusual thiamine pyrophosphate-mediated reaction. J. Am. Chem. Soc. **121:**9223-9224.

Khokhlov, A.S., Tovarova, I.L., Borisova, L.N., Pliner, S.A., Schevchenko, I.L., Kornitskaka, E.Y., Ivkina, N.S., and Rapoport, I.A. 1967. A-factor responsible for the production of streptomycin by a mutant strain of *Actinomyces streptomycini*. Dokl. Akad. SSSR **177**:232-235.

Kieser, T., Bibb, M.J., Buttner, M.J., Charter, K.F., and Hopwood, D.A. 2000. Practical *Streptomyces* genetics. John Innes Foundation, Norwich, England.

Kim, H.S., and Park, Y.I. 2008. Isolation and identification of a novel microorganism producing the immunosuppressant tacrolimus. J. Biosci. Bioeng. **105**(4): 418-421.

Kim, H.S., Lee, Y.J., Lee, C.K., Choi, S.U., Yeo, S.H., Hwang, Y.I., Yu, T.S., Kinoshita, H., and Nihira, T. 2004. Cloning and characterization of a gene encoding the γ-butyrolactone autoregulator receptor from *Streptomyces clavuligerus*. Arch. Microbiol. **182**:44-50.

Kinoshita, H., Tsuji, T., Ipposhi, H., Nihira, T., and Yamada, Y. 1999. Characterization of binding sequences for butyrolactone autoregulator receptors in *Streptomycetes*. J. Bacteriol. **181:**5075-5080.

Kirby, K. S., Fox-Carter, E., and Guest, M. 1967. Isolation of deoxyribonucleic acid and ribosomal ribonucleic acid from bacteria. Biochem. J. **104**:258-262.

Kroos, L. 2005. Eukaryotic-like signaling and gene regulation in a prokaryote that undergoes multicellular development. Proc. Natl. Acad. Sci. USA. **102**(8): 2681-2682.

Kuchma, S.L., Connolly, J.P., and O'Toole, G.A. 2005. A three-component regulatory system regulates biofilm maturation and type III secretion in *Pseudomonas aeruginosa*. J. Bacteriol. **187**:1441-1454.

Kulasekara, H.D., Ventre, I., Kulasekara, B.R., Lazdunski, A., Filloux, A., and Lory, S. 2005. A novel two-component system controls the expression of *Pseudomonas aeruginosa* fimbrial *cup* genes. Mol. Microbiol. **55**:368-380.

Kyung, Y.S., Hu, W.S., and Sherman, D.H. 2001. Analysis of temporal and spatial expression of the CcaR regulatory element in the cephamycin C biosynthetic pathway using green fluorescent protein. Mol. Microbiol. **40**(3): 530-541.

Leskiw, B.K., Bibb, M.J., and Chater, K.F. 1991. The use of a rare codon specifically during development. Mol. Microbiol. **5**:2861-2867.

Li, R., Khaleeli, N., and Townsend, C.A. 2000. Expansion of the clavulanic acid gene cluster: identification and in vivo functional analysis of three new genes required for biosynthesis of clavulanic acid by *Streptomyces clavuligerus*. J. Bacteriol. **182**:4087-4095.

Little, R., and Dixon, R. 2003. The amino-terminal GAF domain of *Azotobacter vinelandii* NifA binds 2-oxoglutarate to resist inhibition of NifL under nitrogen-limiting conditions. J. Biol. Chem. **278**:28711-28718.

Lorenzana, L.M., Perez-Redondo, R., Santamarta, I., Martin, J.F., and Liras, P. 2004. Two oligopeptide-permease-encoding genes in the clavulanic acid cluster of *Streptomyces clavuligerus* are essential for production of the β-lactamase inhibitor. J. Bacteriol. **186**:3431-3438.

MacKenzie, A.K., Kershaw, N.J., Hernandez, H., Robinson, C.V., Schofield, C.J., and Andersson, I. 2007. Clavulanic acid dehydrogenase: Structural and biochemical analysis of the final step in the biosynthesis of the beta-lactamase inhibitor clavulanic acid. Biochemistry **46**(6): 1523-1533.

Mackenzie, A.K., Valegard, K., Iqbal, A., Caines, M.E.C., Kershaw, N.J., Jensen, S.E., Schofield, C.J., and Andersson, I. 2010. Crystal structures of an oligopeptide-binding protein from the biosynthetic pathway of the beta-lactamase inhibitor clavulanic acid. J. Mol. Biol. **396**(2): 332-344.

Marsh, E.N., Chang, M.D., and Townsend, C.A. 1992. Two isozymes of clavaminate synthase central to clavulanic acid formation: cloning and sequencing of both genes from *Streptomyces clavuligerus*. Biochemistry 31:12648-12657.

Martin, J., and Liras, P. 2010. Engineering of regulatory cascades and networks controlling antibiotic biosynthesis in *Streptomyces*. Curr. Opin. Microbiol. **13**(3): 263-273.

Martin, J.F. 2004. Phosphate control of the biosynthesis of antibiotics and other secondary metabolites is mediated by the PhoR-PhoP system: an unfinished story. J. Bacteriol. **186**(16): 5197-5201.

Martinez-Hackert, E., and Stock, A. M. 1997. The DNA-binding domain of OmpR: crystal structures of a winged helix transcription factor. Structure **5**:109-124.

McCarthy, A.J., and Williams, S.T. 1992. Actinomeycetes as agents of biodegradation in the environment-a review. Gene **115**:189-192.

McKenzie, N.L., and Nodwell, J.R. 2007. Phosphorylated AbsA2 negatively regulates antibiotic production in *Streptomyces coelicolor* through interactions with pathway-specific regulatory gene promoters. J. Bacteriol. **189**:5284-5292.

Medema, M.H., Trefzer, A., Kovalchuk, A., van den Berg, M., Muller, U., Heijne, W., Wu, L., Alam, M.T., Ronning, C.M., Nierman, W.C., Bovenberg, R.A.L., Breitling, R., and Takano, E. 2010. The sequence of a 1.8-Mb bacterial linear plasmid reveals a rich evolutionary reservoir of secondary metabolic pathways. Genome Biol. Evol. **2**: 212-224.

Mellado, E., Lorenzana, L.M., Rodriguez-Saiz, M., Diez, B., Liras, P., and Barredo, J.L. 2002. The clavulanic acid biosynthetic cluster of *Streptomyces clavuligerus*: genetic organization of the region upstream of the *car* gene. Microbiology **148**:1427-1438.

Mendez, C., Brana, A.F., Manzanal, M.B., and Hardisson, C. 1985. Role of substrate mycelium in colony development in *Streptomyces*. Can. J. Microbiol. **31**:446-450.

Merrick, M.J. 1976. A morphological and genetic mapping study of bald colony mutants of *Streptomyces coelicolor*. J. Gen. Microbiol. **96**:299-315.

Miller, L.M., Stapley, E.O., and Chailet, L. 1962. Production of synnemantin B by the member of the genus *Streptomyces*. Bacteriol. Proc. **49**:32.

Miller, M.T., Bachmann, B.O., Townsend, C.A., and Rosenzweig, A.C. 2001. Structure of β-lactam synthetase reveals how to synthesize antibiotics instead of asparagine. Nat. Struct. Biol. **8**:684-689.

Mosher, R.H., Paradkar, A.S., Anders, C., Barton, B., and Jensen, S.E. 1999. Genes specific for the biosynthesis of clavam metabolites antipodal to clavulanic acid are clustered with the gene for clavaminate synthase 1 in *Streptomyces clavuligerus*. Antimicrob. Agents Chemother. **43:**1215-1224.

Nagarajan, R., Boeck, L.D., Gorman, M., Hamill, R.L., Higgens, C.E., Hoehn, M.M., Stark, W.M., and Whitney, J.G. 1971. Beta-lactam antibiotics from *Streptomyces*. J. Am. Chem. Soc. **93:**2308-2310.

Nicholson, N.H., Baggaley, K.H., Cassels, R., Davison, M., Elson, S.W., Fulston, M., Tyler, J.W., and Woroniecki, S.R. 1994. Evidence that the immediate biosynthetic precursor of clavulanic acid is its *N*-aldehyde analogue. J. Chem. Soc. Chem. Commun. **1994**:1281-1282.

Ochi, K. 1986. Occurrence of the stringent response in *Streptomyces* sp. and its significance for the initiation of morphological and physiological differentiation. J. Gen. Microbiol. **132**:2621-2631.

Ohnishi, Y., Ishikawa, J., Hara, H., Suzuki, H., Ikenoya, M., Ikeda, H., Yamashita, A., Hattori, M., and Horinouchi, S. 2008. Genome sequence of the streptomycin-producing microorganism *Streptomyces griseus* IFO 13350. J. Bacteriol. **190**(11): 4050-4060.

Paradkar, A.S., Aidoo, K.A., and Jensen, S.E. 1998. A pathway-specifictranscriptional activator regulates late steps of clavulanic acid biosynthesis in *Streptomyces clavuligerus*. Mol. Microbiol. **27**:831-843.

Paradkar, A.S., and Jensen, S.E. 1995. Functional analysis of the gene encoding the clavaminate synthase 2 isoenzyme involved in clavulanic acid biosynthesis in *Streptomyces clavuligerus*. J. Bacteriol. **177**:1307-1314.

Paradkar, A.S., Jensen, S.E., and Mosher, R.H. 1997. Comparative genetics and molecular biology of β-lactam biosynthesis. *In* Biotechnology of antibiotics. *Edited by* W.J. Strohl. Marcel Dekker, Inc., New York. Pp. 241-277.

Pérez-Llarena, F.J., Liras, P., Rodríguez-García, A., and Martin, J.F. 1997. A regulatory gene (*ccaR*) required for cephamycin and clavulanic acid production in *Streptomyces clavuligerus*: Amplification results in overproduction of both β-lactam compounds. J. Bacteriol. **179:**2053-2059.

Pérez-Redondo, R., Rodríguez-García, A., Martín, J.F., and Liras, P. 1998. The *claR* gene of *Streptomyces clavuligerus*, encoding a LysR-type regulatory protein controlling clavulanic acid biosynthesis, is linked to the clavulanate-9-aldehyde reductase (*car*) gene. Gene **211:**311-321.

Pruess, D.L., and Kellett, M. 1983. Ro 22-5417, a new clavam antibiotic from *Streptomyces clavuligerus*. I. Discovery and biological activity. J. Antibiot. **36**:208-212.

Retzlaff, L., and Distler, J. 1995. The regulator of streptomycin gene expression, StrR, of *Streptomyces griseus* is a DNA binding activator protein with multiple recognition sites. Mol. Microbiol. **18**:151-162.

Romagnoli, S., and Tabita, F.R. 2006. A novel three-protein two-component system provides a regulatory twist on an established circuit to moculate expression of the cbb_I region *Rhodopseudomonas palustris* CGA010. J. Bacteriol. **188**:2780-2791.

Romagnoli, S., and Tabita, F.R. 2007. Phosphotransfer reactions of the CbbRRS three-protein two-component system from *Rhodopseudomonas palustris* CGA010 appear to be controlled by an internal molecular switch on the sensor kinase. J. Bacteriol. **189**(2): 325-335.

Ryding, N.J., Anderson, T.B., and Champness, W.C. 2002. Regulation of the *Streptomyces coelicolor* calcium-dependent antibiotic by *absA*, encoding a cluster-linked two-component system. J. Bacteriol. **184**(3): 794-805.

Salowe, S.P., Krol, W.J., Iwata-Reuyl, D., and Townsend, C.A. 1991. Elucidation of the order of oxidations and identification of an intermediate in the multistep clavaminate synthase reaction. Biochemistry **30**:2281-2292.

Salowe, S.P., Marsh, E.N., and Townsend, C.A. 1990. Purification and characterization of clavaminate synthase from *Streptomyces clavuligerus*: an unusual oxidative enzyme in natural product biosynthesis. Biochemistry **29**:6499-6508.

Sambrook, J., Fritsch, E.F., and Maniatas, T. 1989. Molecular cloning: a laboratory manual. 2nd ed. Cold Spring Harbor Laboratory Press, Cold Spring Harbor, N.Y.

Santamarta, I., Pérez-Redondo, R., Lorenzana, L.M., Martín, J.F., and Liras, P. 2005. Different proteins bind to the butyrolactone receptor protein ARE sequence located upstream of the regulatory *ccaR* gene of *Streptomyces clavuligerus*. Mol. Microbiol. **56:**824-835.

Santamarta, I., Rodríguez-García, A., Pérez-Redondo, R., Martín, J.F., and Liras, P. 2002. CcaR is an autoregulatory protein that binds to the *ccaR* and *cefD-cmcI* promoters of the cephamycin C-clavulanic acid cluster in *Streptomyces clavuligerus*. J. Bacteriol. **184:**3106-3113.

Santos-Beneit, F., Rodriguez-Garcia, A., Sola-Landa, A., and Martin, J.F. 2009. Cross-talk between two global regulators in *Streptomyces*: PhoP and AfsR

interact in the control of *afsS*, *pstS* and *phoRP* transcription. Mol. Microbiol. **72**(1): 53-68.

Sardiwal, S., Kendall, S.L., Movahedzadeh, F., Rison, S.C.G., Stoker, N.G., and Djordjevic, S. 2005. A GAF domain in the hypoxia/NO-inducible *Mycobacterium tuberculosis* DosS protein binds haem. J. Mol. Biol. **353**:929-936.

Schmidt, A.J., Ryjenkov, D.A., and Gomelsky, M. 2005. The ubiquitous protein domain EAL is a cyclic diguanylate-specific phosphodiesterase: Enzymatically active and inactive EAL domains. J. Bacteriol. **187**(14): 4774-4781.

Skatrud, P.L., Schwecke, T., Liempt, H.V., and Tobin, M.B. 1997. Advances in the molecular genetics of β-lactam antibiotic biosynthesis. *In* Biotechnology. *Edited by* H. Kleinkauf and H. von Döhren. VCH, Weinheim, Germany. pp. 247-270.

Sola-Landa, A., Moura, R.S., and Martin, J.F. 2003. The two-component PhoR-PhoP system controls both primary metabolism and secondary metabolite biosynthesis in *Streptomyces lividans*. Proc. Natl. Acad. Sci. USA. **100**:6133-6138.

Song, J.Y., Kim, E.S., Kim, D.W., Jensen, S.E., and Lee, K.J. 2009. A gene located downstream of the clavulanic acid gene cluster in *Streptomyces clavuligerus* ATCC 27064 encodes a putative response regulator that affects clavulanic acid production. J. Ind. Microbiol. Biotechnol. **36**(2): 301-311.

Studholme, D.J., and Dixon, R. 2003. Domain architectures of sigma(54)-dependent transcriptional activators. J. Bacteriol. **185**(6): 1757-1767.

Stuttard, C. 1982. Temperate phages of *Streptomyces venezuelae*: lysogeny and host specificity shown by phages SV1 and SV2. J. Gen. Microbiol. **128**:115-121.

Tahlan, K. 2005. Characterization of the carboxyethylarginine synthase genes involved in clavulanic acid and 5S clavam metabolite biosynthesis in *Streptomyces clavuligerus*. Ph.D. thesis, University of Alberta, Edmonton, Alta.

Tahlan, K., Anders, C., and Jensen, S.E. 2004a. The paralogous pairs of genes involved in clavulanic acid and clavam metabolite biosynthesis are differently regulated in *Streptomyces clavuligerus*. J. Bacteriol. **186:**6286-6297.

Tahlan, K., Park, H.U., and Jensen, S.E. 2004b. Three unlinked gene clusters are involved in clavam metabolite biosynthesis in *Streptomyces clavuligerus*. Can. J. Microbiol. **50:**803-810.

Tahlan, K., Park, H.U., Wong, A., Beatty, P.H., and Jensen, S.E. 2004c. Two sets of paralogous genes encode the enzymes involved in the early stages of clavulanic acid and clavam metabolite biosynthesis in *Streptomyces clavuligerus*. Antimicrob. Agents Chemother. 48**:**903-939.

Tahlan, K., Anders, C., Wong, A., Mosher, R.H., Beatty, P.H., Brumlik, M.J., Griffin, A., Hughes, C., Griffin, J., Barton, B., and Jensen, S.E. 2007. 5*S* clavam biosynthetic genes are located in both the clavam and paralog gene clusters in *Streptomyces clavuligerus*. Chem. Biol. **14**(2): 131-142.

Thai, W., Paradkar, A.S. and Jensen, S.E. 2001. Construction and analysus of β-lactamase-inhibitory protein (BLIP) non-producer mutants of *Streptomyces clavuligerus*. Microbiology **147**:325-335.

Tipper, D.J., and Strominger, J.L. 1965. Mechanism of action of penicillins: a proposal based on their structural similarity to acyl-D-alanyl-D-alanine. Proc. Natl. Acad. Sci. USA. **54**:1133-1141.

Trepanier, N.K., Jensen, S.E., Alexander, D.C., and Leskiw, B.K. 2002. The positive activator of cephamycin C and clavulanic acid production in *Streptomyces clavuligerus* is mistranslated in a *bldA* mutant. Microbiology **148**:643-656.

Viswanathan, P., Ueki, T., Inouye, S., and Kroos, L. 2007. Combinatorial regulation of genes essential for *Myxococcus xanthus* development involves a response regulator and a LysR-type regulator. Proc. Natl. Acad. Sci. USA. **104**(19): 7969-7974.

Vogtli, M., Chang, P.C., and Cohen, S.N. 1994. Afsr2 - a previously undetected gene encoding a 63-amino-acid protein that stimulates antibiotic production in *Streptomyces lividans*. Mol. Microbiol. **14**(4): 643-653.

Waksman, S.A., and Henrici, A.T. 1943. The nomenclature and classification of the actinomycetes. J. Bacteriol. **46**:337-341.

Walsh, C. 2003. Antibiotics. American Society for Micriobiology Press, Washington, DC.

Ward, J.M., and Hodgson, J.E. 1993. The biosynthetic genes for clavulanic acid and cephamycin production occur as a 'super-cluster' in three *Streptomyces*. FEMS Microbiol. Lett. **110:**239-242.

Wietzorrek, A., and Bibb, M. 1997. A novel family of proteins that regulates antibiotic production in *Streptomycetes* appears to contain an OmpR-like DNA-binding fold. Mol. Microbiol. **25:**1181-1184.

Wildermuth, H. 1970. Development and organization of the aerial mycelium in *Streptomyces coelicolor*. J. Gen. Microbiol. **60**:43-50.

Wise, E.M., and Park, J.T. 1965. Penicillin: its basic site of action as an inhibitor of a peptide cross-linking reaction in cell wall mucopeptide synthesis. Proc. Natl. Acad. Sci. USA. **54**:75-81.

Zelyas, N. 2007. Identification and analysis of genes involved in 5*S* clavam biosynthesis in *Streptomyces clavuligerus*. M.Sc. thesis, University of Alberta, Edmonton, Alta.

Zelyas, N.J., Cai, H., Kwong, T., and Jensen, S.E. 2008. Alanylclavam biosynthetic genes are clustered together with one group of clavulanic acid biosynthetic genes in *Streptomyces clavuligerus*. J. Bacteriol. **190**(24): 7957-7965.